

Supporting Information

for

**C<sub>1</sub>-Symmetric {Cyclopentadienyl/Indenyl}-Metallocene Catalysts: Synthesis, Structure,  
Isospecific Polymerization of Propylene and Mechanism of Stereocontrol**

Dimitra Theodosopoulou,<sup>a</sup> Miguel Alonso De La Pena,<sup>a</sup> Sary Abou Derhamine,<sup>a</sup> Iskander Douair,<sup>b</sup> Thierry Roisnel,<sup>c</sup> Marie Cordier,<sup>c</sup> Lorenzo Piola,<sup>d</sup> Alvaro Fernandez,<sup>d</sup> Alexandre Welle,<sup>d</sup> Laurent Maron,<sup>b</sup> Jean-François Carpentier<sup>a,\*</sup> and Evgueni Kirillov<sup>a,\*</sup>

<sup>a</sup> Univ Rennes, CNRS, Institut des Sciences Chimiques de Rennes (ISCR), UMR 6226, F-35042 Rennes, France

<sup>b</sup> Univ Toulouse, INSA, UPS and CNRS, LPCNO, UMR 5215, 135 avenue de Rangueil, F-31077 Toulouse, France

<sup>c</sup> Centre de diffraction X, Univ Rennes, CNRS, ISCR (Institut des Sciences Chimiques de Rennes), UMR 6226, F-35700 Rennes, France

<sup>d</sup> Total Research & Technology Feluy, Zone Industrielle Feluy C, B-7181 Seneffe, Belgium

---

\* Correspondence to Jean-François Carpentier ([jean-francois.carpentier@univ-rennes.fr](mailto:jean-francois.carpentier@univ-rennes.fr)) and Evgueni Kirillov ([evgueni.kirillov@univ-rennes.fr](mailto:evgueni.kirillov@univ-rennes.fr)).

## Table of contents

### Experimental section

#### General considerations

#### Instruments and Measurements

#### Homogeneous polymerization of propylene

#### Heterogeneous polymerization of propylene using supported catalysts

#### Syntheses of precursors, proligands and complexes

**Figure S1.**  $^1\text{H}$  NMR spectrum (400 MHz, 25 °C,  $\text{CDCl}_3$ ) of chloro-(3,4-dimethyl-2,5-diphenylcyclopenta-2,4-dien-1-yl)dimethylsilane.

**Figure S2.**  $^{13}\text{C}\{^1\text{H}\}$  NMR spectrum (100 MHz, 25 °C,  $\text{CDCl}_3$ ) of chloro-(3,4-dimethyl-2,5-diphenylcyclopenta-2,4-dien-1-yl)dimethylsilane.

**Figure S3.**  $^1\text{H}$  NMR spectrum (400 MHz, 25 °C,  $\text{CDCl}_3$ ) of chloro(3,4-diisopropyl-2,5-dimethylcyclopenta-2,4-dien-1-yl)dimethylsilane (resulting crude product from the reaction).

**Figure S4.**  $^1\text{H}$  NMR spectrum (400 MHz, 25 °C,  $\text{CDCl}_3$ ) of 2-methyl-4-(3',5'-di-*tert*-butyl-4'-methoxy)-phenyl-5-methoxy-6-*tert*-butyl-1*H*-indene.

**Figure S5.**  $^{13}\text{C}\{^1\text{H}\}$  NMR spectrum (100 MHz, 25 °C,  $\text{CDCl}_3$ ) of 2-methyl-4-(3',5'-di-*tert*-butyl-4'-methoxy)-phenyl-5-methoxy-6-*tert*-butyl-1*H*-indene.

**Figure S6.**  $^1\text{H}$  NMR spectrum (400 MHz, 25 °C,  $\text{CDCl}_3$ ) of 6-*tert*-butyl-5-methoxy-4-(3,5-di-*tert*-butyl-4-methoxy)-phenyl-2-ethyl-1*H*-indene.

**Figure S7.**  $^{13}\text{C}\{^1\text{H}\}$  NMR spectrum (100 MHz, 25 °C,  $\text{CDCl}_3$ ) of 6-*tert*-butyl-5-methoxy-4-(3,5-di-*tert*-butyl-4-methoxy)-phenyl-2-ethyl-1*H*-indene.

**Figure S8.**  $^1\text{H}$  NMR spectrum (400 MHz, 25 °C,  $\text{CDCl}_3$ ) of 2,3-diisopropyl-1,4-dimethylcyclopenta-1,3-diene (resulting crude product from the reaction).

**Figure S9.**  $^1\text{H}$  NMR spectrum (400 MHz, 25 °C,  $\text{CDCl}_3$ ) of **1c** (resulting crude product from the reaction).

**Figure S10.**  $^{13}\text{C}\{^1\text{H}\}$  NMR spectrum (100 MHz, 25 °C,  $\text{CDCl}_3$ ) of **1c** (resulting crude product from the reaction).

**Figure S11.**  $^1\text{H}$  NMR spectrum (400 MHz, 25 °C,  $\text{CDCl}_3$ ) of **1d** (resulting crude product from the reaction).

**Figure S12.**  $^{13}\text{C}\{^1\text{H}\}$  NMR spectrum (100 MHz, 25 °C,  $\text{CDCl}_3$ ) of **1d** (resulting crude product from the reaction).

**Figure S13.**  $^1\text{H}$  NMR spectrum (400 MHz, 25 °C,  $\text{CDCl}_3$ ) of **1e**.

**Figure S14.**  $^{13}\text{C}\{^1\text{H}\}$  NMR spectrum (100 MHz, 25 °C,  $\text{CDCl}_3$ ) of **1e**.

**Figure S15.**  $^1\text{H}$  NMR spectrum (400 MHz, 25 °C,  $\text{CDCl}_3$ ) of **1f** (resulting crude product from the reaction).

**Figure S16.**  $^{13}\text{C}\{^1\text{H}\}$  NMR spectrum (100 MHz, 25 °C,  $\text{CDCl}_3$ ) of **1f** (resulting crude product from the reaction).

**Figure S17.**  $^1\text{H}$  NMR spectrum (400 MHz, 25 °C,  $\text{CDCl}_3$ ) of **1g** (resulting crude product from the reaction).

**Figure S18.**  $^{13}\text{C}\{^1\text{H}\}$  NMR spectrum (100 MHz, 25 °C,  $\text{CDCl}_3$ ) of **1g** (resulting crude product from the reaction).

**Figure S19.**  $^1\text{H}$  NMR spectrum (400 MHz, 25 °C,  $\text{CDCl}_3$ ) of **1h**.

**Figure S20.**  $^{13}\text{C}\{^1\text{H}\}$  NMR spectrum (100 MHz, 25 °C,  $\text{CDCl}_3$ ) of **1h**.

**Figure S21.**  $^1\text{H}$  NMR spectrum (400 MHz, 25 °C,  $\text{CDCl}_3$ ) of **1i** (resulting crude product from the reaction).

**Figure S22.**  $^1\text{H}$  NMR spectrum (100 MHz, 25 °C,  $\text{CDCl}_3$ ) of **1j**.

**Figure S23.**  $^1\text{H}$  NMR spectrum (400 MHz, 25 °C,  $\text{CDCl}_3$ ) of **1k**.

**Figure S24.**  $^1\text{H}$  NMR spectrum (400 MHz, 25 °C,  $\text{CDCl}_3$ ) of **2b-Zr**.

**Figure S25.**  $^{13}\text{C}\{^1\text{H}\}$  NMR spectrum (100 MHz, 25 °C,  $\text{CDCl}_3$ ) of **2b-Zr**.

**Figure S26.**  $^1\text{H}$  NMR spectrum (400 MHz, 25 °C,  $\text{CDCl}_3$ ) of **2b-Hf**.

**Figure S27.**  $^{13}\text{C}\{^1\text{H}\}$  NMR spectrum (100 MHz, 25 °C,  $\text{CDCl}_3$ ) of **2b-Hf**.

**Figure S28.**  $^1\text{H}$  NMR spectrum (400 MHz, 25 °C,  $\text{CDCl}_3$ ) of **2c-Zr**.

**Figure S29.**  $^{13}\text{C}\{^1\text{H}\}$  NMR spectrum (100 MHz, 25 °C,  $\text{CDCl}_3$ ) of **2c-Zr**.

**Figure S30.**  $^1\text{H}$  NMR spectrum (400 MHz, 25 °C,  $\text{CDCl}_3$ ) of **2d-Zr**.

**Figure S31.**  $^{13}\text{C}\{^1\text{H}\}$  NMR spectrum (100 MHz, 25 °C,  $\text{CDCl}_3$ ) of **2d-Zr**.

**Figure S32.**  $^1\text{H}$  NMR spectrum (400 MHz, 25 °C,  $\text{CDCl}_3$ ) of **2d-Hf**.

**Figure S33.**  $^{13}\text{C}\{^1\text{H}\}$  NMR spectrum (100 MHz, 25 °C,  $\text{CDCl}_3$ ) of **2d-Hf**.

**Figure S34.**  $^1\text{H}$  NMR spectrum (400 MHz, 25 °C,  $\text{CDCl}_3$ ) of **2e-Zr**.

**Figure S35.**  $^{13}\text{C}\{^1\text{H}\}$  NMR spectrum (100 MHz, 25 °C,  $\text{CDCl}_3$ ) of **2e-Zr**.

**Figure S36.**  $^1\text{H}$  NMR spectrum (400 MHz, 25 °C,  $\text{CDCl}_3$ ) of **2f-Zr**.

**Figure S37.**  $^{13}\text{C}\{^1\text{H}\}$  NMR spectrum (100 MHz, 25 °C,  $\text{CDCl}_3$ ) of **2f-Zr**.

**Figure S38.**  $^1\text{H}$  NMR spectrum (400 MHz, 25 °C,  $\text{CDCl}_3$ ) of **2g-Zr**.

**Figure S39.**  $^{13}\text{C}\{^1\text{H}\}$  NMR spectrum (100 MHz, 25 °C,  $\text{CDCl}_3$ ) of **2g-Zr**.

**Figure S40.**  $^1\text{H}$  NMR spectrum (400 MHz, 25 °C,  $\text{CDCl}_3$ ) of **2h-Zr**.

**Figure S41.**  $^{13}\text{C}\{^1\text{H}\}$  NMR spectrum (100 MHz, 25 °C,  $\text{CDCl}_3$ ) of **2h-Zr**.

**Figure S42.**  $^1\text{H}$  NMR spectrum (400 MHz, 25 °C,  $\text{C}_6\text{D}_6$ ) of **2i-Zr**.

**Figure S43.**  $^{13}\text{C}\{^1\text{H}\}$  NMR spectrum (100 MHz, 25 °C,  $\text{C}_6\text{D}_6$ ) of **2i-Zr**.

**Figure S44.**  $^1\text{H}$  NMR spectrum (400 MHz, 25 °C,  $\text{C}_6\text{D}_6$ ) of **2j-Zr**.

**Figure S45.**  $^{13}\text{C}\{^1\text{H}\}$  NMR spectrum (100 MHz, 25 °C,  $\text{C}_6\text{D}_6$ ) of **2j-Zr**.

**Figure S46.**  $^1\text{H}$  NMR spectrum (400 MHz, 25 °C,  $\text{CD}_2\text{Cl}_2$ ) of **2k-Zr**.

**Figure S47.**  $^{13}\text{C}\{^1\text{H}\}$  NMR spectrum (100 MHz, 25 °C,  $\text{CD}_2\text{Cl}_2$ ) of **2k-Zr**.

**Figure S48.**  $^{13}\text{C}\{^1\text{H}\}$  NMR spectrum (125 MHz, 135 °C,  $\text{C}_6\text{D}_6/\text{C}_6\text{H}_3\text{Cl}_3$ ) of an iPP sample obtained with precursor **2h-Zr** (Table 2, entry 14).

**Figure S49.**  $^{13}\text{C}\{^1\text{H}\}$  NMR spectrum (125 MHz, 135 °C,  $\text{C}_6\text{D}_6/\text{C}_6\text{H}_3\text{Cl}_3$ ) of an iPP sample obtained with precursor **2e-Zr** (Table 2, entry 8).

### Computational details

**Table S1.** Steric maps generated for the DFT-optimized (B3PW91/LANL2DZ) geometries of the synthesized  $\{\text{Cp/Ind}\}$  *ansa*-zirconocenes with sphere radius = 5 Å.

**Figure S50.** Plot of probabilistic descriptor  $b$  vs the  $\Delta\%V_{\text{free,Q1}}$  of quadrants Q1 in metallocene complexes **2a–h,k-Zr**.

**Figure S51.** GPC trace for the iPP obtained with **2e-Zr** (Table 2, entry 9).

**Figure S52.** DSC curve for the iPP obtained with **2e-Zr** (Table 2, entry 9).

**Figure S53.**  $^1\text{H}$  NMR spectrum (400 MHz,  $\text{CDCl}_3$ , 25 °C) of oligomers produced with **2i-Zr** complex.

**Figure S54.**  $^{13}\text{C}\{^1\text{H}\}$  NMR spectrum (100 MHz, 25 °C,  $\text{CDCl}_3$ ) of oligomers produced with **2i-Zr/MAO**.

**Figure S55.** Molecular structure of **2b-Hf**.

**Figure S56.** Molecular structure of **2d-Hf**.

**Table S2.** Summary of Crystal and Refinement Data for Complexes **2a-Zr**, **2b-Zr**, **2b-Hf**, **2d-Zr**, **2d-Hf**, **2e-Zr**, **2f-Zr**, **2j-Zr** and **2k-Zr**.

**Table S3.** Energetic data ( $\text{kcal}\cdot\text{mol}^{-1}$ ) calculated for the three first propylene insertion steps with systems  $[\mathbf{2c-Zr-Me}]^+$  and  $[\mathbf{2d-Zr-Me}]^+$ .

## Experimental part

**General considerations.** All manipulations were performed under a purified argon atmosphere using standard Schlenk techniques or in a glovebox. Solvents were distilled: THF from Na/benzophenone, toluene from Na/K alloy, hexane and heptane from CaH<sub>2</sub> under nitrogen, degassed thoroughly and stored under argon prior to use. Diethyl ether and dichloromethane were used directly from a Solvent Purification System and stored under argon and molecular sieves (3A, 8 to 12 mesh) prior to use. Deuterated solvents (benzene-*d*<sub>6</sub>, THF-*d*<sub>8</sub>; >99.5% D, Deutero GmbH and Eurisotop) were vacuum-transferred from Na/K alloy into storage tubes; CDCl<sub>3</sub> and CD<sub>2</sub>Cl<sub>2</sub> were kept over CaH<sub>2</sub> and vacuum-transferred before use. MAO (30 wt.% solution in toluene, Grace) and complex *rac*-{Me<sub>2</sub>Si(2-Me-4-Ph-Ind)<sub>2</sub>}ZrCl<sub>2</sub> (**I**) were generously provided by TotalEnergies Petrochemicals and used as received. The following ligand precursors were prepared as described in the literature: chlorodimethyl(2,3,4,5-tetramethylcyclopenta-2,4-dien-1-yl)silane,<sup>1,2</sup> (1,2-diphenyl, 3,4-dimethyl)-cyclopentadiene,<sup>3</sup> 4-bromo-6-*tert*-butyl-5-methoxy-2-methyl-1-indanone, 6-*tert*-butyl-5-methoxy-4-phenyl-2-methyl-1*H*-indene and 4-bromo-6-*tert*-butyl-5-methoxy-2-ethyl-1-indanone,<sup>4</sup> 6-*tert*-butyl-4-phenyl-2-methyl-1*H*-indene,<sup>5</sup> and (3,5-di-*tert*-butyl-4-methoxy-phenyl)boronic acid,<sup>6</sup> 2-methyl-4-phenyl-1*H*-indene **1e**,<sup>7</sup> (3,6-di-*tert*-butyl-9-(2-methyl-1*H*-inden-7-yl)-9*H*-carbazole,<sup>8</sup> 2,3-diisopropyl-1,4-dimethylcyclopenta-1,3-diene,<sup>9</sup> (6*r*,11*s*)-2-methyl-6,11-dihydro-3*H*-6,11-[1,2]benzenocyclopenta[*a*]anthracene,<sup>10</sup> and reference metallocenes **2a-Zr**<sup>11,12</sup> and **2b-Zr**.<sup>13</sup> Other starting materials were purchased from Acros, Alfa, Strem and Aldrich, and used as received.

**Instruments and Measurements.** NMR spectra of air- and moisture- sensitive compounds were recorded on Bruker AM-300, AM-400 and AM-500 spectrometers in Teflon-valved NMR tubes at room temperature. <sup>1</sup>H and <sup>13</sup>C chemical shifts are reported in ppm vs. SiMe<sub>4</sub> (0.00), as determined by reference to the residual solvent signals. Assignments of signals were carried out from 2D <sup>1</sup>H–<sup>13</sup>C HMQC and HMBC NMR experiments. Coupling constants are given in Hertz.

<sup>13</sup>C{<sup>1</sup>H} NMR analyses of iPP samples were run in the research center of TotalEnergies OneTech Belgium on a AM-500 Bruker spectrometer equipped with a high temperature 10 mm cryoprobe using the following conditions: The sample was prepared by dissolving a sufficient

amount of polymer in 1,2,4-trichlorobenzene (TCB, 99 %, spectroscopic grade) at 130 °C and occasional agitation to homogenize the sample, followed by the addition of hexadeuterobenzene ( $C_6D_6$ , spectroscopic grade) and a minor amount of hexamethyldisiloxane (HMDS, 99.5+ %) as internal standard (2.03 ppm). To give an example, about 600 mg of polymer were dissolved in 2.0 mL of TCB, followed by addition of 0.5 mL of  $C_6D_6$  and 2 to 3 drops of HMDS.

DSC measurements were performed on a SETARAM Instrumentation DSC 131 differential scanning calorimeter, under a continuous flow of helium and using aluminum capsules, at a heating rate of 10 °C/min; first and second runs were recorded after cooling to 30 °C; the melting temperatures reported in tables correspond to the second run.

GPC analyses of iPP samples were carried out in 1,2,4-trichlorobenzene at 135 °C in the research center of TotalEnergies Petrochemicals in Feluy (Belgium), using polystyrene standards for universal calibration.

### **Homogeneous polymerization of propylene.**

**Protocol 1: typical propylene homopolymerization with MAO (scavenger and activator).** Polymerization experiments were performed in a 300 mL high-pressure glass reactor equipped with a mechanical stirrer (Pelton turbine) and externally heated with a double mantle with a circulating water bath. The reactor was charged with toluene (150 mL) and the desired quantity of MAO (30% wt. solution in toluene). The reactor was thermally equilibrated at the desired temperature for 30 min and vented with propylene. A solution of the catalyst precursor in toluene (ca. 2 mL) was added by syringe and the reactor was pressurized at 5 bar of propylene (Air Liquide, 99.99%). The propylene pressure was immediately increased to 5 bar (kept constant with a back regulator) and the solution was stirred for the desired time (typically 30 min). The temperature inside the reactor was monitored using a thermocouple. The polymerization was stopped by venting the vessel and quenching with a 10% solution of aqueous HCl in methanol (ca. 1 mL). The polymer was precipitated in methanol (ca. 200 mL) and 35% aqueous HCl (ca. 3 mL) was added to dissolve possible catalyst residues. The polymer was collected by filtration, washed with methanol (ca. 200 mL), and dried in a vacuum oven at 40 °C for 4 h.

**Protocol 2: propylene homopolymerization with TIBAL/[Ph<sub>3</sub>C]<sup>+</sup>[(C<sub>6</sub>F<sub>5</sub>)<sub>4</sub>]<sup>-</sup>.** The reactor was charged with toluene (130 to 150 mL) and TIBAL (1,000–2,000 equiv vs [Zr]<sub>0</sub>, 1.1 M

solution in toluene), and propylene (5 bar, Air Liquide, 99.99%) was introduced. The reactor was thermally equilibrated at the desired temperature for 1 h. Propylene pressure was reduced to 1 bar and a solution of the catalyst precursor in toluene (1–2 mL) was added by syringe, and after 15 min the trityl tetrakis(pentafluorophenyl)borate solution (5 equiv vs  $[Zr]_0$ , in 10 mL of toluene) was added to start the polymerization. The propylene pressure was immediately increased to 5 bar (kept constant with a back regulator) and the solution was stirred for the desired time (typically 30 min). The polymerization was stopped and the polymer was isolated following the same steps as those described in Protocol 1.

**Protocol 3: propylene homopolymerization with TIBAL/MAO.** The reactor was charged with toluene (130 to 150 mL) and TIBAL (5,000 equiv vs  $[Zr]_0$ , 1.1 M solution in toluene). For preactivation, the desired quantity of the metallocene was dissolved in 10 mL of toluene, MAO (5,000 equiv, 30% wt. solution in toluene) was added and the resulting solution was stirred for 1 h at room temperature. The reactor was thermally equilibrated at the desired temperature for 1 h and vented with propylene. The solution of the preactivated catalyst in toluene (ca. 10 mL) was added by syringe and the reactor was pressurized at 5 bar of propylene. The polymerization was stopped and the polymer was isolated following the same steps as those described in Protocol 1.

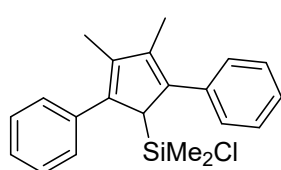
**Heterogeneous polymerization of propylene using supported catalysts *supp-2b-Zr*, *supp-2c-Zr*, *supp-2d-Zr* and *supp-2e-Zr*.** Catalysts **2b–e-Zr** were supported according to the ACM methodology, using Radley apparatus, as described below (all reactions were carried out under strictly anhydrous conditions):

Dry silica (TS-F202, 20.011 g) was suspended in toluene (200 mL) and mechanical stirring was started at a very low speed. MAO (38 mL, 30 wt% solution in toluene) was added dropwise, aiming at 16 wt% deposition of Al. An additional amount of toluene (87 mL) was added, and the mixture was heated at 110 °C for 4 h. The mixture was then filtered and the solid was washed 3 times with both toluene and pentane and then dried in a frit connected to a pump. The metallocene (ca. 10 mg, in order to reach 1.25 wt% of supported metallocene) was dissolved in toluene (5 mL). Silica/MAO (8.0 g, prepared as described above) was added and toluene (5 mL) was used to wash the glassware and added to the mixture. The mixture was stirred at room temperature for 3 h and then was filtered. The solid was washed 3 times with toluene and 3 times with pentane and then dried under vacuum. The supported catalyst was then dispersed in dry oil

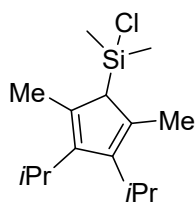
(Finavestan A 360 B) in order to have a solid content of around 20 wt%. The samples were analyzed for zirconium and aluminum content (%wt) using ICP-AES spectrometer.

An 8-L reactor was heated at 130 °C and flushed with N<sub>2</sub> prior to being used. The reactor was then flushed with 1 L of propylene and cooled to 40 °C. Subsequently, 3 L of propylene were pushed in the reactor together with the required amount of H<sub>2</sub>. Mechanical stirring at 20 rpm was started and once the reactor was stabilized, a mixture of TIBAL (1 mL), the supported catalyst and the co-catalyst were injected in the reactor together with 1.5 L of propylene. The reactor was then ramped to 70 °C and once the temperature was reached, it was left to react for 1 h. The reactor was then vented, and the polymer was left under a light stream of N<sub>2</sub> to dry. The polymer was then collected and left to dry further for additional 2 h.

### Syntheses of precursors, proligands and complexes



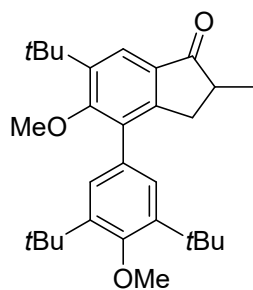
**Chloro-(3,4-dimethyl-2,5-diphenylcyclopenta-2,4-dien-1-yl)dimethylsilane.** (1,2-diphenyl,3,4-dimethyl)-cyclopentadiene (0.36 g, 0.0015 mol) was dissolved in THF (15 mL) and the solution was stirred while cooling to -78 °C. To this solution, *n*-BuLi (0.61 mL of a 2.26 M solution in hexane, 0.0015 mol) was added by syringe and the temperature was raised to room temperature. A pink solution formed which was stirred overnight at room temperature. After cooling at -78 °C, Me<sub>2</sub>SiCl<sub>2</sub> (0.35 mL, 0.003 mol, 2 equiv) was added slowly by syringe and the mixture was then allowed to warm at room temperature and stirred overnight. Volatiles were then evaporated under vacuum. Petroleum ether (30 mL) was added and LiCl was removed *via* cannula filtration. Volatiles were then evaporated under vacuum to give a colourless viscous oil (0.40 g, 80%). <sup>1</sup>H NMR (400 MHz, CDCl<sub>3</sub>, 25 °C): δ 7.42–7.32 (m, 8H, Ar-*H*), 7.29–7.24 (m, 2H, Ar-*H*), 4.38 (p, *J* = 1.6, 1H, Cp-*H*), 2.14 (d, *J* = 1.6, 6H, (CH<sub>3</sub>)<sub>2</sub>-Cp), -0.20 (s, 6H, Si-(CH<sub>3</sub>)<sub>2</sub>). <sup>13</sup>C{<sup>1</sup>H} NMR (100 MHz, CDCl<sub>3</sub>, 25 °C): δ 139.46, 139.10, 137.87, 129.52, 128.29, 126.56, 53.79 (CH-Cp), 12.71 ((CH<sub>3</sub>)<sub>2</sub>-Cp), 0.61 (Si-(CH<sub>3</sub>)<sub>2</sub>).



**Chloro(3,4-diisopropyl-2,5-dimethylcyclopenta-2,4-dien-1-yl)dimethylsilane.** Following a procedure similar to that described for chloro(3,4-dimethyl-2,5-diphenylcyclopenta-2,4-dien-1-yl)dimethylsilane, chloro(3,4-



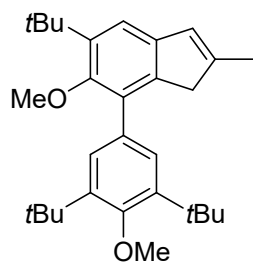
diisopropyl-2,5-dimethylcyclopenta-2,4-dien-1-yl)dimethylsilane was obtained as a yellow oil (5.83 g, 86%). <sup>1</sup>H NMR (400 MHz, CDCl<sub>3</sub>, 25 °C): δ 3.11 (dt, *J* = 10.9, 1.0, 1H, C<sub>5</sub>H<sub>1</sub>), 2.88 (q, *J* = 7.3, 2H, CH(CH<sub>3</sub>)<sub>2</sub>), 2.16–1.43 (m, 6H, CH<sub>3</sub>), 1.18 (dd, *J* = 7.2, 6.3, 3H, CH(CH<sub>3</sub>)<sub>2</sub>), 1.09–1.05 (m, 3H, CH(CH<sub>3</sub>)<sub>2</sub>), 0.94–0.82 (m, 6H, CH(CH<sub>3</sub>)<sub>2</sub>), 0.51–0.02 (m, 6H, Si-(CH<sub>3</sub>)<sub>2</sub>). EI-MS *m/z*: [M]<sup>+</sup> 270.



**6-*Tert*-butyl-5-methoxy-4-(3',5'-di-*tert*-butyl-4'-methoxy)-phenyl-2-**

**methyl-1-indanone.** Pd(OAc)<sub>2</sub> (0.13 g, 3 mol%) and RuPhos (0.53 g, 6 mol%) were added under an Ar flush to a well-stirred mixture of 4-bromo-6-*tert*-butyl-5-methoxy-2-methyl-1-indanone (5.90 g, 0.019 mol), (3,5-di-*tert*-butyl-4-methoxy-phenyl)-boronic acid (8.00 g, 0.030 mol), K<sub>3</sub>PO<sub>4</sub> (12.0 g, 0.057 mol) in THF (72 mL) and water (14 mL). The reaction

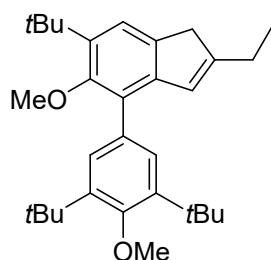
mixture was refluxed overnight. Then, the reaction mixture was cooled, poured into water (100 mL) and extracted with CH<sub>2</sub>Cl<sub>2</sub> (3 × 100 mL). The combined organic phases were washed with water (200 mL) and 2.0 M aqueous solution of Na<sub>2</sub>CO<sub>3</sub> (200 mL) dried over MgSO<sub>4</sub> and evaporated under vacuum. Then, a concentrated solution of the crude product in dichloromethane was prepared, from which the desired product was precipitated as a white solid by adding an excess of hexane. The pure product was obtained as a white crystalline solid after dissolution in 30 mL of CH<sub>2</sub>Cl<sub>2</sub>, filtration over a short pad of silica-gel using CH<sub>2</sub>Cl<sub>2</sub>/hexane 1:1 *v/v* followed by evaporation of the volatiles to yield the product (6.0 g, 70%). <sup>1</sup>H NMR (400 MHz, CDCl<sub>3</sub>, 25 °C): δ 7.73 (s, 1H, Ar'-*H*), 7.27 (s, 2H, Ar'-*H*), 3.74 (s, 3H, 4'-(OCH<sub>3</sub>)-Ph), 3.25 (s, 3H, Ind-OCH<sub>3</sub>), 3.18 (dd, *J* = 17.4, 7.8, 1H, 2*H*-ind), 2.71–2.43 (m, 2H, 3*H*-Ind), 1.46 (s, 18H, (CH<sub>3</sub>)<sub>3</sub>'), 1.42 (s, 9H, (CH<sub>3</sub>)<sub>3</sub>), 1.27 (d, *J* = 7.5, 3H, Ind-CH<sub>3</sub>).



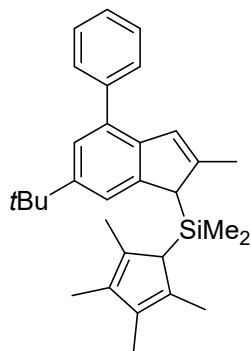
**2-Methyl-4-(3',5'-di-*tert*-butyl-4'-methoxy)-phenyl-5-methoxy-6-*tert*-butyl-1*H*-indene.**

6-*Tert*-butyl-5-methoxy-4-(3',5'-di-*tert*-butyl-4'-methoxy)-phenyl-2-methyl-1-indanone (6.00 g, 0.013 mol) was dissolved in THF (25 mL) and added dropwise at 0 °C to a mixture of LiAlH<sub>4</sub> (0.25 g, 0.0066 mol) in THF (50 mL). After 1 h of stirring, water was slowly added (20 mL) and then 5 wt% aqueous HCl (20 mL) was added. The organic phase was separated, washed with an aqueous solution of Na<sub>2</sub>CO<sub>3</sub> (5% *w/w*, 100 mL), dried over MgSO<sub>4</sub>

and evaporated. The residue was dissolved in toluene (80 mL), PTSA (0.23 g, 9 mol%) was added and the resulting mixture was refluxed for 30 min, cooled, washed with water, dried over MgSO<sub>4</sub> and evaporated to obtain a white crystalline solid (5.20 g, 89%). <sup>1</sup>H NMR (400 MHz, CDCl<sub>3</sub>, 25 °C): δ 7.35 (s, 2H, Ar'-H), 7.19 (s, 1H, Ind-7H), 6.44 (bs, *J* = 1.6, 1H, 1H-Ind), 3.73 (s, 3H, 4'-(OCH<sub>3</sub>)-Ph), 3.18 (s, 3H, OCH<sub>3</sub>-Ind), 3.15 (s, 2H, 3H-Ind), 2.08 (s, 3H, Ind-CH<sub>3</sub>), 1.45 (s, 18H, (CH<sub>3</sub>)<sub>3</sub>'), 1.43 (s, 9H, (CH<sub>3</sub>)<sub>3</sub>). <sup>13</sup>C{<sup>1</sup>H} NMR (100 MHz, CDCl<sub>3</sub>, 25 °C): δ 158.41, 154.60, 145.30, 143.33, 141.84, 141.09, 140.79, 134.30, 132.41, 132.18, 128.04, 127.11, 116.96, 64.48 (4'-(OCH<sub>3</sub>)-Ph), 60.28 (Ind-OCH<sub>3</sub>), 43.13 (3C-Ind), 36.00, 35.31, 32.44, 32.16, 31.13, 16.87 (Ind-CH<sub>3</sub>).

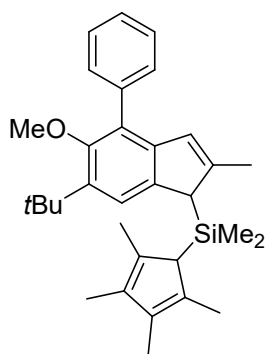


**6-*Tert*-butyl-5-methoxy-4-(3,5-di-*tert*-butyl-4-methoxy)-phenyl-2-ethyl-1*H*-indene.** Using a procedure similar to that described for 6-*tert*-butyl-5-methoxy-4-(3',5'-di-*tert*-butyl-4'-methoxy)-phenyl-2-methyl-1*H*-indene, the desired compound was obtained as a pale yellow crystalline solid (1.1 g, 92%) starting from 6-*tert*-butyl-5-methoxy-4-(3',5'-di-*tert*-butyl-4'-methoxy)-phenyl-2-ethyl-1-indanone **1l** (1.24 g, 0.0027 mol), obtained using a procedure similar to that described for **1i** starting from **1k** (4.0 g, 0.012 mol) and **1c** (5.2 g, 0.020 mol). <sup>1</sup>H NMR (400 MHz, CDCl<sub>3</sub>, 25 °C): δ 7.38 (s, 2H, Ar'-H), 7.24 (s, 1H, Ind-7H), 6.48 (s, 1H, 1H-Ind), 3.75 (s, 3H, 4'-(OCH<sub>3</sub>)-Ph), 3.20 (s, 2H, OCH<sub>3</sub>-Ind), 3.19 (s, 3H, 3H-Ind), 2.45 (qd, *J* = 7.5, 1.7, 2H, CH<sub>2</sub>CH<sub>3</sub>), 1.47 (s, 18H, (CH<sub>3</sub>)<sub>3</sub>'), 1.45 (s, 9H, CH<sub>3</sub>)<sub>3</sub>), 1.17 (t, *J* = 7.5, 3H, CH<sub>2</sub>CH<sub>3</sub>). <sup>13</sup>C{<sup>1</sup>H} NMR (100 MHz, CDCl<sub>3</sub>, 25 °C): δ 158.42, 154.66, 151.83, 143.33, 141.56, 141.15, 140.59, 132.40, 132.25, 128.08, 125.20, 117.14, 64.48 (4'-(OCH<sub>3</sub>)-Ph), 60.28 (OCH<sub>3</sub>-Ind), 41.35 (3C-Ind), 36.00, 35.32, 32.44, 31.13, 24.42 (CH<sub>2</sub>CH<sub>3</sub>), 13.64 (CH<sub>2</sub>CH<sub>3</sub>).



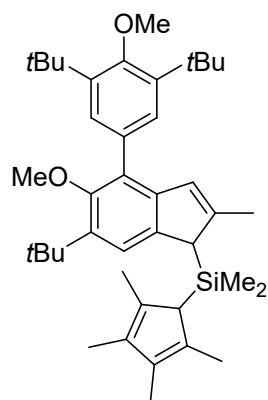
**(6-*Tert*-butyl-4-phenyl-2-methyl-1*H*-inden-1-yl)dimethyl(2,3,4,5-tetramethylcyclopenta-2,4-dien-1-yl)silane (1c).** 6-*Tert*-butyl-4-phenyl-2-methyl-1*H*-indene (2.40 g, 0.0092 mol) was dissolved in Et<sub>2</sub>O (40 mL) and cooled down at -78 °C. To this solution, *n*-BuLi (4.05 mL of a 2.26 M solution in hexane, 0.0092 mol) was added by syringe and the temperature was raised to room temperature. The resulting mixture was stirred overnight. Then, CuCN (0.33 g, 0.0037 mol) was added in at -60 °C. After

10 min of stirring, chlorodimethyl(2,3,4,5-tetramethylcyclopenta-2,4-dien-1-yl)silane (1.67 g, 0.0092 mol) was added dropwise at the same temperature and the resulting mixture was allowed to warm at room temperature and stirred overnight. The mixture was poured into water (50 mL), the organic layer was separated and the aqueous layer was extracted with diethyl ether (2 × 50 mL). The combined organic phases were dried over Na<sub>2</sub>SO<sub>4</sub> and then evaporated to dryness to give a yellow viscous oil (3.80 g, 94%) which was used without further purification. <sup>1</sup>H NMR (CDCl<sub>3</sub>, 400 MHz, 25 °C) (mixture of tautomers): δ 7.55 (d, *J* = 6.8, 3H, Ar-*H*), 7.49–7.41 (m, 5H, Ar-*H*), 7.37–7.31 (m, 2H, Ar-*H*), 6.71 (s, 1H, 3*H*-Ind), 3.66 (s, 1H, 1*H*-Ind), 3.24 (s, 1H, Cp-*H*), 2.22 (s, 3H, 2-CH<sub>3</sub>-Ind), 2.01 (d, *J* = 17.2, 6H, (CH<sub>3</sub>)<sub>2</sub>-Cp), 1.85 (d, *J* = 4.9, 6H, (CH<sub>3</sub>)<sub>2</sub>-Cp), 1.37 (s, 9H, C(CH<sub>3</sub>)<sub>3</sub>), -0.26 (d, *J* = 14.8, 6H, Si(CH<sub>3</sub>)<sub>2</sub>). <sup>13</sup>C{<sup>1</sup>H} NMR (CDCl<sub>3</sub>, 100 MHz, 25 °C): δ 147.61, 146.14, 146.03, 142.16, 140.47, 136.87, 136.79, 133.24, 129.10, 128.43, 126.68, 125.39, 122.67, 119.67, 47.86 (1-CH-ind), 43.18, 42.53, 34.79, 31.93, 31.88, 31.85, 27.07, 18.18 (2-CH<sub>3</sub>-Ind), 15.03, 14.92 ((CH<sub>3</sub>)<sub>2</sub>-Cp), 11.41 ((CH<sub>3</sub>)<sub>2</sub>-Cp), -5.17 (Si(CH<sub>3</sub>)<sub>2</sub>), -5.20 (Si(CH<sub>3</sub>)<sub>2</sub>). ASAP-MS *m/z* calcd for C<sub>31</sub>H<sub>40</sub>Si: 440.2894, found: 440.2895.

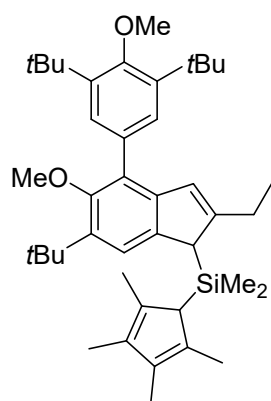


**(2-Methyl-4-phenyl-5-methoxy-6-*tert*-butyl-1*H*-inden-1-yl)dimethyl(2,3,4,5-tetramethylcyclopenta-2,4-dien-1-yl)silane (1d).**

Using a procedure similar to that described for **1c**, proligand **1d** was obtained from 6-*tert*-butyl-5-methoxy-4-phenyl-2-methyl-1*H*-indene (0.62 g, 0.0021 mol), *n*BuLi (0.93 mL of a 2.26 M solution in hexane, 0.0021 mol) and chlorodimethyl(2,3,4,5-tetramethylcyclopenta-2,4-dien-1-yl)silane (0.45 g, 0.0021 mol, 1 equiv). Workup afforded **2d** as a viscous yellow solid (0.90 g, 91%). <sup>1</sup>H NMR (CDCl<sub>3</sub>, 400 MHz, 25 °C): δ 7.54–7.29 (m, 9H, Ar-*H*), 6.41 (s, 1H, 3*H*-Ind), 3.58 (s, 1H, 1*H*-Ind), 3.23 (s, 3H, OCH<sub>3</sub>), 3.20 (s, 1H, Cp-*H*), 2.16 (d, *J* = 1.7, 3H, 2-CH<sub>3</sub>-Ind), 1.99 (d, *J* = 7.7, 9H, (CH<sub>3</sub>)<sub>2</sub>-Cp), 1.84 (s, 9H, (CH<sub>3</sub>)<sub>2</sub>-Cp), 1.44 (s, 11H, C(CH<sub>3</sub>)<sub>3</sub>), -0.24 (d, *J* = 3.2, 6H, Si(CH<sub>3</sub>)<sub>2</sub>). <sup>13</sup>C{<sup>1</sup>H} NMR (CDCl<sub>3</sub>, 100 MHz, 25 °C): δ 155.29, 148.14, 147.52, 143.68, 141.32, 139.93, 138.55, 137.01, 130.36, 130.23, 128.83, 128.45, 128.27, 127.23, 126.64, 125.54, 120.75, 60.59 (OCH<sub>3</sub>-Ind), 47.71 (1-CH-Ind), 35.23, 31.36, 31.29, 31.23, 31.19, 31.13, 27.01, 22.43, 18.06, 16.92, 16.74, 14.97, 14.76, 14.23, 14.17, 11.37, 11.34, -5.06 (Si(CH<sub>3</sub>)<sub>2</sub>), -5.18 (Si(CH<sub>3</sub>)<sub>2</sub>). ASAP-MS *m/z* calcd for C<sub>32</sub>H<sub>42</sub>OSi: 470.2999, found: 470.3001.

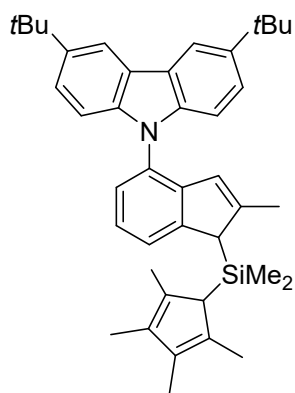


**[2-Methyl-4-(3',5'-di-*tert*-butyl-4'-methoxy)-phenyl-5-methoxy-6-*tert*-butyl-1*H*-inden-1-yl]dimethyl(2,3,4,5-tetramethylcyclopenta-2,4-dien-1-yl)silane (1e).** The same experimental procedure than that used for the previous synthesized proligands was followed starting from 2-methyl-4-(3',5'-di-*tert*-butyl-4'-methoxy)-phenyl-5-methoxy-6-*tert*-butyl-1*H*-indene (0.54 g, 0.0012 mol). A yellow viscous oil was obtained (0.85 g, 98%), which was used on the next step without further purification.  $^1\text{H}$  NMR (400 MHz,  $\text{CDCl}_3$ , 25 °C):  $\delta$  7.36 (d,  $J = 12.7$ , 3H, Ar-*H*), 6.47 (s, 1H, 3*H*-Ind), 3.75 (s, 3H, 4'-( $\text{OCH}_3$ )-Ph), 3.74 (s, 1H, Cp-*H*), 3.57 (s, 1H, 1*H*-Ind), 3.19 (s, 3H,  $\text{OCH}_3$ -Ind), 2.19 (s, 3H, 2- $\text{CH}_3$ -Ind), 2.02 (s, 3H), 1.98 (d,  $J = 7.3$ , 6H,  $(\text{CH}_3)_2$ -Cp), 1.85 (d,  $J = 4.4$ , 6H,  $(\text{CH}_3)_2$ -Cp), 1.82 (s, 3H), 1.47 (s, 24H,  $\text{C}(\text{CH}_3)_3$ ), 1.44 (s, 14H,  $\text{C}(\text{CH}_3)_3$ ), -0.22 (d,  $J = 6.4$ , 6H,  $\text{Si}(\text{CH}_3)_2$ ).  $^{13}\text{C}\{^1\text{H}\}$  NMR (100 MHz,  $\text{CDCl}_3$ , 25 °C):  $\delta$  158.22, 155.53, 147.76, 143.70, 143.06, 139.77, 137.07, 132.44, 128.79, 127.61, 125.96, 120.35, 68.12 (CH-Cp), 64.48 (4'-( $\text{OCH}_3$ )-Ph), 60.09 ( $\text{OCH}_3$ -Ind), 47.65 (1-CH-Ind), 35.94, 35.29, 32.45, 32.27, 31.38, 25.77, 18.23 (2- $\text{CH}_3$ -Ind), 15.01, 14.81 ( $(\text{CH}_3)_2$ -Cp), 11.41 ( $(\text{CH}_3)_2$ -Cp), -4.99 ( $\text{Si}(\text{CH}_3)_2$ ), -5.05 ( $\text{Si}(\text{CH}_3)_2$ ). ASAP-MS  $m/z$  calcd for  $\text{C}_{41}\text{H}_{60}\text{O}_2\text{Si}$ : 612.4357, found: 612.4359.



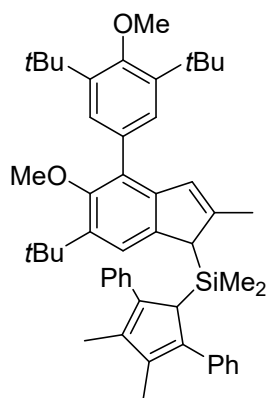
**[2-Ethyl-4-(3',5'-di-*tert*-butyl-4'-methoxy)-phenyl-5-methoxy-6-*tert*-butyl-1*H*-inden-1-yl]dimethyl(2,3,4,5-tetramethylcyclopenta-2,4-dien-1-yl)silane (1f).** Using a procedure similar to that described for the previous synthesized proligands, the desired compound was obtained starting from 6-*tert*-butyl-5-methoxy-4-(3',5'-di-*tert*-butyl-4'-methoxy)-phenyl-2-ethyl-1*H*-indene (0.60 g, 0.0014 mol). A yellow viscous oil was obtained (0.95 g, 84%), which was used on the next step without further purification.  $^1\text{H}$  NMR (400 MHz,  $\text{CDCl}_3$ , 25 °C):  $\delta$  7.42–7.34 (m, 3H, Ar-*H*), 6.54–6.45 (m, 1H, 3*H*-Ind), 3.75 (d,  $J = 2.7$ , 3H, 4'-( $\text{OCH}_3$ )-Ph), 3.74 (s, 1H, Cp-*H*), 3.65 (s, 1H, 1*H*-Ind), 3.18 (s, 3H,  $\text{OCH}_3$ -Ind), 2.64–2.38 (m, 2H,  $\text{CH}_2\text{CH}_3$ ), 2.01 (s, 3H), 1.96 (s, 6H), 1.83 (t,  $J = 5.8$ , 6H), 1.53–1.39 (m, 36H,  $\text{C}(\text{CH}_3)_3$ ), 1.16 (td,  $J = 7.5$ , 2.8, 3H,  $\text{CH}_2\text{CH}_3$ ), 0.21 (s, 1H), 0.03 (s, 1H), -0.04 (s, 2H,  $\text{Si}(\text{CH}_3)_2$ ), -0.24 (d,  $J = 9.0$ , 4H,  $\text{Si}(\text{CH}_3)_2$ ).  $^{13}\text{C}\{^1\text{H}\}$  NMR ( $\text{CDCl}_3$ , 100 MHz, 25 °C):  $\delta$  158.33, 155.88, 154.64, 153.53, 151.83, 143.32, 143.17, 143.02,

141.55, 141.14, 140.58, 139.14, 138.65, 138.34, 137.50, 132.38, 132.24, 131.99, 128.86, 128.79, 128.07, 125.19, 124.24, 120.29, 117.13, 64.47 (4'-(OCH<sub>3</sub>)-Ph), 60.26, 60.15 (OCH<sub>3</sub>-Ind), 55.80, 47.55 (1-CH-Ind), 41.34, 35.99, 35.92, 35.30, 35.25, 32.41, 31.38, 31.28, 31.12, 25.24, 24.41, 13.16, 11.79, 11.39, 9.29, -0.56 (Si(CH<sub>3</sub>)<sub>2</sub>), -0.99 (Si(CH<sub>3</sub>)<sub>2</sub>). ASAP-MS *m/z* calcd for C<sub>42</sub>H<sub>62</sub>O<sub>2</sub>Si: 626.4514, found: 626.4509.



**[4-(3,6'-Di-*tert*-butylcarbazol-9-yl)-2-methyl-1*H*-inden-1-yl]dimethyl(2,3,4,5-tetramethylcyclopenta-2,4-dien-1-yl)silane (1g).**

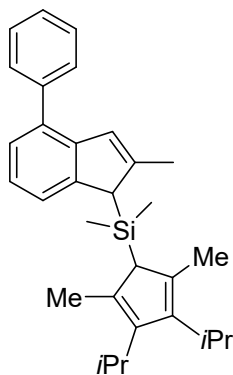
Using a procedure similar to that described for the previous synthesized proligands, the desired compound was obtained from (3,6-di-*tert*-butyl-9-(2-methyl-1*H*-inden-7-yl)-9*H*-carbazole (0.74 g, 0.0018 mol). A crystalline white solid was obtained, which was used on the next step without further purification (1.20 g, 94%). <sup>1</sup>H NMR (400 MHz, CDCl<sub>3</sub>, 25 °C): δ 8.18 (d, *J* = 2.0, 4H), 7.52 (d, *J* = 7.2, 1H), 7.43 (dt, *J* = 8.6, 2.1, 4H), 7.33–7.26 (m, 3H), 7.18 (d, *J* = 8.8, 1H), 7.05 (d, *J* = 8.6, 1H), 6.20 (s, 1H, 3*H*-Ind), 3.82 (s, 1H, 1*H*-Ind), 3.32 (s, 1H, Cp-*H*), 2.16 (s, 3H, 2-CH<sub>3</sub>-Ind), 2.12–2.02 (m, 6H, (CH<sub>3</sub>)<sub>2</sub>-Cp), 1.89 (d, *J* = 7.0, 6H, (CH<sub>3</sub>)<sub>2</sub>-Cp), 1.49 (s, 36H, C(CH<sub>3</sub>)<sub>3</sub>), -0.21 (d, *J* = 7.5, 6H, Si(CH<sub>3</sub>)<sub>2</sub>). <sup>13</sup>C{<sup>1</sup>H} NMR (100 MHz, CDCl<sub>3</sub>, 25 °C): δ 148.97, 147.75, 142.81, 142.42, 142.33, 139.96, 139.91, 137.16, 129.36, 124.47, 124.30, 123.67, 123.56, 123.54, 123.23, 123.21, 122.55, 116.24, 116.19, 109.75, 48.52 (1-CH-Ind), 34.87, 32.22, 18.18 (2-CH<sub>3</sub>-Ind), 17.49, 15.03 ((CH<sub>3</sub>)<sub>2</sub>-Cp), 11.43 ((CH<sub>3</sub>)<sub>2</sub>-Cp), -5.43 (Si(CH<sub>3</sub>)<sub>2</sub>), -5.58 (Si(CH<sub>3</sub>)<sub>2</sub>). ASAP-MS *m/z* calcd for C<sub>41</sub>H<sub>51</sub>NSi: 585.3785, found: 585.3787.



**[2-Methyl-4-(3',5'-di-*tert*-butyl,4'-methoxy)-phenyl-6-*tert*-butyl-1*H*-inden-1-yl]dimethyl(3,4-dimethyl-2,5-diphenylcyclopenta-2,4-dien-1-yl)silane (1h).**

Using a procedure similar to that described for the previous synthesized proligands, the desired compound was obtained from 6-*tert*-butyl-5-methoxy-4-(3',5'-di-*tert*-butyl-4'-methoxyphenyl)-2-methyl-1*H*-indene (0.50 g, 0.0012 mol). A white solid was obtained (0.70 g, 82%), which was used on the next step without further purification. <sup>1</sup>H NMR (500 MHz, CDCl<sub>3</sub>, 25 °C): δ 7.53–7.21 (m, 25H, Ar-*H*), 6.29 (d, *J* = 1.4,

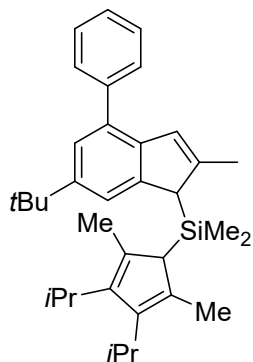
1H, 3*H*-Ind), 4.80–4.73 (bs, 1H), 3.74 (d, *J* = 1.2, 3H, 4'-(OCH<sub>3</sub>)-Ph), 3.17 (d, *J* = 1.1, 3H, OCH<sub>3</sub>-Ind), 2.59 (s, 1H), 2.22 (d, *J* = 8.2, 6H), 2.03 (s, 3H), 1.53 (d, *J* = 1.2, 9H, (CH<sub>3</sub>)<sub>2</sub>-Cp), 1.45 (d, *J* = 1.2, 18H, C(CH<sub>3</sub>)<sub>3</sub>), -0.85 (d, *J* = 8.2, 6H, Si(CH<sub>3</sub>)<sub>2</sub>). <sup>13</sup>C{<sup>1</sup>H} NMR (100 MHz, CDCl<sub>3</sub>, 25 °C): δ 158.13, 155.24, 147.68, 143.44, 142.95, 141.15, 140.85, 139.96, 139.89, 138.61, 138.53, 138.49, 138.30, 138.18, 137.94, 136.74, 132.36, 129.73, 129.56, 129.40, 128.68, 128.55, 128.38, 128.00, 127.38, 126.52, 126.06, 125.37, 119.90, 64.41 (4'-(OCH<sub>3</sub>)-Ph), 60.03 (OCH<sub>3</sub>-ind), 54.20, 51.38, 46.01 (1-CH-Ind), 35.87, 35.27, 32.40, 32.29, 31.43, 17.91, 12.72, 12.69, 12.58, -1.70 (Si(CH<sub>3</sub>)<sub>2</sub>), -6.47 (Si(CH<sub>3</sub>)<sub>2</sub>), -7.01 (Si(CH<sub>3</sub>)<sub>2</sub>). ASAP-MS *m/z* calcd for C<sub>51</sub>H<sub>64</sub>O<sub>2</sub>Si: 736.4670, found: 736.4669.



**(2-Methyl-4-phenyl-1*H*-inden-1-yl)dimethyl(3,4-diisopropyl-2,5-**

**dimethylcyclopenta-2,4-dien-1-yl)silane (1i).** Using a procedure similar to that described above for the previous synthesized proligands, **1i** was isolated as a viscous yellow oil (2.4 g, 42%). <sup>1</sup>H NMR (400 MHz, CDCl<sub>3</sub>, 25 °C): 7.57–7.49 (m, 2H, Ar-*H*), 7.49–7.41 (m, 3H, Ar-*H*), 7.41–7.28 (m, 2H, Ar-*H*), 7.17 (dt, *J* = 14.8, 7.5, 1H, Ar-*H*), 6.80–6.52 (m, 1H, 3*H*-Ind), 4.21–3.78 (m, 1H), 3.52–3.29 (m, 2H), 3.04–2.93 (m, 1H), 2.27 (s, 2H), 2.15 (d, *J* = 3.9, 1H), 2.09 (d, *J* = 7.7, 2H), 2.00–1.43 (m, 5H), 1.25 (dd, *J* = 7.2, 3.8, 5H), 1.12–1.08 (m, 2H), 1.03–0.91 (m, 8H), 0.76 (s, 1H), 0.35–0.04 m, -0.29 d, *J* = 11.4, 6H, Si(CH<sub>3</sub>)<sub>2</sub>). EI-MS *m/z*: [M]<sup>+</sup>

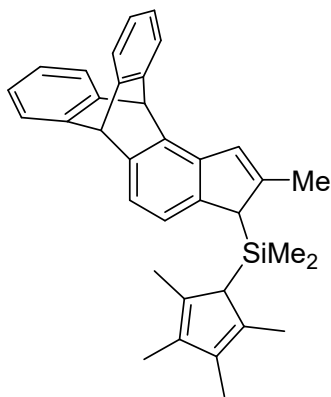
440.



**(6-*Tert*-butyl-2-methyl-4-phenyl-1*H*-inden-1-yl)dimethyl(3,4-**

**diisopropyl-2,5-dimethylcyclopenta-2,4-dien-1-yl)silane (1j).** Using a procedure similar to that described above for the previous synthesized proligands, was obtained as a white solid (0.96 g, 54%). <sup>1</sup>H NMR (400 MHz, CDCl<sub>3</sub>, 25 °C): 7.58 (d, *J* = 7.5, 2H, Ar-*H*), 7.49 (d, *J* = 7.1, 2H, Ar-*H*), 7.36 (d, *J* = 7.2, 2H, Ar-*H*), 7.31 (d, *J* = 1.8, 1H, Ar-*H*), 6.75 (d, *J* = 14.0, 1H, 3*H*-Ind), 3.73 (d, *J* = 31.5, 1H, 1*H*-Ind), 3.40 (d, *J* = 62.1, 1H,

Cp-*H*), 3.00 (dddd, *J* = 14.8, 12.2, 6.9, 3.5, 2H, CH(CH<sub>3</sub>)<sub>2</sub>), 2.25 (d, *J* = 27.8, 3H, Cp-CH<sub>3</sub>), 2.11 (d, *J* = 3.3, 3H, 2-CH<sub>3</sub>-Ind), 1.46 (d, *J* = 13.5, 3H, Cp-CH<sub>3</sub>), 1.41 (s, 9H, C(CH<sub>3</sub>)<sub>3</sub>), 1.28 (td, *J* = 8.0, 5.4, 12H, CH(CH<sub>3</sub>)<sub>2</sub>), -0.25 (d, *J* = 8.4, 6H, Si(CH<sub>3</sub>)<sub>2</sub>).

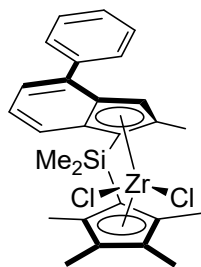


**Dimethyl((6r,11s)-2-methyl-6,11-dihydro-3H-6,11-[1,2]benzenocyclopenta[a]anthracen-3-yl)(2,3,4,5-**

**tetramethylcyclopenta-2,4-dien-1-yl)silane (1k).** Using a procedure similar to that described for **1c**, proligand **1k** was obtained from (6r,11s)-2-methyl-6,11-dihydro-1H-6,11-

[1,2]benzenocyclopenta[a]anthracene (0.960 g, 3.13 mmol), *n*-BuLi (1.4 mL, 3.44 mmol, 2.5 M in hexanes) and chlorodimethyl(2,3,4,5-tetramethylcyclopenta-2,4-dien-1-yl)silane. The purification was performed by column chromatography (4:1 cyclohexane/CH<sub>2</sub>Cl<sub>2</sub>),

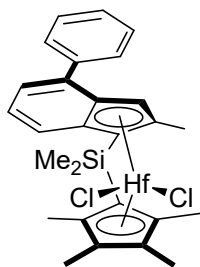
affording the desired product as a slightly yellow powder (0.380 g, 25%) as a mixture of tautomers. <sup>1</sup>H NMR (400 MHz, CDCl<sub>3</sub>, 25 °C): δ 7.42–7.31 (m, 4H), 7.16 (d, *J* = 7.5, 1H), 7.04 (d, *J* = 7.5, 1H), 7.02–6.87 (m, 4H), 5.63 (s, 1H), 5.43 (s, 1H), 3.46 (s, 1H), 2.71 (s, 2H), 2.29 (s, 2H), 1.89 (s, 6H), 1.78 (s, 6H), 0.36 (s, 3H), 0.06 (s, 3H). ASAP-MS *m/z* calcd. for C<sub>35</sub>H<sub>37</sub>Si: 485.2659 found: 485.2647.



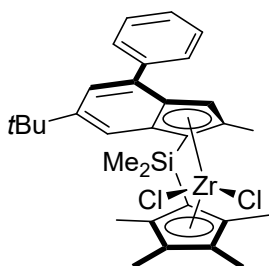
**Synthesis of 2b-Zr.** Following the literature procedure,<sup>12</sup> *n*-BuLi (2.30 mL of a 2.26 M solution in hexanes, 0.0052 mol) was added dropwise to a solution of **1b** (1.00 g, 0.0026 mol) in Et<sub>2</sub>O (30 mL) at –78 °C; the resulting mixture was stirred overnight. To this solution, ZrCl<sub>4</sub> (0.61 g, 0.0026 mol) was added in at –80 °C and the resulting mixture was allowed to warm at room temperature and stirred overnight.

The mixture was evaporated to dryness, and dichloromethane/heptane (40 mL, 1:1 *v/v*) was added and the precipitated LiCl was filtered *via* cannula to give an orange solution. The latter was concentrated to ca. 1/3 *v*; a yellow microcrystalline powder formed which was separated *via* cannula filtration from the solution and then dried under vacuum (0.60 g, 42%). <sup>1</sup>H NMR (400 MHz, CDCl<sub>3</sub>, 25 °C): δ 7.71–7.65 (m, 2H, Ar-*H*), 7.57 (d, *J* = 8.7, 1H, Ar-*H*), 7.46 (t, *J* = 7.5, 3H, Ar-*H*), 7.37 (t, *J* = 7.4, 2H, Ar-*H*), 7.31 (s, 1H, 3*H*-Ind), 7.09–7.02 (m, 2H, Ar-*H*), 2.30 (s, 3H, C-CH<sub>3</sub>), 2.09 (s, 3H, Cp-CH<sub>3</sub>), 2.01 (s, 3H, Cp-CH<sub>3</sub>), 1.92 (d, *J* = 10.2, 6H, Cp-CH<sub>3</sub>), 1.22 (s, 3H, Si-CH<sub>3</sub>), 1.11 (s, 3H, Si-CH<sub>3</sub>). <sup>13</sup>C{<sup>1</sup>H} NMR (125 MHz, CD<sub>2</sub>Cl<sub>2</sub>, 25 °C): δ 139.87, 137.85, 135.52, 134.61, 133.73, 128.62, 128.50, 128.31, 127.85, 127.61, 125.96, 125.67, 124.66, 94.49 (Si-*C*(Cp)), 83.87 (Si-*C*(Ind)), 18.03 (Ind-CH<sub>3</sub>), 15.71 (CH<sub>3</sub>-Cp), 15.44 (CH<sub>3</sub>-Cp),

12.27 (CH<sub>3</sub>-Cp), 11.89 (CH<sub>3</sub>-Cp), 2.82 (Si-CH<sub>3</sub>), 2.73 (Si-CH<sub>3</sub>). ASAP-MS *m/z* calcd for C<sub>27</sub>H<sub>30</sub>Cl<sub>2</sub>SiZr [M+H]<sup>+</sup>: 542.0541, found: 542.0541.

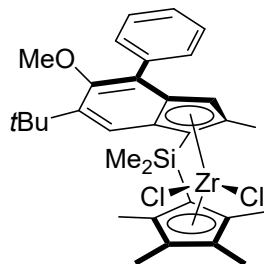


**Synthesis of 2b-Hf.** Using a procedure similar to that described above for **2b-Zr**, complex **2b-Hf** was synthesized from **1b** (1.00 g, 0.0026 mol), *n*BuLi (2.30 mL of a 2.26 M solution in hexanes, 0.0052 mol), HfCl<sub>4</sub> (0.84 g, 0.0026 mol) and isolated as a yellow microcrystalline powder (0.49 g, 30%). <sup>1</sup>H NMR (400 MHz, CDCl<sub>3</sub>, 25 °C) δ 7.68 (d, *J* = 7.0, 2H, Ar-*H*), 7.60 (d, *J* = 8.8, 1H, Ar-*H*), 7.45 (t, *J* = 7.5, 2H, Ar-*H*), 7.37 (t, *J* = 7.4, 1H, Ar-*H*), 7.28 (d, *J* = 6.8, 1H, Ar-*H*), 7.03 (dd, *J* = 8.7, 6.9, 1H, Ar-*H*), 6.96 (bs, 1H, 3*H*-Ind), 2.39 (s, 3H, C-CH<sub>3</sub>), 2.20 (s, 3H, Cp-CH<sub>3</sub>), 2.03 (d, *J* = 5.5, 6H, Cp-CH<sub>3</sub>), 1.93 (s, 3H, Cp-CH<sub>3</sub>), 1.22 (s, 3H, Si-CH<sub>3</sub>), 1.11 (s, 3H, Si-CH<sub>3</sub>). <sup>13</sup>C{<sup>1</sup>H} NMR (125 MHz, CDCl<sub>3</sub>, 25 °C): δ 140.05, 137.91, 136.80, 133.74, 133.39, 133.26, 128.86, 128.68, 127.71, 125.95, 125.15, 124.67, 124.59, 124.48, 124.23, 118.84, 96.44 (Si-C(Cp)), 84.55 (Si-C(Ind)), 18.25 (Ind-CH<sub>3</sub>), 15.75 (CH<sub>3</sub>-Cp), 15.49 (CH<sub>3</sub>-Cp), 12.49 (CH<sub>3</sub>-Cp), 12.12 (CH<sub>3</sub>-Cp), 3.26 (Si-CH<sub>3</sub>), 3.14 (Si-CH<sub>3</sub>). ASAP-MS *m/z* calcd for C<sub>27</sub>H<sub>30</sub>Cl<sub>2</sub>HfZr [M+H]<sup>+</sup>: 632.0959, found: 632.0942.

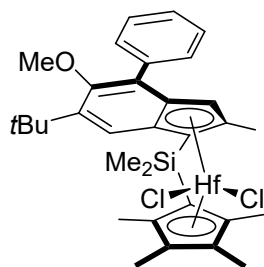


**Synthesis of 2c-Zr.** Using a procedure similar to that described above for **2b-Zr**, complex **2c-Zr** was synthesized from *n*-BuLi (2.00 mL of a 2.26 M solution in hexanes, 0.0045 mol), **1c** (1.00 g, 0.0023 mol) and ZrCl<sub>4</sub> (0.53 g, 0.0023 mol). After workup, **2c-Zr** was isolated as a yellow microcrystalline powder (0.62 g, 45%). <sup>1</sup>H NMR (CDCl<sub>3</sub>, 400 MHz, 25 °C): δ 7.69 (d, *J* = 7.0, 2H, Ar-*H*), 7.51–7.43 (m, 3H, Ar-*H*), 7.41 (d, *J* = 1.6, 1H, Ar-*H*), 7.37 (t, *J* = 7.3, 1H, Ar-*H*), 6.99 (s, 1H, 3*H*-Ind), 2.29 (s, 3H, C-CH<sub>3</sub>), 2.09 (s, 3H, Cp-CH<sub>3</sub>), 2.01 (s, 3H, Cp-CH<sub>3</sub>), 1.93 (d, *J* = 9.3, 6H, Cp-CH<sub>3</sub>), 1.31 (s, 9H, (CH<sub>3</sub>)<sub>3</sub>), 1.24 (s, 3H, Si-CH<sub>3</sub>), 1.11 (s, 3H, Si-CH<sub>3</sub>). <sup>13</sup>C{<sup>1</sup>H} NMR (100 MHz, CDCl<sub>3</sub>, 25 °C): δ 147.90, 140.38, 137.73, 137.62, 135.08, 134.59, 132.15, 128.88, 128.69, 127.67, 127.38, 126.58, 126.01, 120.75, 118.89, 94.09 (Si-C(Cp)), 83.03 (Si-C(Ind)), 35.20 C(CH<sub>3</sub>)<sub>3</sub>, 30.97 (CH<sub>3</sub>)<sub>3</sub>, 18.22 (ind-CH<sub>3</sub>), 16.18 (CH<sub>3</sub>-Cp), 15.65 (CH<sub>3</sub>-Cp), 12.66, 12.33 (CH<sub>3</sub>-Cp), 3.34 (Si-CH<sub>3</sub>), 3.27 (Si-CH<sub>3</sub>). ASAP-MS *m/z* calcd for C<sub>31</sub>H<sub>38</sub>Cl<sub>2</sub>SiZr [M+H]<sup>+</sup>: 598.1167, found: 598.1167.

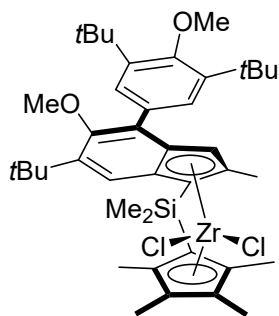




**Synthesis of 2d-Zr.** Using a procedure similar to that described above for metallocene complex **2b-Zr**, complex **2d-Zr** was synthesized from **1d** (0.9 g, 0.0019 mmol) and isolated as a yellow microcrystalline powder (0.60 g, 50%). <sup>1</sup>H NMR (400 MHz, CDCl<sub>3</sub>, 25 °C): δ 7.66 (s, 1H, Ar-*H*), 7.50–7.42 (m, 3H, Ar-*H*), 7.35 (t, *J* = 7.5, 1H, Ar-*H*), 6.66 (s, 1H, 3*H*-Ind), 3.37 (s, 3H, OCH<sub>3</sub>), 2.21 (s, 3H, C-CH<sub>3</sub>), 2.07 (s, 3H, Cp-CH<sub>3</sub>), 2.02 (s, 3H, Cp-CH<sub>3</sub>), 1.93 (d, *J* = 13.2, 6H, Cp-CH<sub>3</sub>), 1.37 (s, 9H, (CH<sub>3</sub>)<sub>3</sub>), 1.20 (s, 3H, Si-CH<sub>3</sub>), 1.08 (s, 3H, Si-CH<sub>3</sub>). <sup>13</sup>C{<sup>1</sup>H} NMR (100 MHz, CDCl<sub>3</sub>, 25 °C): δ 159.49, 143.44, 137.59, 137.27, 135.56, 135.13, 134.94, 129.95, 128.68, 127.37, 127.12, 126.72, 121.98, 121.33, 120.21, 93.84 (Si-C(Cp)), 82.43(Si-C(Ind)), 62.72 (OCH<sub>3</sub>), 35.88 C(CH<sub>3</sub>)<sub>3</sub>, 30.52 (CH<sub>3</sub>)<sub>3</sub>, 18.19 (Ind-CH<sub>3</sub>), 16.06 (CH<sub>3</sub>-Cp), 15.64 (CH<sub>3</sub>-Cp), 12.68 (CH<sub>3</sub>-Cp), 12.32 (CH<sub>3</sub>-Cp), 3.23 (Si-CH<sub>3</sub>), 3.10 (Si-CH<sub>3</sub>). ASAP-MS *m/z* calcd for C<sub>32</sub>H<sub>40</sub>Cl<sub>2</sub>OSiZr [M+H]<sup>+</sup>: 628.1273, found: 628.1273.

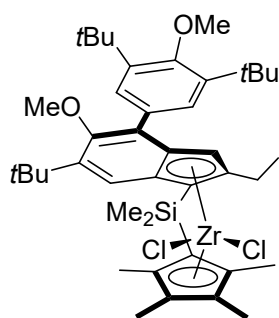


**Synthesis of 2d-Hf.** Using a procedure similar to that described above for **2b-Zr**, complex **2d-Hf** was synthesized from **1d** (1.35 g, 0.0026 mol) and isolated as a yellow microcrystalline powder (0.45 g, 23%). <sup>1</sup>H NMR (400 MHz, CDCl<sub>3</sub>, 25 °C) δ 7.65 (s, 2H, Ar-*H*), 7.51–7.40 (m, 3H, Ar-*H*), 7.34 (t, *J* = 7.4, 1H, Ar-*H*), 6.57 (s, 1H, 3*H*-Ind), 3.36 (s, 3H, OCH<sub>3</sub>), 2.30 (s, 3H, C-CH<sub>3</sub>), 2.17 (s, 3H, Cp-CH<sub>3</sub>), 2.05 (s, 3H, Cp-CH<sub>3</sub>), 1.98 (d, *J* = 13.4, 6H, Cp-CH<sub>3</sub>), 1.38 (s, 9H, (CH<sub>3</sub>)<sub>3</sub>), 1.19 (s, 3H, Si-CH<sub>3</sub>), 1.08 (s, 3H, Si-CH<sub>3</sub>). <sup>13</sup>C{<sup>1</sup>H} NMR (125 MHz, CDCl<sub>3</sub>, 25 °C): δ 159.39, 143.00, 137.38, 136.22, 135.02, 133.36, 132.97, 129.95, 128.65, 127.32, 126.25, 124.38, 123.65, 121.40, 120.36, 118.31, 95.99 (Si-C(Cp)), 83.39 (Si-C(Ind)), 62.71 (OCH<sub>3</sub>), 53.56 C(CH<sub>3</sub>)<sub>3</sub>, 35.83 (CH<sub>3</sub>)<sub>3</sub>, 30.55 (CH<sub>3</sub>)<sub>3</sub>, 18.09 (Ind-CH<sub>3</sub>), 15.79 (CH<sub>3</sub>-Cp), 15.38 (CH<sub>3</sub>-Cp), 12.51 (CH<sub>3</sub>-Cp), 12.15 (CH<sub>3</sub>-Cp), 3.21 (Si-CH<sub>3</sub>), 3.06 (Si-CH<sub>3</sub>). ASAP-MS *m/z* calcd for C<sub>32</sub>H<sub>40</sub>Cl<sub>2</sub>HfOSi [M+H]<sup>+</sup>: 718.1691, found: 718.1674.



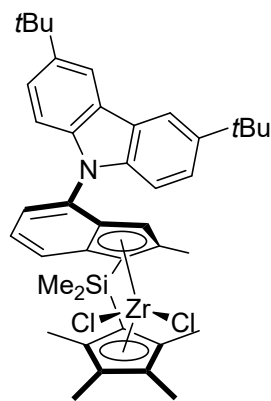
**Synthesis of 2e-Zr.** Using a procedure similar to that described above for **2b-Zr**, complex **2e-Zr** was synthesized from **1e** (0.80 g, 0.0013 mol), *n*BuLi (1.16 mL of a 2.25 M solution in hexanes, 0.0026 mol) and ZrCl<sub>4</sub> (0.31 g, 0.0013 mol) and isolated as a yellow microcrystalline powder (0.30 g, 30%). <sup>1</sup>H NMR (400 MHz, CDCl<sub>3</sub>, 25 °C): δ 7.41 (s, 3H, Ar-*H*),

6.67 (s, 1H, 3*H*-Ind), 3.73 (s, 3H, ind-OCH<sub>3</sub>), 3.32 (s, 3H, 4'-(OCH<sub>3</sub>)-Ph), 2.22 (s, 3H, C-CH<sub>3</sub>), 2.04 (d, *J* = 17.9, 6H, Cp-CH<sub>3</sub>), 1.91 (d, *J* = 12.4, 6H, Cp-CH<sub>3</sub>), 1.43 (s, 21H, (CH<sub>3</sub>)<sub>3</sub>), 1.36 (s, 9H, (CH<sub>3</sub>)<sub>3</sub>), 1.19 (s, 3H, Si-CH<sub>3</sub>), 1.07 (s, 3H, Si-CH<sub>3</sub>). <sup>13</sup>C{<sup>1</sup>H} NMR (100 MHz, CDCl<sub>3</sub>, 25 °C): δ 159.47 (C-OCH<sub>3</sub>), 158.61 (C-OCH<sub>3</sub>), 143.37, 137.35, 135.89, 135.00, 134.72, 131.19, 127.31, 126.97, 126.75, 121.91, 120.73, 120.13, 93.80 (Si-C(Cp)), 82.45 (Si-C(Ind)), 64.44 (O-CH<sub>3</sub>), 62.22 (O-CH<sub>3</sub>), 35.87, 32.47, 32.05, 30.51, 22.86, 18.34 (Ind-CH<sub>3</sub>), 16.10 (CH<sub>3</sub>-Cp), 15.65 (CH<sub>3</sub>-Cp), 14.28 (CH<sub>3</sub>-Cp), 12.66 (CH<sub>3</sub>-Cp), 12.35 (CH<sub>3</sub>-Cp), 3.25 (Si-CH<sub>3</sub>), 3.14 (Si-CH<sub>3</sub>). ASAP-MS *m/z* calcd for C<sub>41</sub>H<sub>58</sub>Cl<sub>2</sub>O<sub>2</sub>SiZr [M+H]<sup>+</sup>: 770.2630, found: 770.2630.



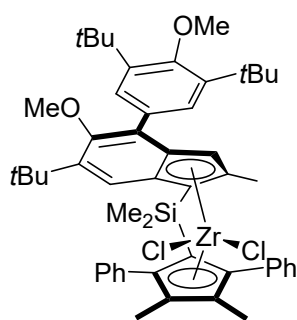
**Synthesis of 2f-Zr.** Using a procedure similar to that described above for **2b-Zr**, complex **2f-Zr** was synthesized from **1f** (0.95 g, 0.0015 mol), *n*BuLi (1.21 mL of a 2.5 M solution in hexanes, 0.0031 mol) and ZrCl<sub>4</sub> (0.35 g, 0.0015 mol), and isolated as a yellow microcrystalline powder (0.27 g, 23%). <sup>1</sup>H NMR (400 MHz, CDCl<sub>3</sub>, 25 °C): δ 7.56 (s, 2H, Ar-*H*), 7.44 (s, 1H, Ar-*H*), 6.70 (s, 1H, 3*H*-Ind), 3.73 (s, 3H, ind-OCH<sub>3</sub>), 3.30 (s,

3H, 4'-(OCH<sub>3</sub>)-Ph), 2.55 (qt, *J* = 14.4, 7.4, 2H, CH<sub>2</sub>CH<sub>3</sub>), 2.03 (d, *J* = 13.2, 6H, Cp-CH<sub>3</sub>), 1.91 (d, *J* = 12.3, 6H, Cp-CH<sub>3</sub>), 1.46 (s, 18H, (CH<sub>3</sub>)<sub>3</sub>), 1.36 (s, 9H, (CH<sub>3</sub>)<sub>3</sub>), 1.19 (s, 3H, Si-CH<sub>3</sub>), 1.11 (t, *J* = 7.5, 3H, CH<sub>2</sub>CH<sub>3</sub>), 1.06 (s, 3H, Si-CH<sub>3</sub>). <sup>13</sup>C{<sup>1</sup>H} NMR (100 MHz, CDCl<sub>3</sub>, 25 °C): δ 159.51, 158.62, 143.49, 142.08, 137.39, 135.92, 134.73, 131.16, 128.57, 127.36, 127.18, 126.68, 122.20, 120.86, 118.17, 93.60 (Si-C(Cp)), 81.35 (Si-C(Ind)), 64.44 (O-CH<sub>3</sub>), 62.19 (O-CH<sub>3</sub>), 36.13, 35.88, 32.48, 30.51, 25.88, 17.71 (Ind-CH<sub>3</sub>), 16.09 (CH<sub>3</sub>-Cp), 15.60 (CH<sub>3</sub>-Cp), 12.66 (CH<sub>3</sub>-Cp), 12.35 (CH<sub>3</sub>-Cp), 3.30 (Si-CH<sub>3</sub>), 3.27 (Si-CH<sub>3</sub>). ASAP-MS *m/z* calcd for C<sub>42</sub>H<sub>60</sub>Cl<sub>2</sub>O<sub>2</sub>SiZr [M+H]<sup>+</sup>: 784.2781, found: 784.2785.

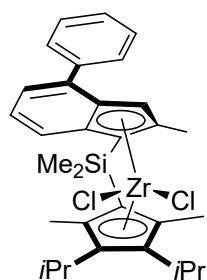


**Synthesis of 2g-Zr.** Using a procedure similar to that described above for **2b-Zr**, complex **2g-Zr** was synthesized from **1g** (1.0 g, 0.0017 mol) and isolated as an orange microcrystalline powder (0.40 g, 34%). <sup>1</sup>H NMR (400 MHz, CDCl<sub>3</sub>, 25 °C): δ <sup>1</sup>H NMR (400 MHz, CDCl<sub>3</sub>) δ 8.12 (d, *J* = 11.7, 2H, cbz-*H*), 8.05 (d, *J* = 8.7, 1H, cbz-*H*), 7.68 (d, *J* = 8.8, 1H, cbz-*H*), 7.53 (d, *J* = 7.2, 1H, Ar-*H*), 7.45 (dd, *J* = 8.8, 2.0, 1H, Ar-*H*), 7.32 (dd, *J* = 8.7, 2.0, 1H, Ar-*H*), 7.15 (t, *J* = 7.9, 1H, Ar-*H*), 6.83 (s, 1H, Ar-

*H*), 6.81 (s, 1H, 3*H*-Ind), 2.31 (s, 3H, C-CH<sub>3</sub>), 2.07 (d, *J* = 13.8, 6H, Cp-CH<sub>3</sub>), 1.97 (d, *J* = 8.7, 6H, Cp-CH<sub>3</sub>), 1.47 (s, 18H, (CH<sub>3</sub>)<sub>3</sub>), 1.28 (s, 3H, Si-CH<sub>3</sub>), 1.14 (s, 3H, Si-CH<sub>3</sub>). <sup>13</sup>C{<sup>1</sup>H} NMR (100 MHz, CDCl<sub>3</sub>, 25 °C): δ 142.95, 142.73, 139.57, 139.27, 138.31, 135.52, 135.25, 134.63, 133.21, 128.54, 128.00, 126.74, 125.12, 124.79, 124.67, 124.15, 123.89, 123.83, 122.99, 119.69, 116.33, 115.82, 112.33, 110.29, 94.46 (Si-C(Cp)), 84.05 (Si-C(Ind)), 34.86, 32.18, 29.18, 18.61 (Ind-CH<sub>3</sub>), 16.16 (CH<sub>3</sub>-Cp), 15.82 (CH<sub>3</sub>-Cp), 14.27 (CH<sub>3</sub>-Cp), 12.71 (CH<sub>3</sub>-Cp), 12.34 (CH<sub>3</sub>-Cp), 3.26 (Si-CH<sub>3</sub>), 3.19 (Si-CH<sub>3</sub>). ASAP-MS *m/z* calcd for C<sub>41</sub>H<sub>49</sub>NCl<sub>2</sub>SiZr [M+H]<sup>+</sup>: 743.2053, found: 743.2058.

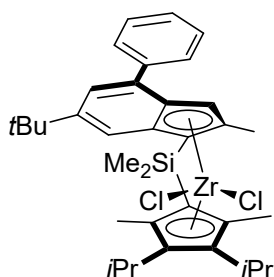


**Synthesis of 2h-Zr.** Using a procedure similar to that described above for **2b-Zr**, complex **2h-Zr** was synthesized from **1h** (0.65 g, 0.00088 mol) and isolated as an orange microcrystalline powder (0.08 g, 10%). <sup>1</sup>H NMR (400 MHz, CDCl<sub>3</sub>, 25 °C): δ <sup>1</sup>H NMR (400 MHz, CDCl<sub>3</sub>) δ 7.75 (s, 1H, Ar-*H*), 7.48–7.28 (m, 8H, Ar-*H*), 7.06 (d, *J* = 5.0, 1H, Ar-*H*), 6.79 (s, 1H, Ar-*H*), 6.67 (bs, *J* = 0.7, 1H, 3*H*-Ind), 3.75 (s, 3H, Ind-OCH<sub>3</sub>), 3.40 (s, 3H, 4'-(OCH<sub>3</sub>)-Ph), 2.06 (s, 3H, C-CH<sub>3</sub>), 1.91 (s, 3H, Cp-CH<sub>3</sub>), 1.68 (s, 3H, Cp-CH<sub>3</sub>), 1.49 (s, 18H, (CH<sub>3</sub>)<sub>3</sub>), 1.22 (s, 9H, (CH<sub>3</sub>)<sub>3</sub>), 0.53 (d, *J* = 14.1, 6H, Si-CH<sub>3</sub>). <sup>13</sup>C{<sup>1</sup>H} NMR (100 MHz, CDCl<sub>3</sub>, 25 °C): δ 160.09, 158.67, 143.76, 137.13, 136.12, 136.03, 135.58, 135.46, 135.39, 134.91, 134.80, 134.18, 131.13, 130.93, 128.94, 128.58, 127.92, 127.51, 127.47, 123.30, 122.86, 121.02, 97.15 (Si-C(Cp)), 82.84 (Si-C(Ind)), 64.43 (O-CH<sub>3</sub>), 62.28 (O-CH<sub>3</sub>), 36.20, 35.80, 32.53, 32.05, 30.08, 29.18, 22.85, 19.09 (Ind-CH<sub>3</sub>), 14.27 (CH<sub>3</sub>-Cp), 13.00 (CH<sub>3</sub>-Cp), 4.54 (Si-CH<sub>3</sub>), 3.48 (Si-CH<sub>3</sub>). ASAP-MS *m/z* calcd for C<sub>51</sub>H<sub>62</sub>Cl<sub>2</sub>O<sub>2</sub>SiZr [M+H]<sup>+</sup>: 894.2938, found: 894.2940.

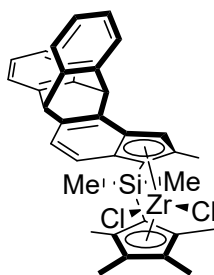


**Synthesis of 2i-Zr.** Using a procedure similar to that described above for **1b-Zr**, complex **2i-Zr** was synthesized from **1i** (0.50 g, 0.0011 mol). The residue was recrystallized from heptane/toluene (5:1 v/v) and obtained as an orange-yellow powder (0.16 g, 27%). <sup>1</sup>H NMR (400 MHz, benzene-*d*<sub>6</sub>, 25 °C): 7.93 (dd, *J* = 7.9, 1.4, 2H, Ar-*H*), 7.44 (d, *J* = 8.7, 1H, Ar-*H*), 7.27 (dd, *J* = 8.4, 7.1, 3H, Ar-*H*), 7.15 (d, *J* = 1.6, 2H, Ar-*H*), 6.85 (dd, *J* = 8.7, 6.9, 1H, 3*H*-Ind), 3.45 (sept, *J* = 7.7, 2H, CH(CH<sub>3</sub>)<sub>2</sub>), 2.09 (d, *J* = 7.0, 6H, Cp-CH<sub>3</sub>), 2.00 (s, 3H, Ind-CH<sub>3</sub>), 1.50 (d,

$J = 7.0$ , 3H,  $\text{CH}(\text{CH}_3)_2$ ), 1.29 (d,  $J = 7.1$ , 3H,  $\text{CH}(\text{CH}_3)_2$ ), 1.21 (d,  $J = 7.4$ , 3H,  $\text{CH}(\text{CH}_3)_2$ ), 1.13 (d,  $J = 7.0$ , 3H,  $\text{CH}(\text{CH}_3)_2$ ), 0.73 (d,  $J = 57.6$ , 6H,  $\text{Si}(\text{CH}_3)_2$ ).  $^{13}\text{C}\{^1\text{H}\}$  NMR (100 MHz, benzene- $d_6$ , 25 °C): 140.16, 138.17, 129.05, 128.56, 128.6, 128.2, 125.88, 125.32, 124.46, 124.16, 97.57 (Si-C(Cp)), 84.68 (Si-C(Ind)), 28.26 ( $\text{CH}(\text{CH}_3)_2$ ), 27.99 ( $\text{CH}(\text{CH}_3)_2$ ), 21.63 ( $\text{CH}(\text{CH}_3)_2$ ), 20.45 ( $\text{CH}(\text{CH}_3)_2$ ), 18.39 (Cp- $\text{CH}_3$ ), 17.83 (Cp- $\text{CH}_3$ ), 15.93 (Ind- $\text{CH}_3$ ), 3.37 ( $\text{Si}(\text{CH}_3)_2$ ), 2.96 ( $\text{Si}(\text{CH}_3)_2$ ). ASAP-MS  $m/z$  calcd for  $\text{C}_{31}\text{H}_{39}\text{Cl}_2\text{SiZr}$   $[\text{M}+\text{H}]^+$ : 599.1240, found: 599.1242.



**Synthesis of 2j-Zr.** Using a procedure similar to that described above for **2b-Zr**, complex **2j-Zr** was synthesized from **1j** (0.96 g, 0.0019 mol). The residue was recrystallized from hot heptane and obtained as pure yellow microcrystalline powder (0.045 g, 5%).  $^1\text{H}$  NMR (400 MHz, benzene- $d_6$ , 25 °C):  $\delta$  8.01–7.91 (m, 2H, Ar- $H$ ), 7.56–7.48 (m, 2H, Ar- $H$ ), 7.29 (t,  $J = 7.7$ , 3H, Ar- $H$ ), 7.11 (s, 1H, 3*H*-Ind), 3.52–3.35 (m, 2H,  $\text{CH}(\text{CH}_3)_2$ ), 2.14 (d,  $J = 7.5$ , 6H, Cp- $\text{CH}_3$ ), 2.02 (s, 3H, Ind- $\text{CH}_3$ ), 1.48 (d,  $J = 7.1$ , 3H,  $\text{CH}(\text{CH}_3)_2$ ), 1.44–1.40 (m, 3H,  $\text{CH}(\text{CH}_3)_2$ ), 1.38 (t,  $J = 2.7$ , 3H,  $\text{CH}(\text{CH}_3)_2$ ), 1.27 (s, 9H,  $\text{C}(\text{CH}_3)_3$ ), 1.16 (d,  $J = 5.6$ , 3H,  $\text{CH}(\text{CH}_3)_2$ ), 0.93 (s, 3H,  $\text{Si}(\text{CH}_3)_2$ ), 0.70 (s, 3H,  $\text{Si}(\text{CH}_3)_2$ ).  $^{13}\text{C}\{^1\text{H}\}$  NMR (100 MHz, benzene- $d_6$ , 25 °C):  $\delta$  146.9, 146.6, 140.56, 137.80, 135.8, 133.7, 129.09, 128.56, 128.3, 128.0, 127.8, 127.6, 127.5, 125.68, 122.6, 120.8, 118.93, 97.36 (Si-C(Cp)), 84.24 (Si-C(Ind)), 31.6 ( $\text{C}(\text{CH}_3)_3$ ), 30.60 ( $\text{C}(\text{CH}_3)_3$ ), 28.25 ( $\text{CH}(\text{CH}_3)_2$ ), 28.02 ( $\text{CH}(\text{CH}_3)_2$ ), 26.7 ( $\text{CH}(\text{CH}_3)_2$ ), 21.5 ( $\text{CH}(\text{CH}_3)_2$ ), 20.4 (Cp- $\text{CH}_3$ ), 18.31 (Cp- $\text{CH}_3$ ), 15.96 (Ind- $\text{CH}_3$ ), 3.54 ( $\text{Si}(\text{CH}_3)_2$ ), 3.07 ( $\text{Si}(\text{CH}_3)_2$ ). ASAP-MS  $m/z$  calcd for  $\text{C}_{35}\text{H}_{47}\text{SiZr}$   $[\text{M}+\text{H}]^+$ : 655.1866, found: 655.1871.



**Synthesis of 2k-Zr.** Using a procedure similar to that described above for **2b-Zr**, complex **2k-Zr** was synthesized from **1k** (0.380 g, 0.78 mmol) and  $\text{ZrCl}_4$  (0.183 g, 0.78 mmol) and isolated as a bright yellow powder (0.185 g, 37%).  $^1\text{H}$  NMR (400 MHz,  $\text{CD}_2\text{Cl}_2$ , 25 °C):  $\delta$  7.47–7.34 (m, 4H), 7.31 (d,  $J = 8.6$  Hz, 1H), 7.19–7.17 (m, 2H), 7.02–6.90 (m, 4H), 5.73 (s, 1H), 5.48 (s, 1H), 2.32 (s, 3H), 2.03 (s, 3H), 1.88 (s, 3H), 1.79 (s, 3H), 1.66 (s, 3H), 1.13 (s, 3H), 1.06 (s, 3H).  $^{13}\text{C}$  NMR (100 MHz,  $\text{CD}_2\text{Cl}_2$ , 25 °C):  $\delta$  146.49, 146.47, 145.49, 145.38, 144.17, 140.67, 137.45, 135.96, 134.26, 132.89, 127.91, 127.73, 127.71, 124.81, 124.71, 124.69, 124.61, 124.45, 123.33, 123.28, 122.55, 122.17, 121.76, 116.54, 94.46, 83.08, 54.20, 51.47,

18.19, 15.64, 15.34, 12.11, 11.76, 2.82, 2.63. ASAP-MS  $m/z$  calcd. for  $C_{35}H_{34}^{35}Cl_2Si^{90}Zr$   $[M+H]^+$ : 642.0848; found: 642.0851.

**Crystal Structure Determination of 2a,b-Zr, 2b-Hf, 2d-Zr,Hf, 2e,f,j,k-Zr.** Diffraction data were collected at 150 K with a D8 VENTURE Bruker AXS diffractometer equipped with a (CMOS) PHOTON 100 detector,  $[MoK\alpha]$  radiation ( $\lambda = 0.71073 \text{ \AA}$ , multilayer monochromator). The structure was solved by dual-space algorithm using the SHELXT program,<sup>14</sup> and then refined with full-matrix least-squares methods based on F2 (SHELXL).<sup>15</sup> For **3j-Zr**, the contribution of the disordered solvent molecules to the calculated structure factors was estimated following the BYPASS algorithm,<sup>16</sup> implemented as the SQUEEZE option in PLATON.<sup>17</sup> All non-hydrogen atoms were refined with anisotropic atomic displacement parameters. H atoms were finally included in their calculated positions and treated as riding on their parent atom with constrained thermal parameters. Crystal data and details of data collection and structure refinement for the different compounds are given in Table S2. Crystal data, details of data collection and structure refinement for all compounds (CCDC 2248323–2248331) can be obtained from the Cambridge Crystallographic Data Centre via [www.ccdc.cam.ac.uk/data\\_request/cif](http://www.ccdc.cam.ac.uk/data_request/cif).

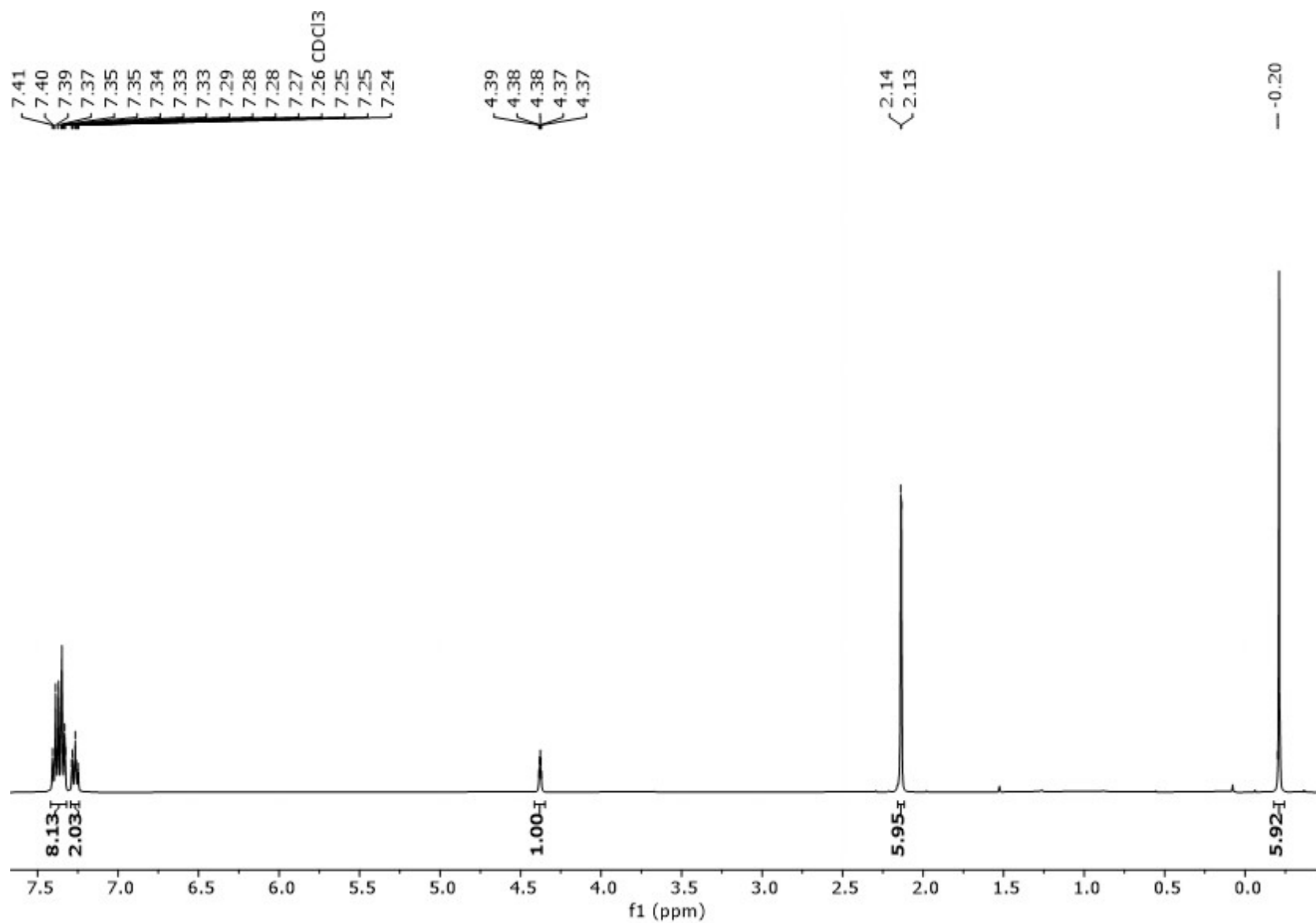


**Figure S1.** <sup>1</sup>H NMR spectrum (400 MHz, 25 °C, CDCl<sub>3</sub>) of chloro-(3,4-dimethyl-2,5-diphenylcyclopenta-2,4-dien-1-yl)dimethylsilane.

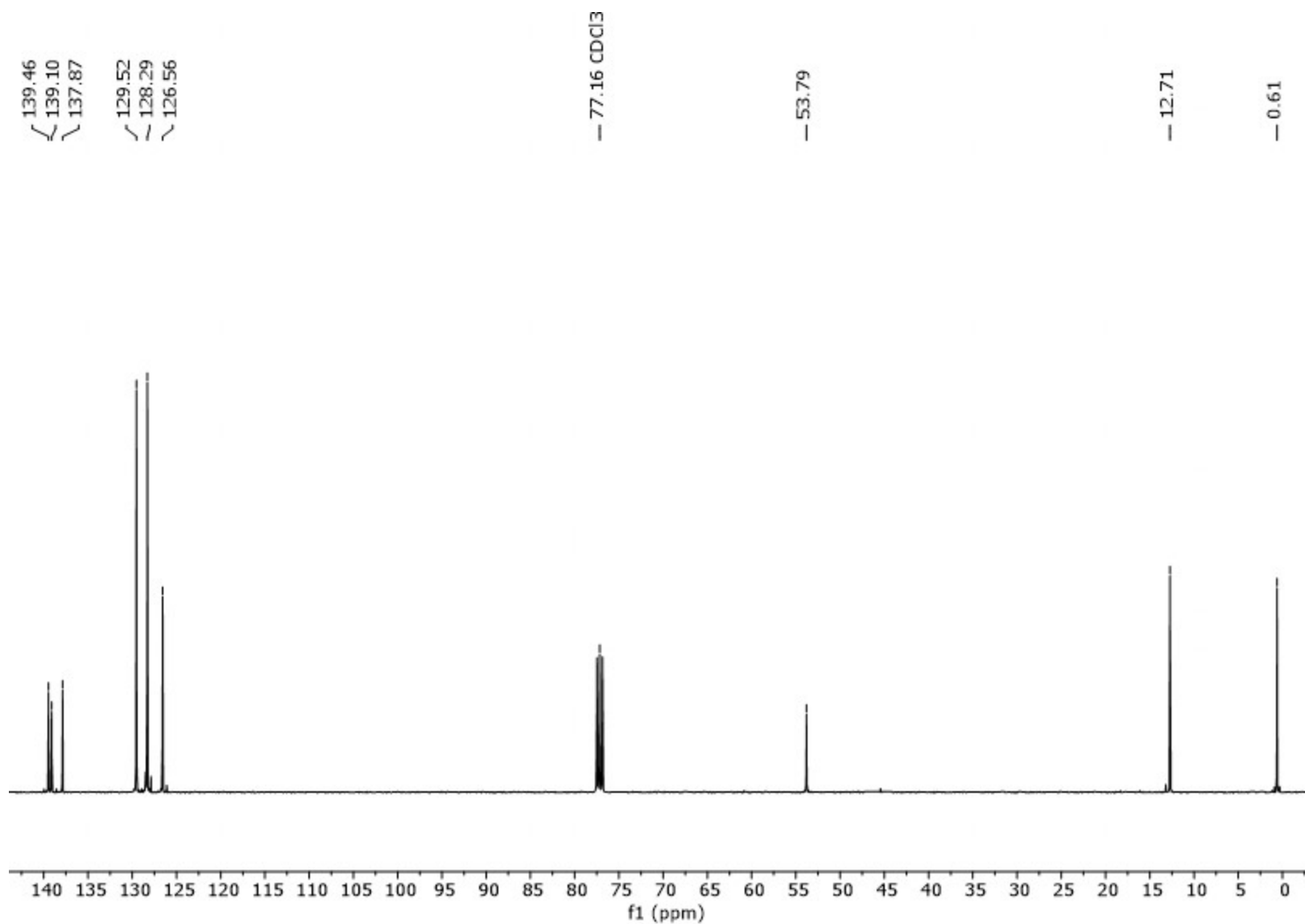


**Figure S2.**  $^{13}\text{C}\{^1\text{H}\}$  NMR spectrum (100 MHz, 25 °C,  $\text{CDCl}_3$ ) of chloro-(3,4-dimethyl-2,5-diphenylcyclopenta-2,4-dien-1-yl)dimethylsilane.

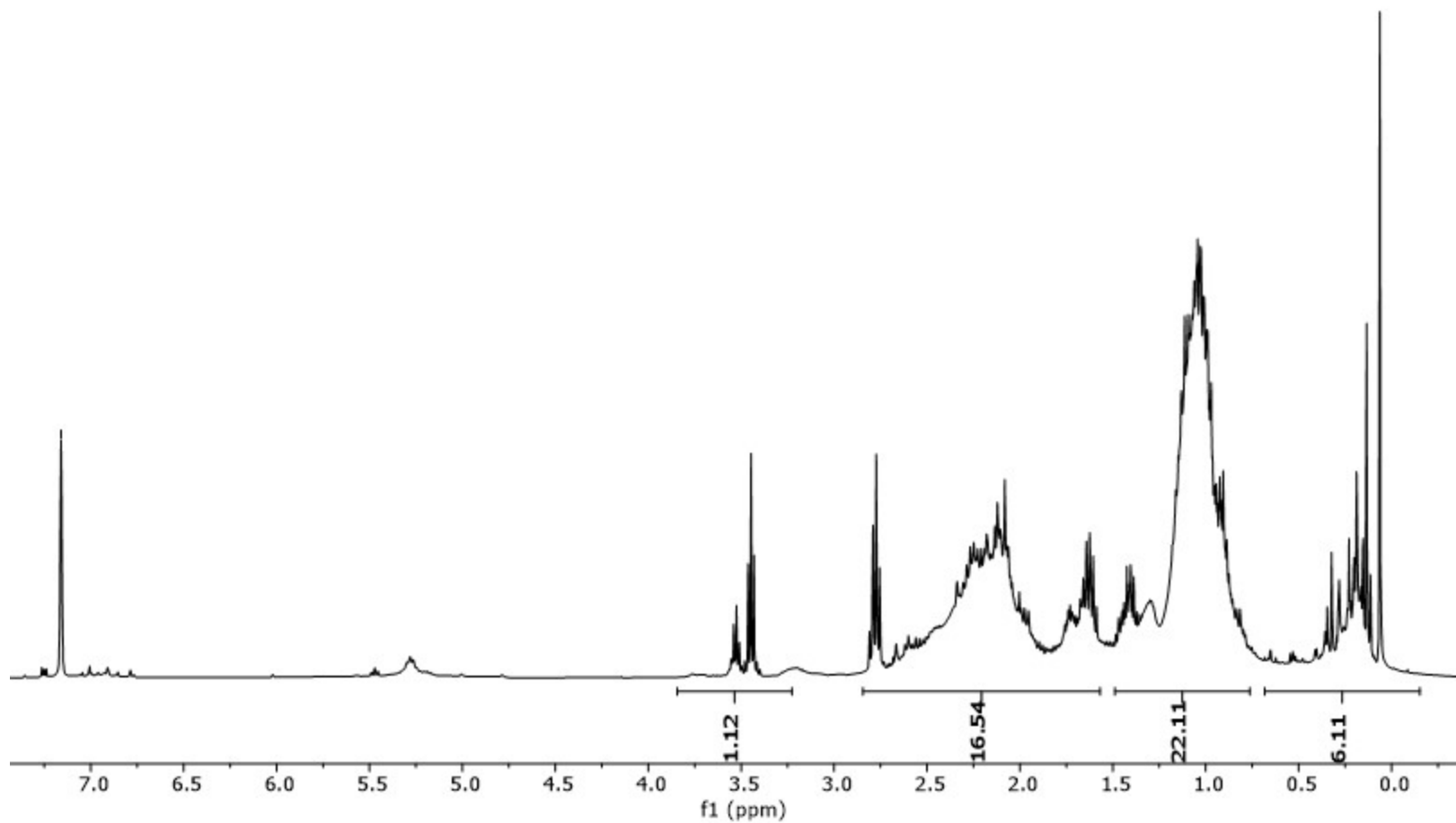


**Figure S3.**  $^1\text{H}$  NMR spectrum (400 MHz, 25 °C,  $\text{CDCl}_3$ ) of chloro(3,4-diisopropyl-2,5-dimethylcyclopenta-2,4-dien-1-yl)dimethylsilane (resulting crude product from the reaction).



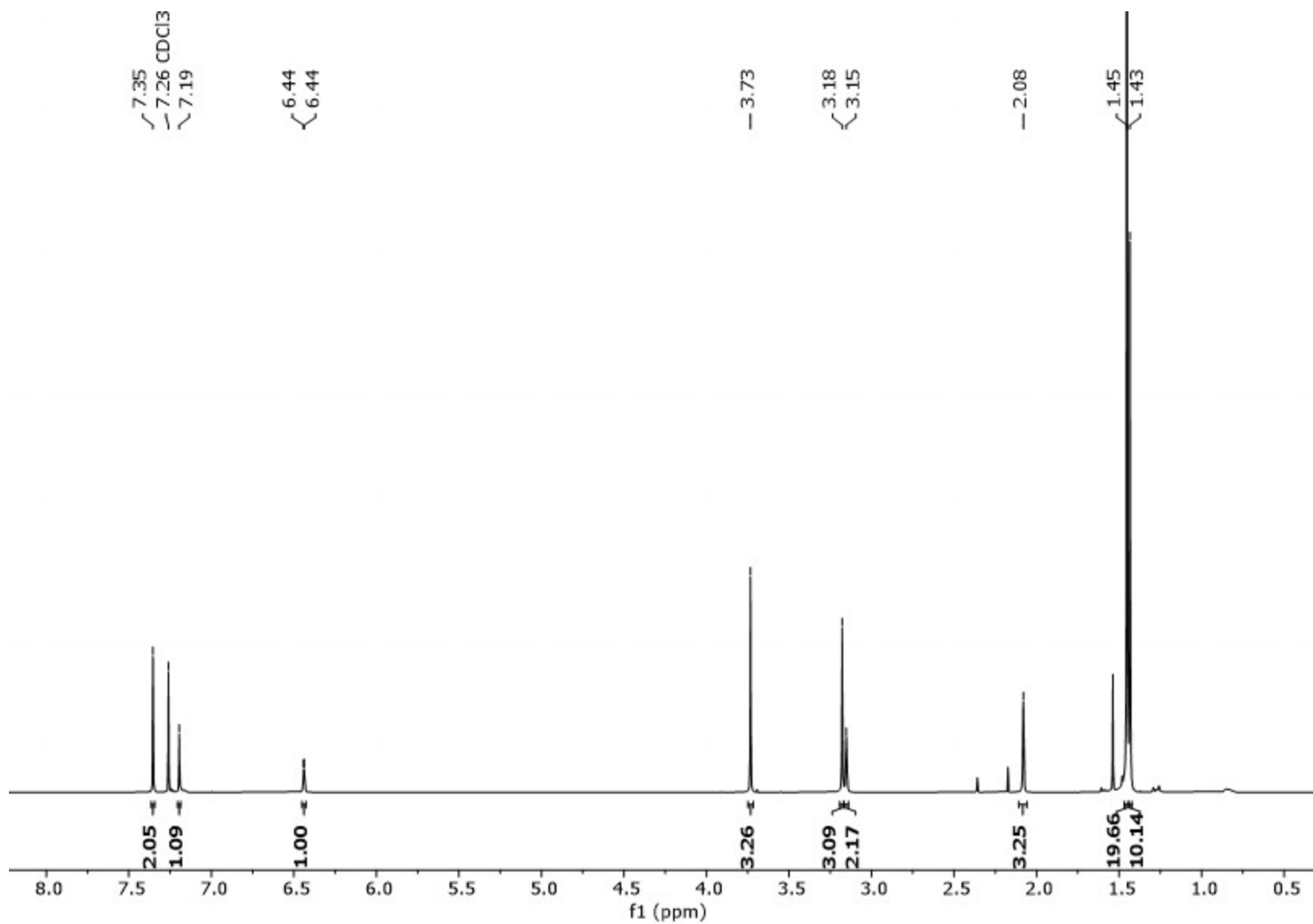


**Figure S4.** <sup>1</sup>H NMR spectrum (400 MHz, 25 °C, CDCl<sub>3</sub>) of 2-methyl-4-(3',5'-di-*tert*-butyl-4'-methoxy)-phenyl-5-methoxy-6-*tert*-butyl-1*H*-indene.

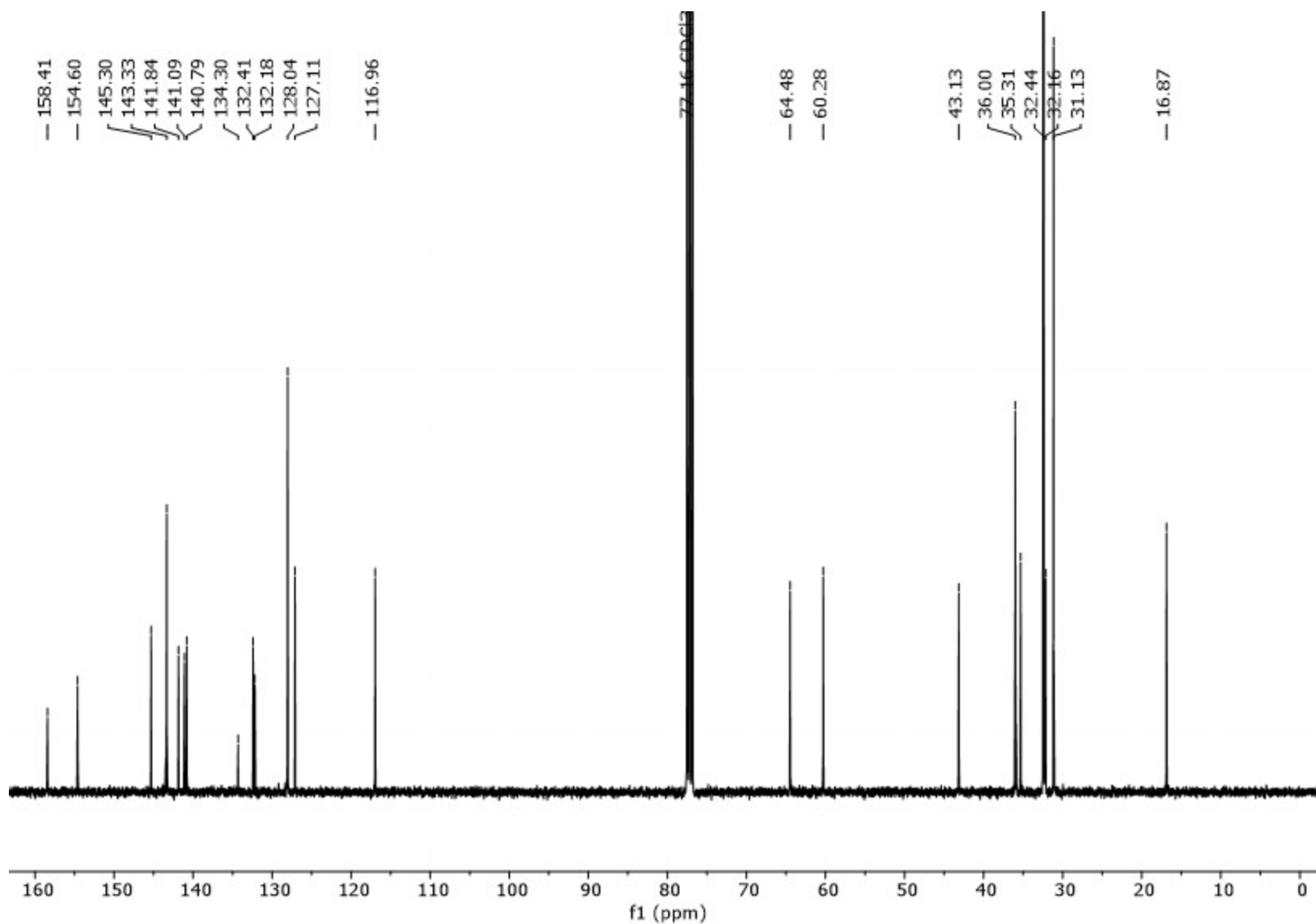


**Figure S5.**  $^{13}\text{C}\{^1\text{H}\}$  NMR spectrum (100 MHz, 25 °C,  $\text{CDCl}_3$ ) of 2-methyl-4-(3',5'-di-*tert*-butyl-4'-methoxy)-phenyl-5-methoxy-6-*tert*-butyl-1*H*-indene.

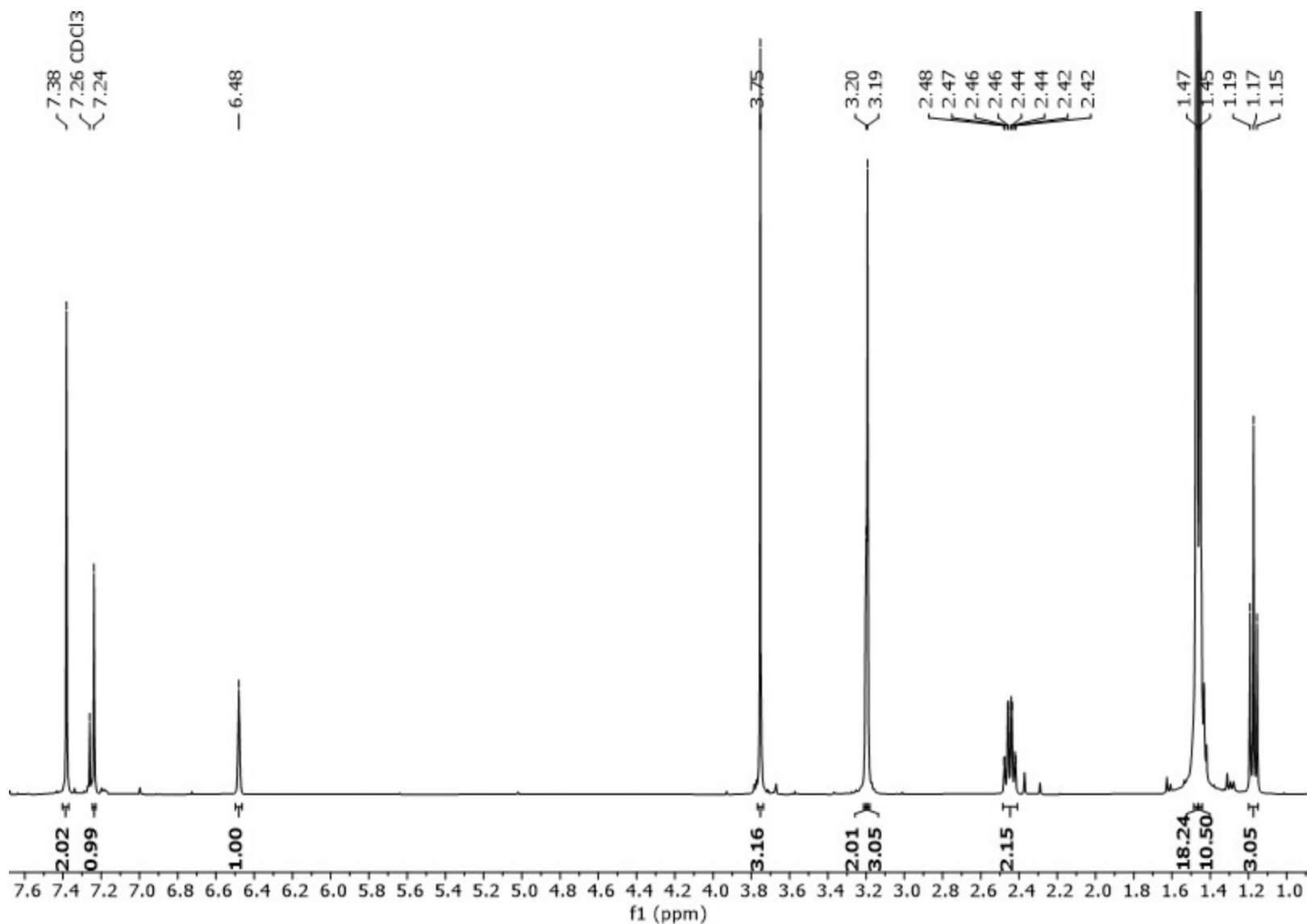


**Figure S6.** <sup>1</sup>H NMR spectrum (400 MHz, 25 °C, CDCl<sub>3</sub>) of 6-*tert*-butyl-5-methoxy-4-(3,5-di-*tert*-butyl-4-methoxy)-phenyl-2-ethyl-1*H*-indene.

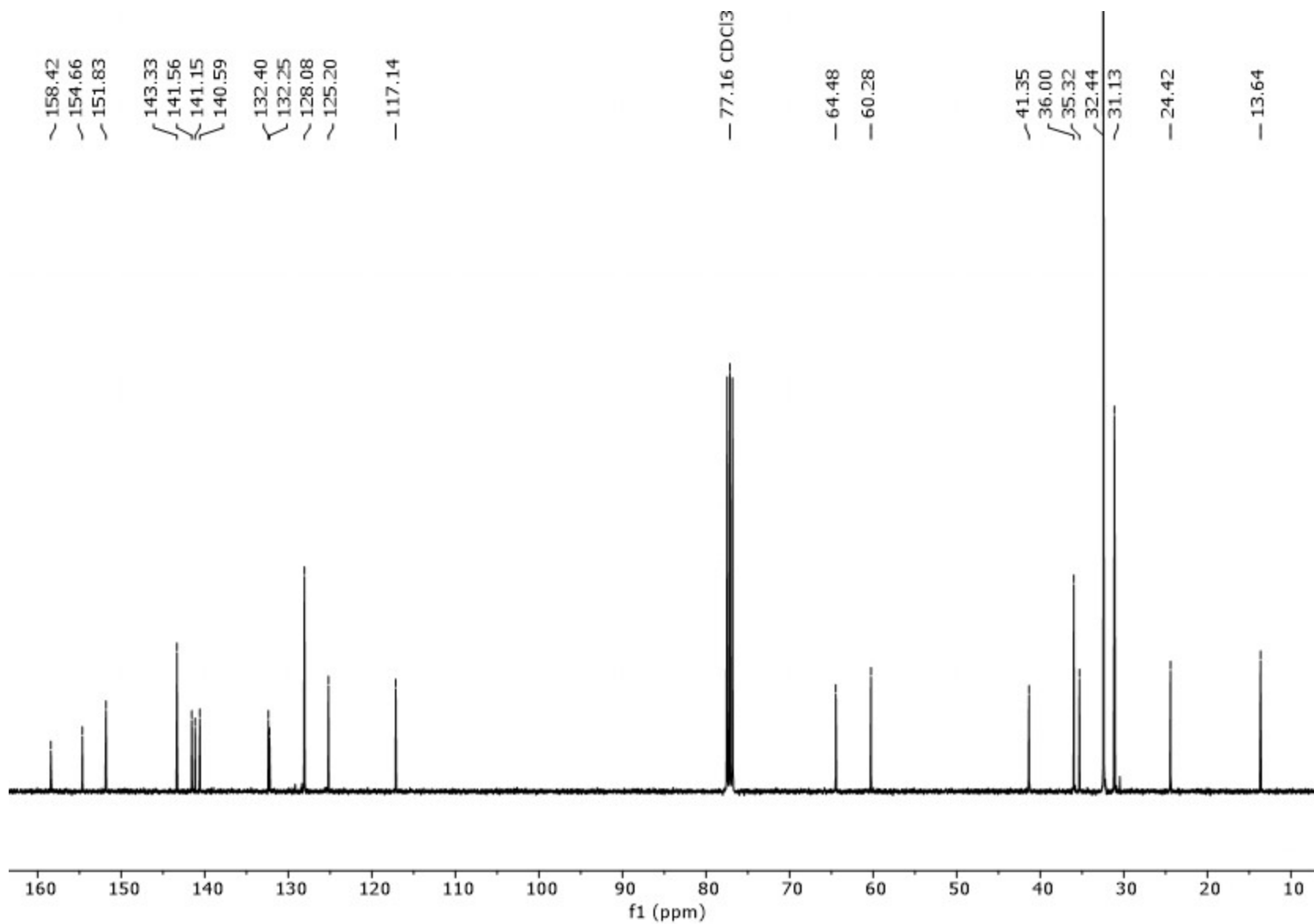


**Figure S7.**  $^{13}\text{C}\{^1\text{H}\}$  NMR spectrum (100 MHz, 25 °C,  $\text{CDCl}_3$ ) of 6-*tert*-butyl-5-methoxy-4-(3,5-di-*tert*-butyl-4-methoxy)-phenyl-2-ethyl-1*H*-indene.

— 7.26 CDCl<sub>3</sub>

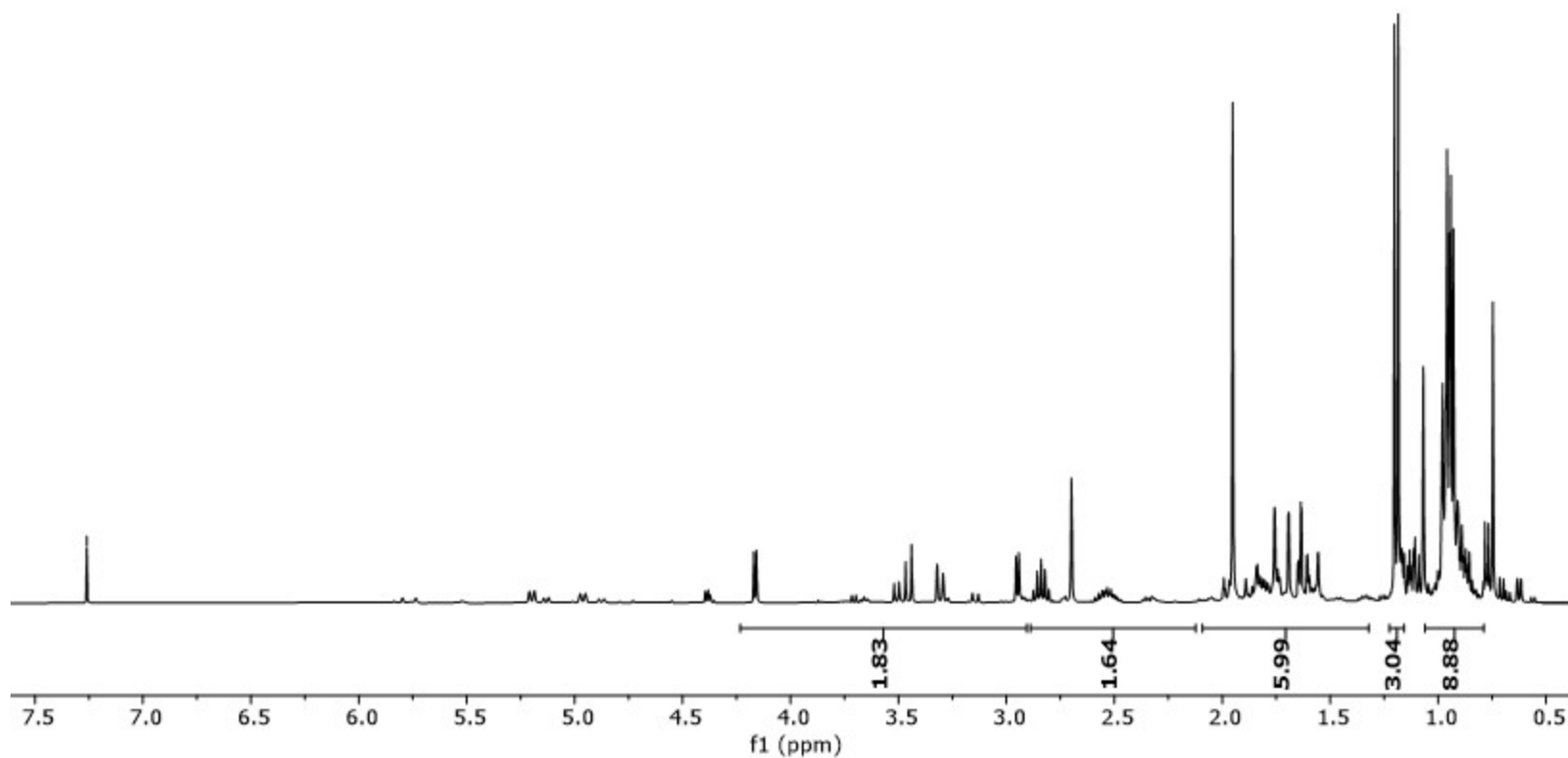


**Figure S8.** <sup>1</sup>H NMR spectrum (400 MHz, 25 °C, CDCl<sub>3</sub>) of 2,3-diisopropyl-1,4-dimethylcyclopenta-1,3-diene (resulting crude product from the reaction).

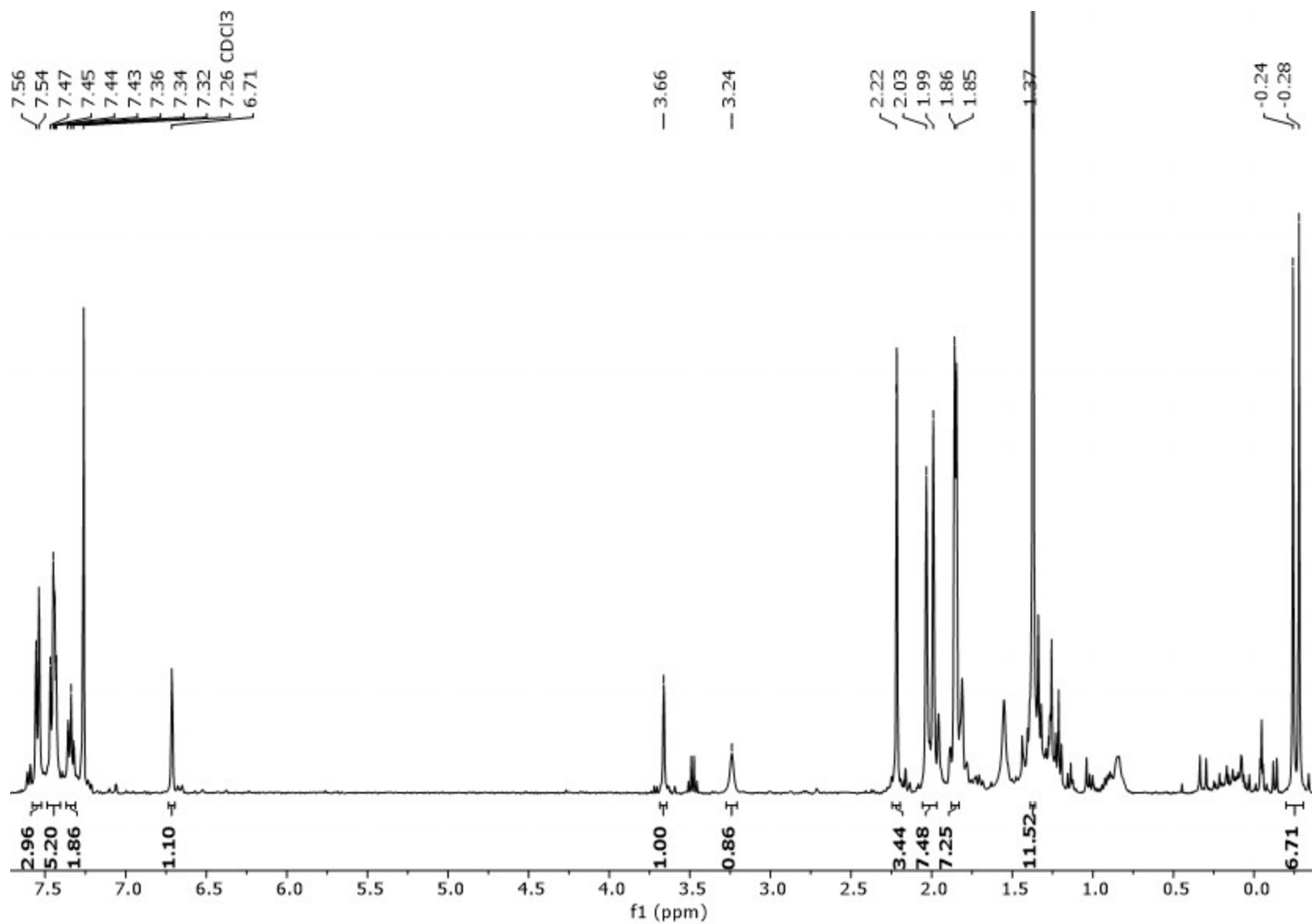


**Figure S9.** <sup>1</sup>H NMR spectrum (400 MHz, 25 °C, CDCl<sub>3</sub>) of **1c** (resulting crude product from the reaction).

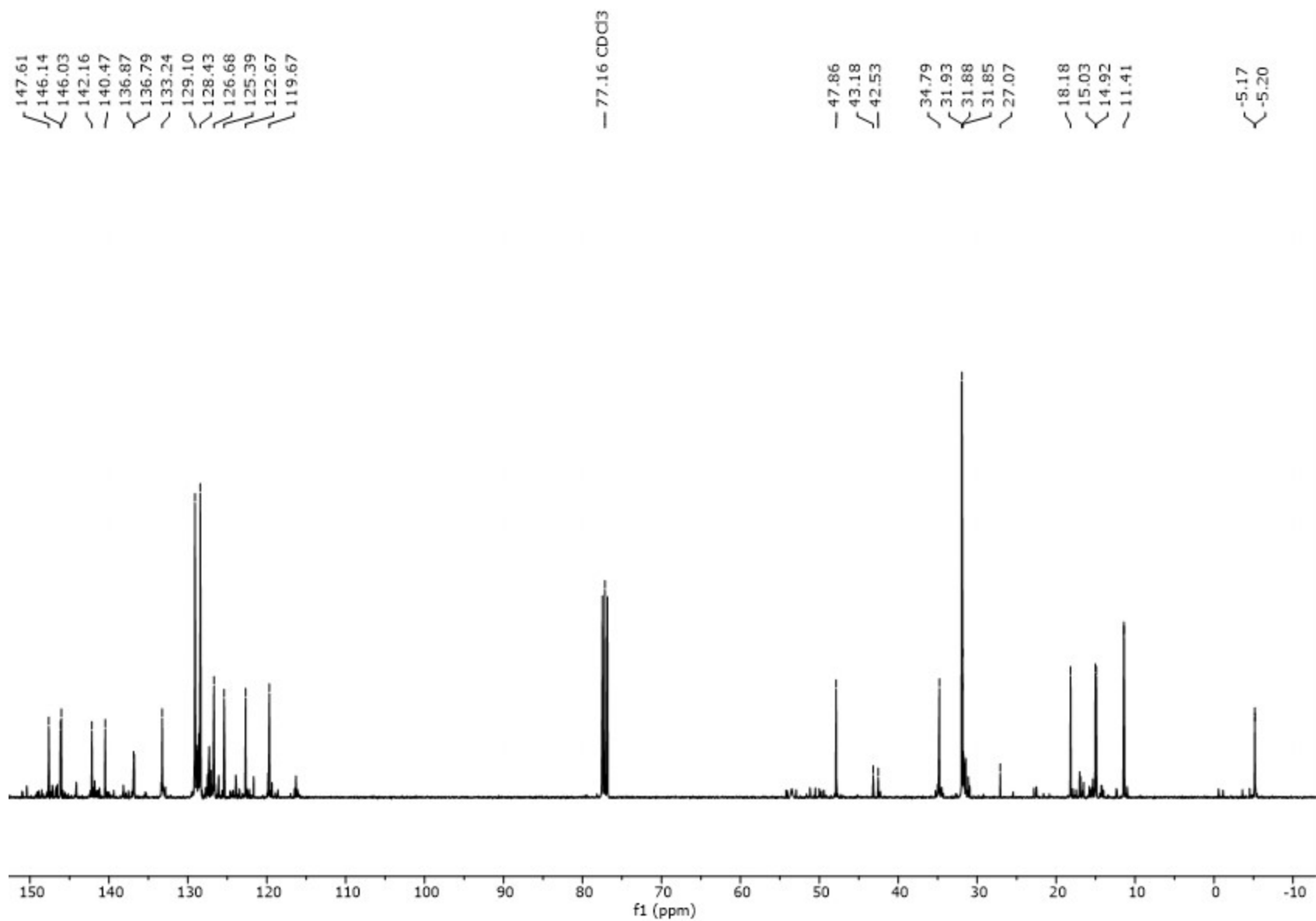


**Figure S10.**  $^{13}\text{C}\{^1\text{H}\}$  NMR spectrum (100 MHz, 25 °C,  $\text{CDCl}_3$ ) of **1c** (resulting crude product from the reaction).

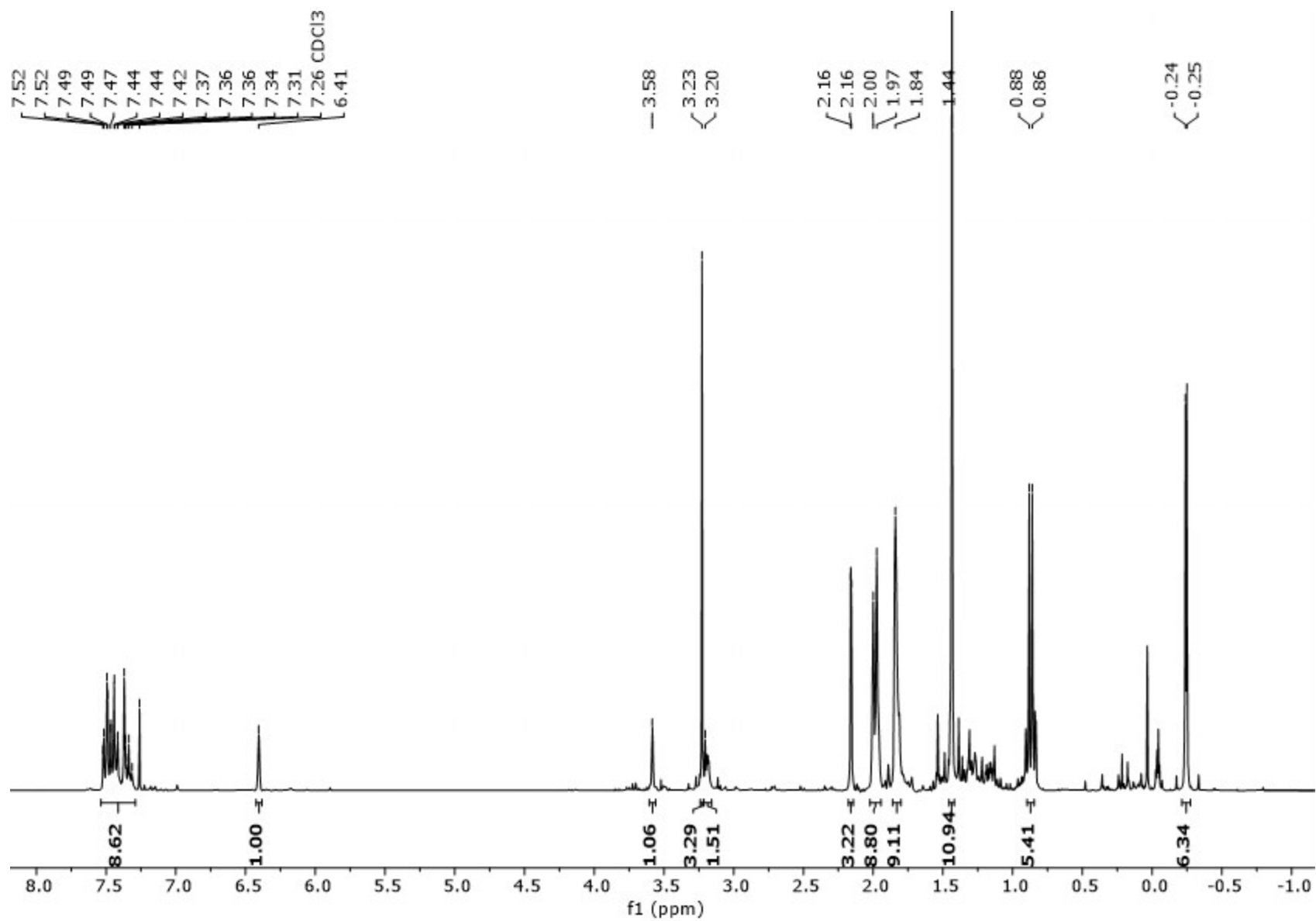


**Figure S11.** <sup>1</sup>H NMR spectrum (400 MHz, 25 °C, CDCl<sub>3</sub>) of **1d** (resulting crude product from the reaction).



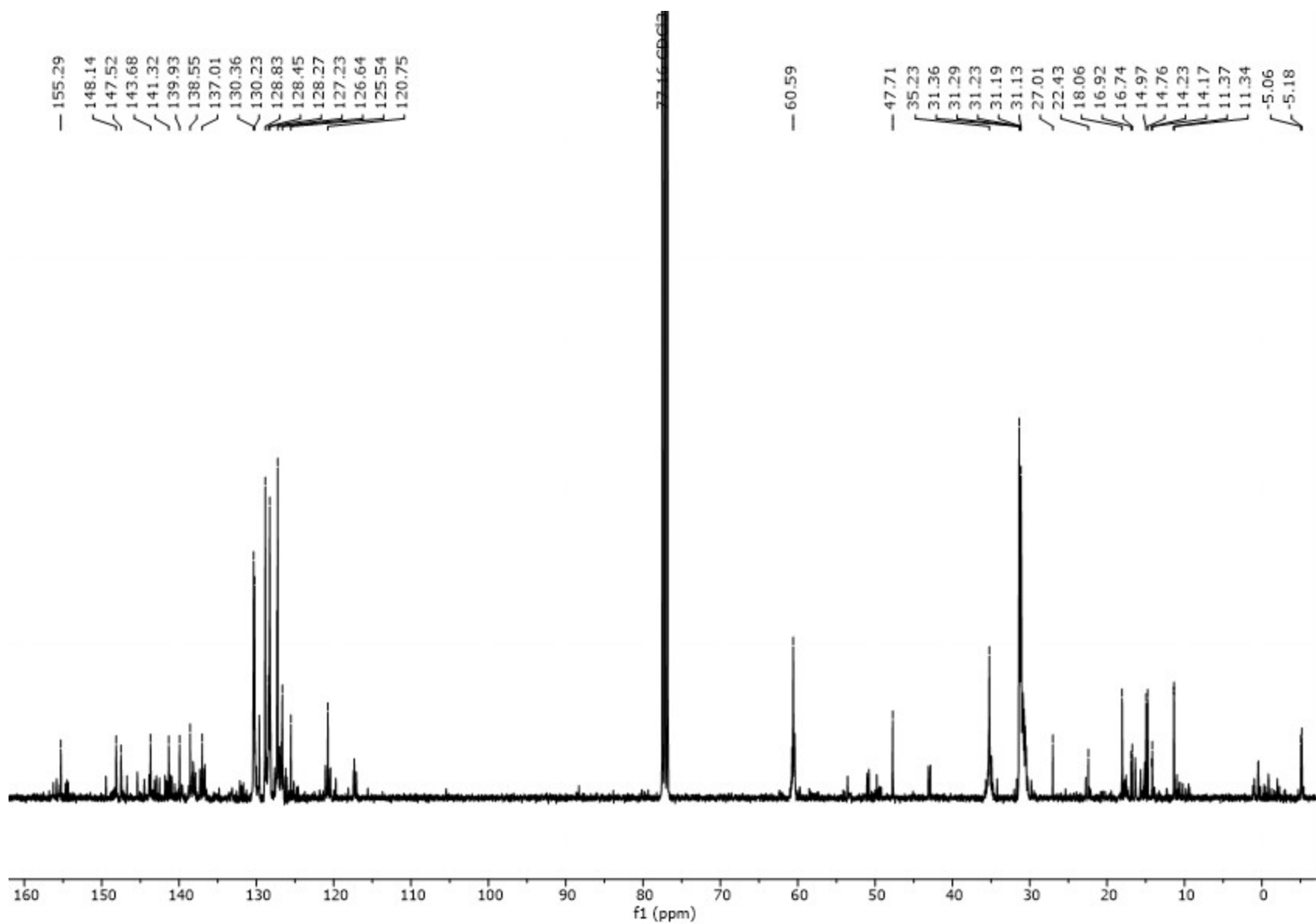


**Figure S12.**  $^{13}\text{C}\{^1\text{H}\}$  NMR spectrum (100 MHz, 25 °C,  $\text{CDCl}_3$ ) of **1d** (resulting crude product from the reaction).

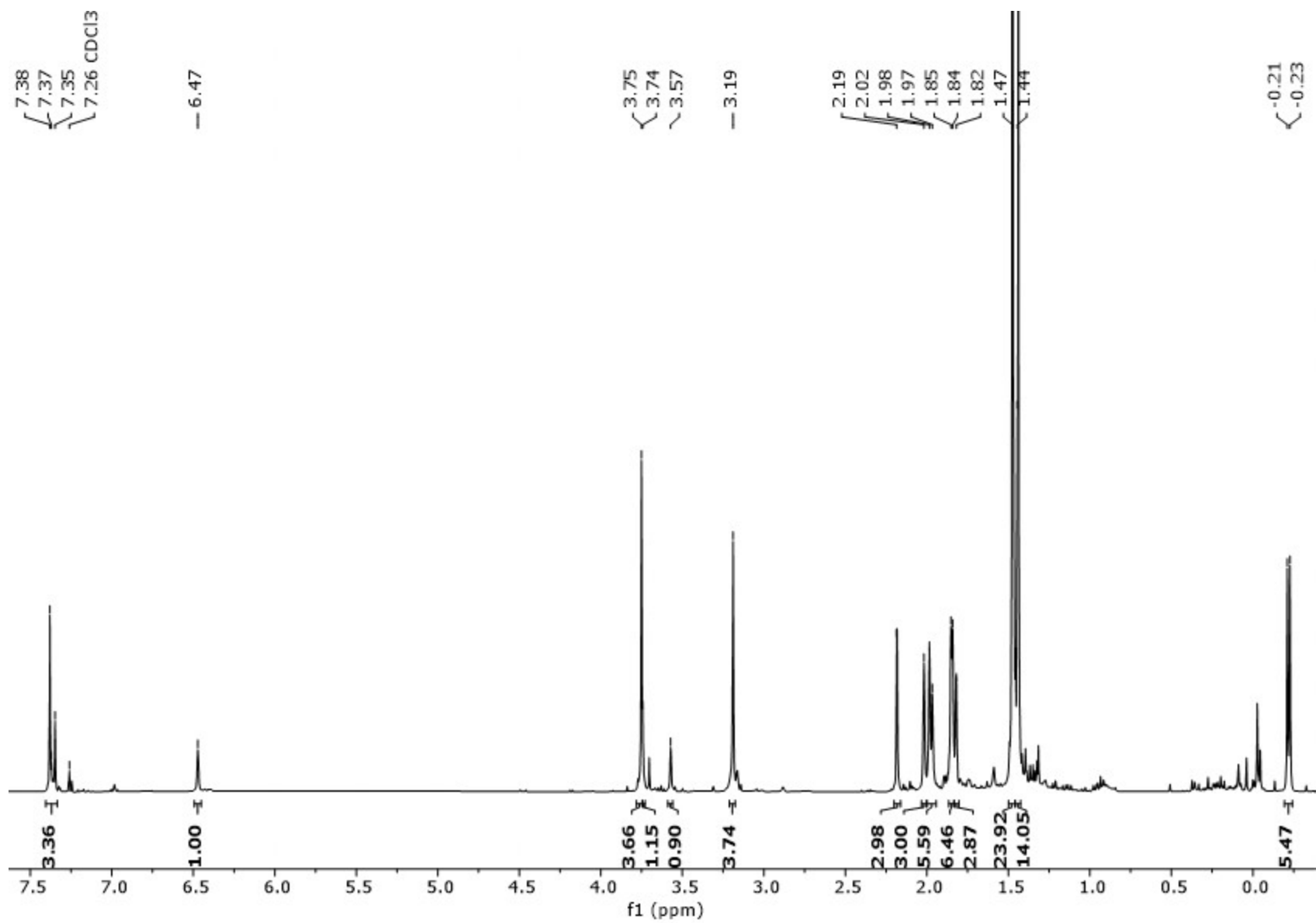


**Figure S13.** <sup>1</sup>H NMR spectrum (400 MHz, 25 °C, CDCl<sub>3</sub>) of **1e**.

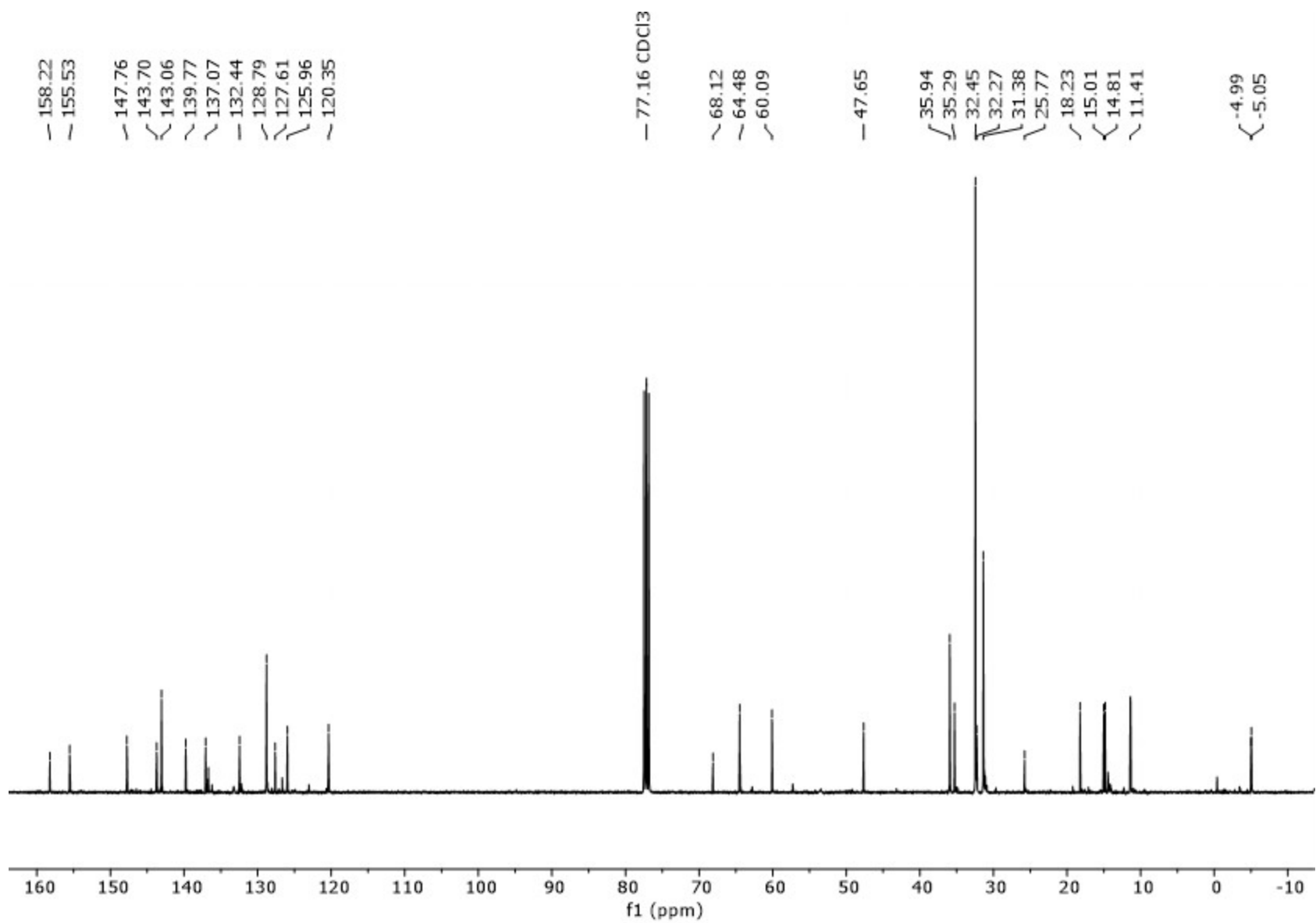


**Figure S14.**  $^{13}\text{C}\{^1\text{H}\}$  NMR spectrum (100 MHz, 25 °C,  $\text{CDCl}_3$ ) of **1e**.

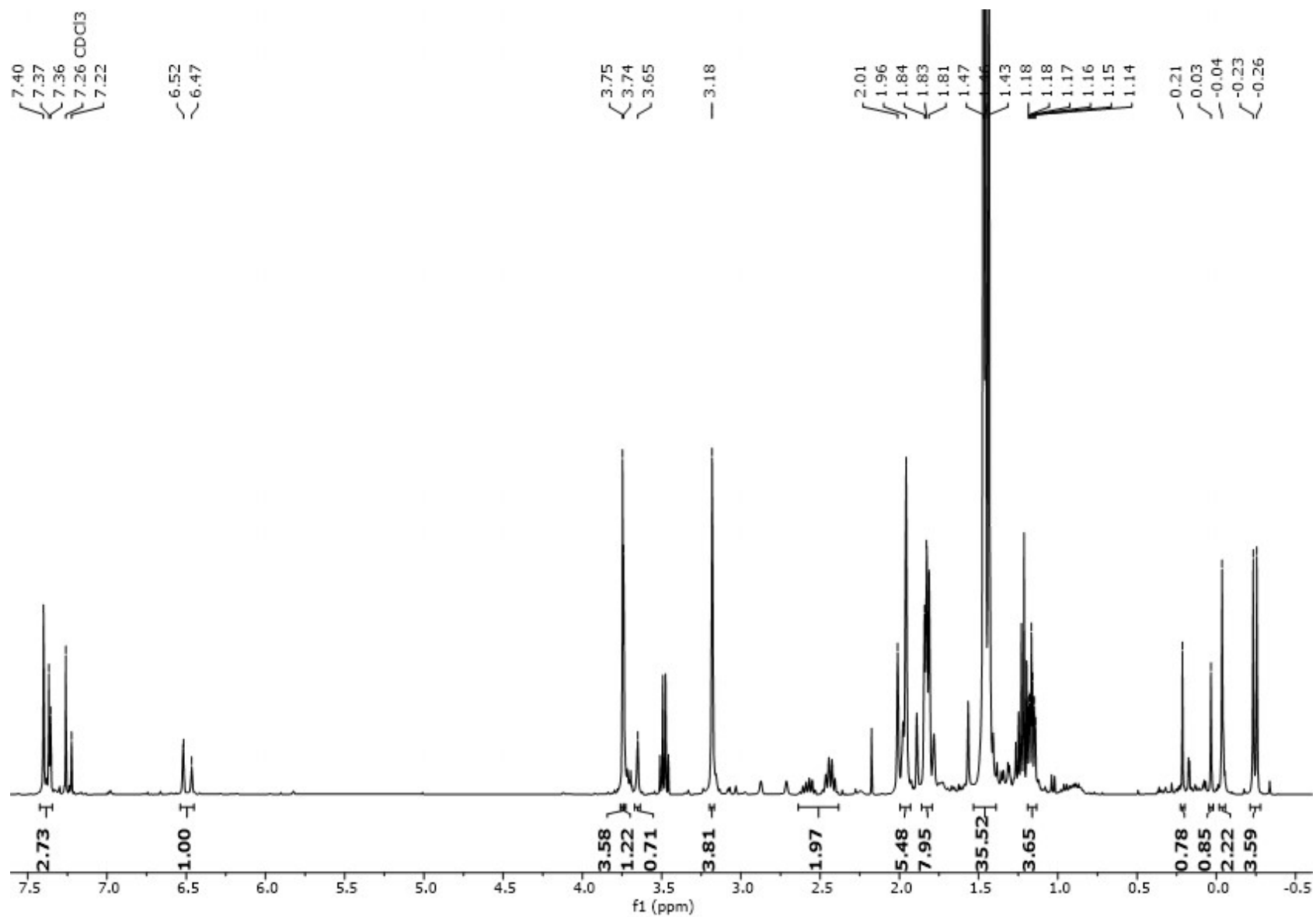


**Figure S15.** <sup>1</sup>H NMR spectrum (400 MHz, 25 °C, CDCl<sub>3</sub>) of **1f** (resulting crude product from the reaction).

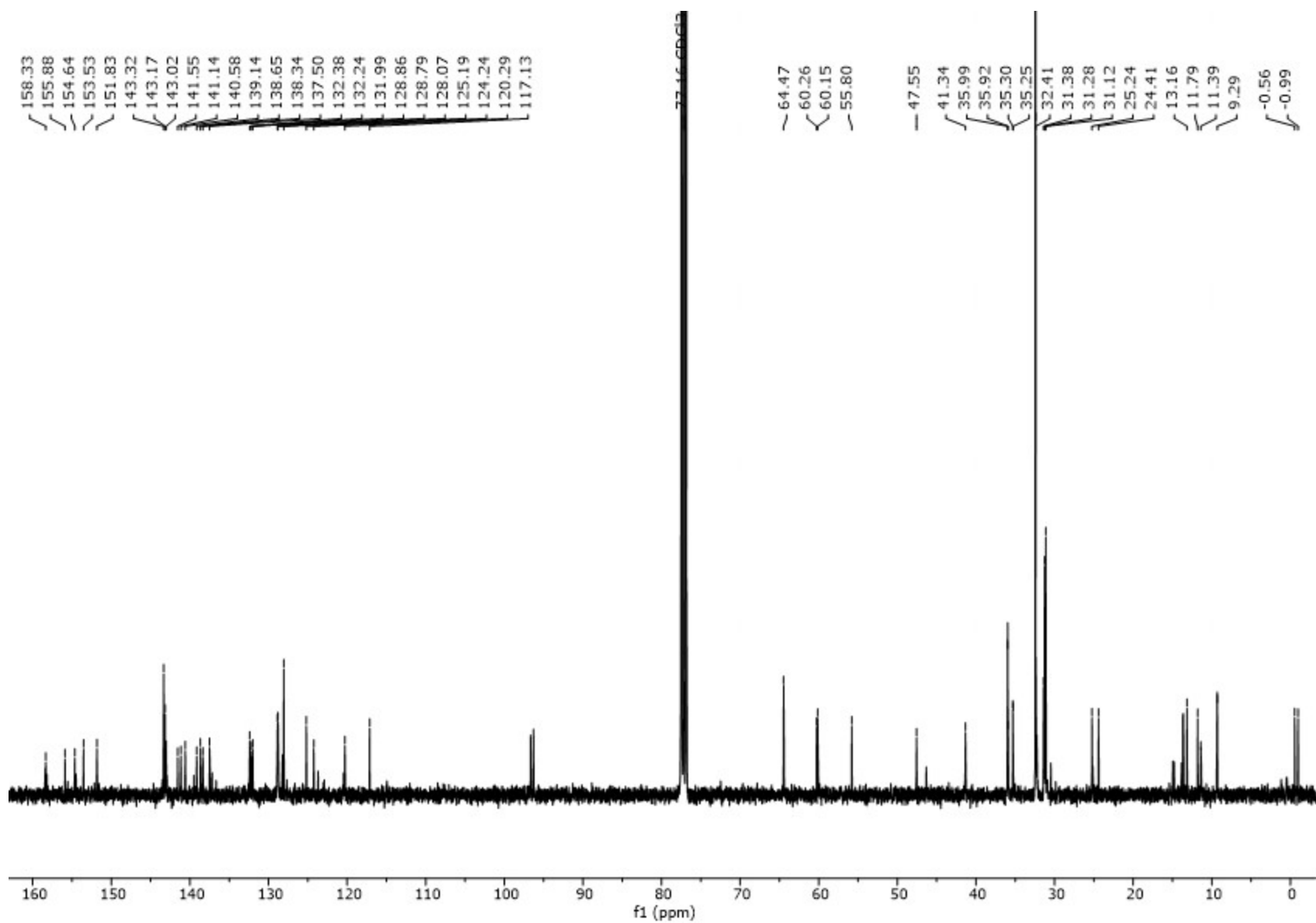


**Figure S16.**  $^{13}\text{C}\{^1\text{H}\}$  NMR spectrum (100 MHz, 25 °C,  $\text{CDCl}_3$ ) of **1f** (resulting crude product from the reaction).

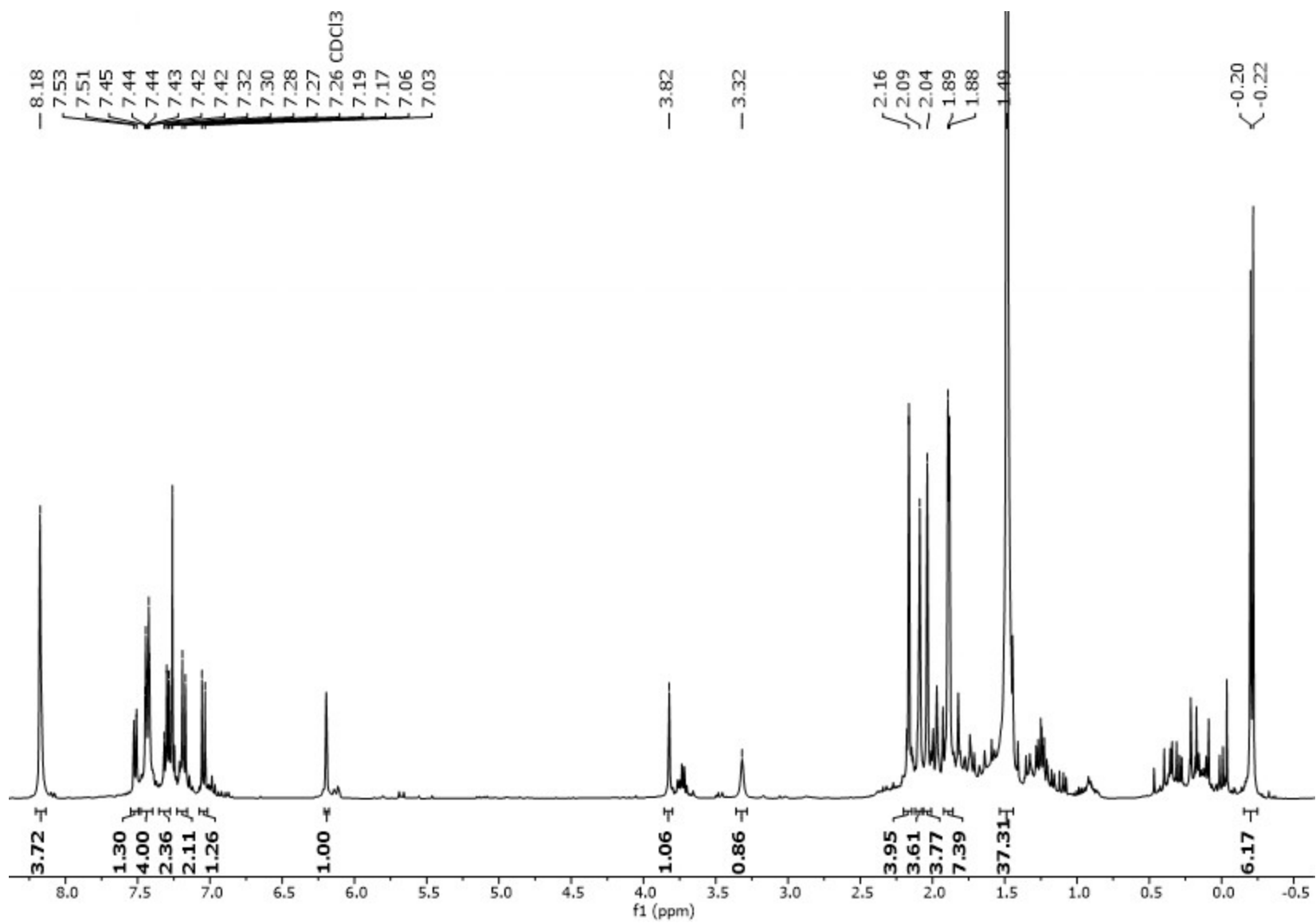


**Figure S17.** <sup>1</sup>H NMR spectrum (400 MHz, 25 °C, CDCl<sub>3</sub>) of **1g** (resulting crude product form the reaction).

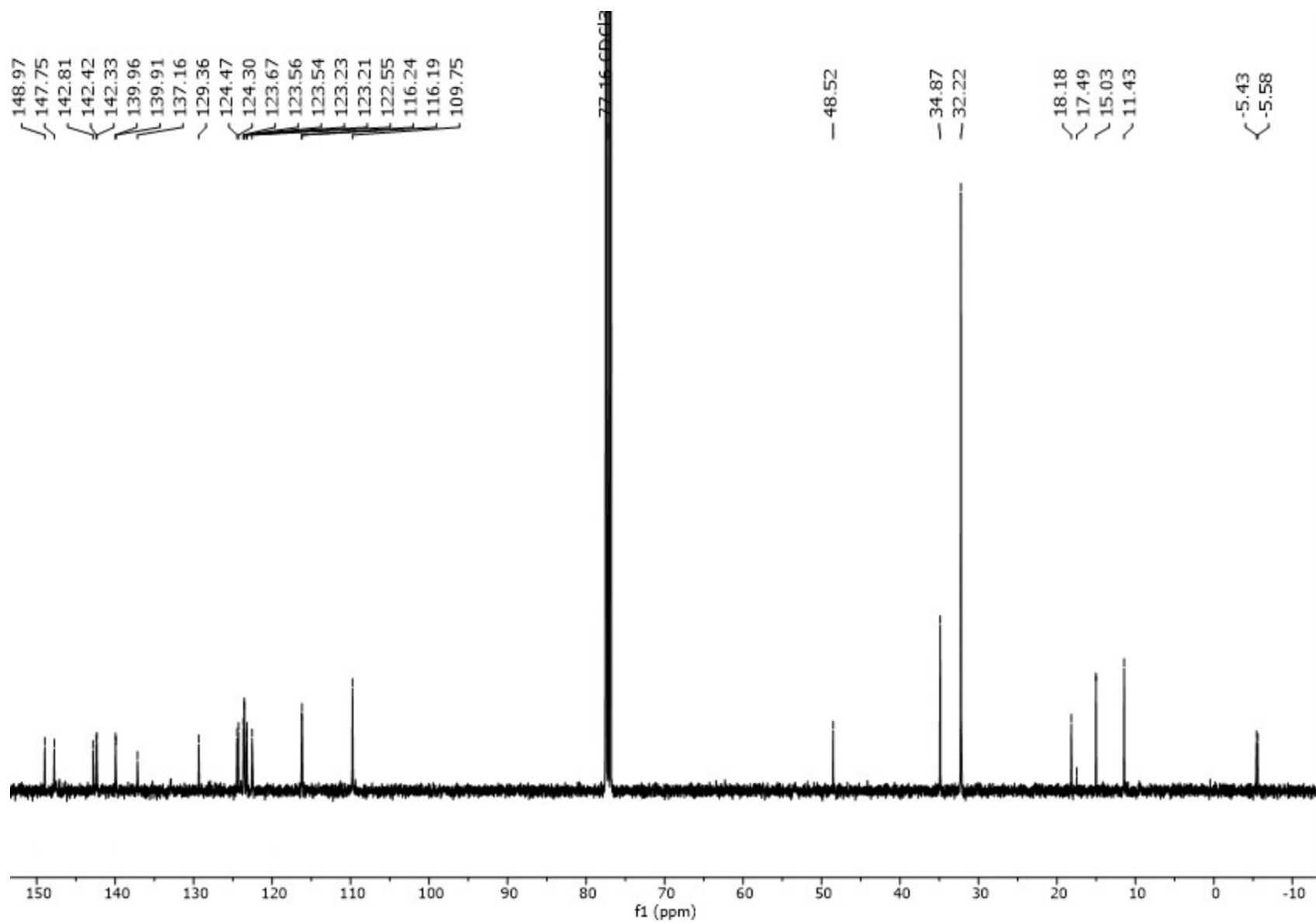


**Figure S18.**  $^{13}\text{C}\{^1\text{H}\}$  NMR spectrum (100 MHz, 25 °C,  $\text{CDCl}_3$ ) of **1g** (resulting crude product from the reaction).

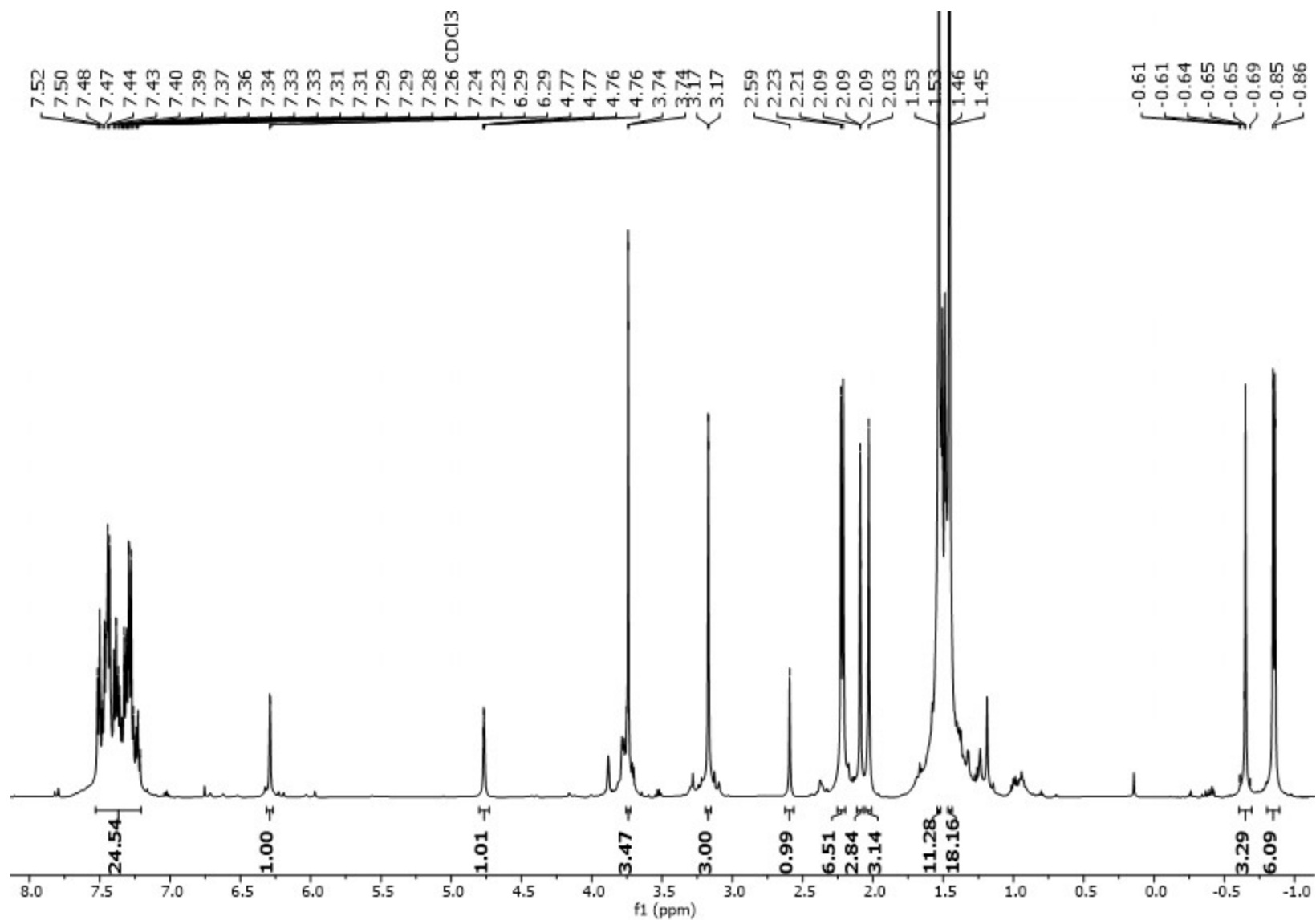


**Figure S19.** <sup>1</sup>H NMR spectrum (400 MHz, 25 °C, CDCl<sub>3</sub>) of **1h**.



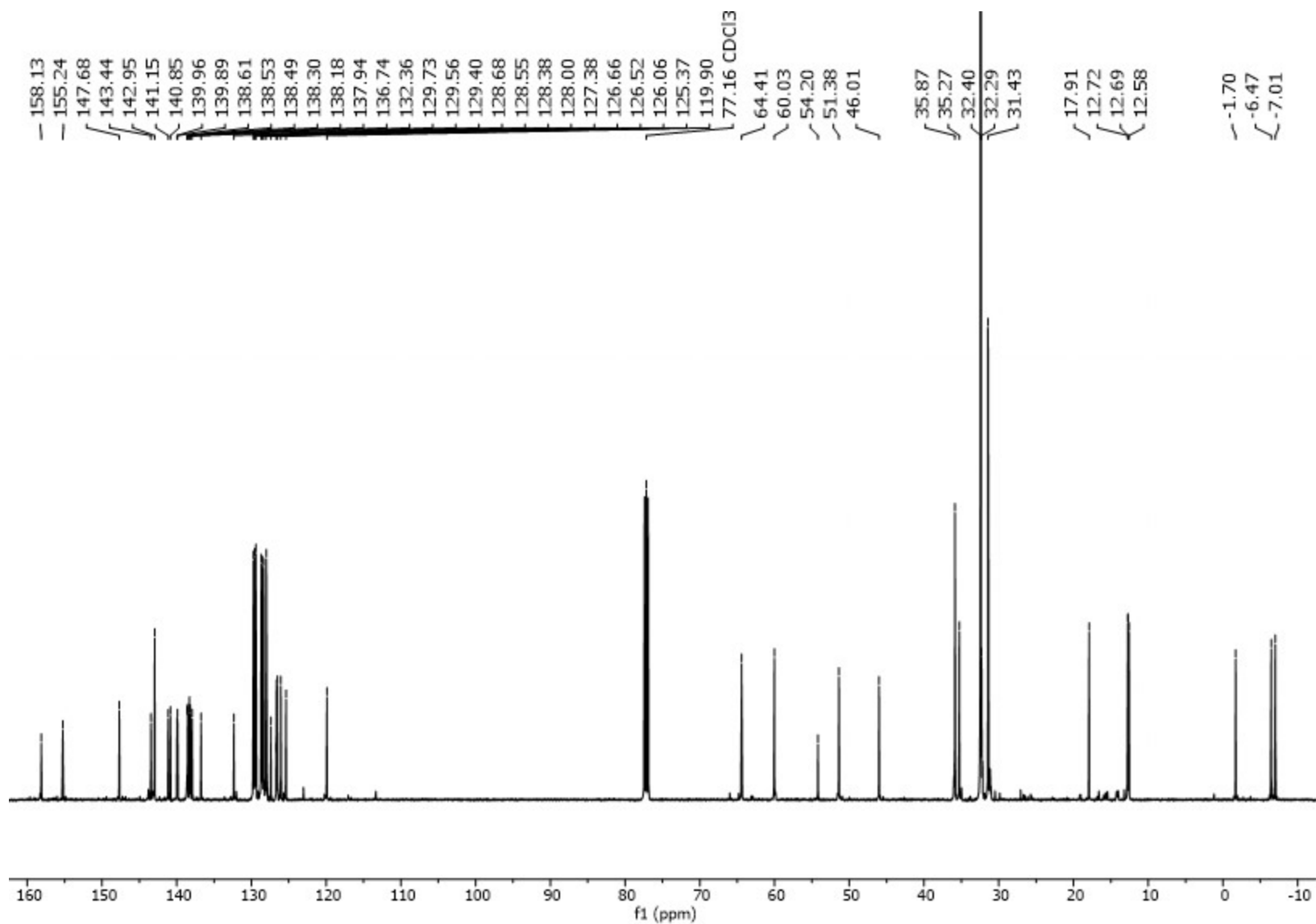


**Figure S20.**  $^{13}\text{C}\{^1\text{H}\}$  NMR spectrum (100 MHz, 25 °C,  $\text{CDCl}_3$ ) of **1h**.

— 7.26 CDCl<sub>3</sub>

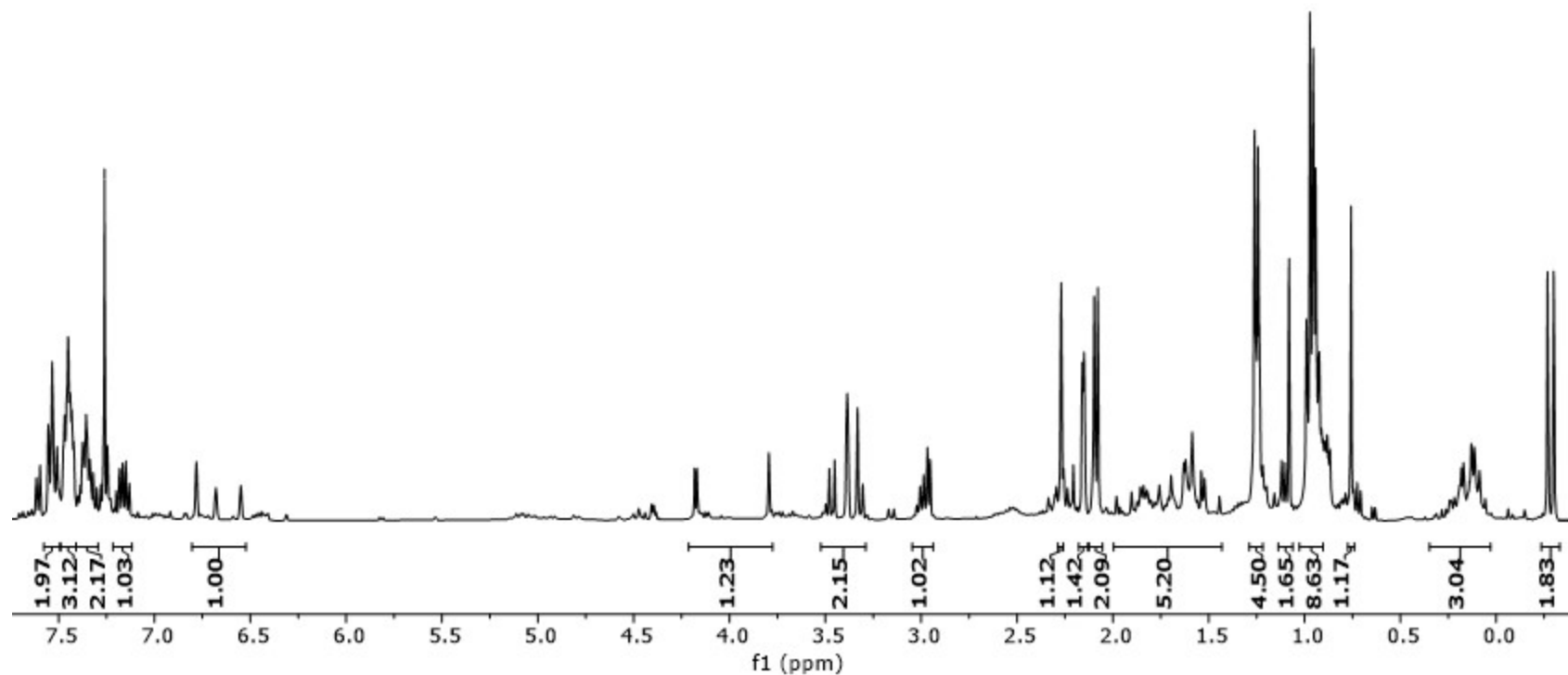


**Figure S21.** <sup>1</sup>H NMR spectrum (400 MHz, 25 °C, CDCl<sub>3</sub>) of **1i** (resulting crude product from the reaction).

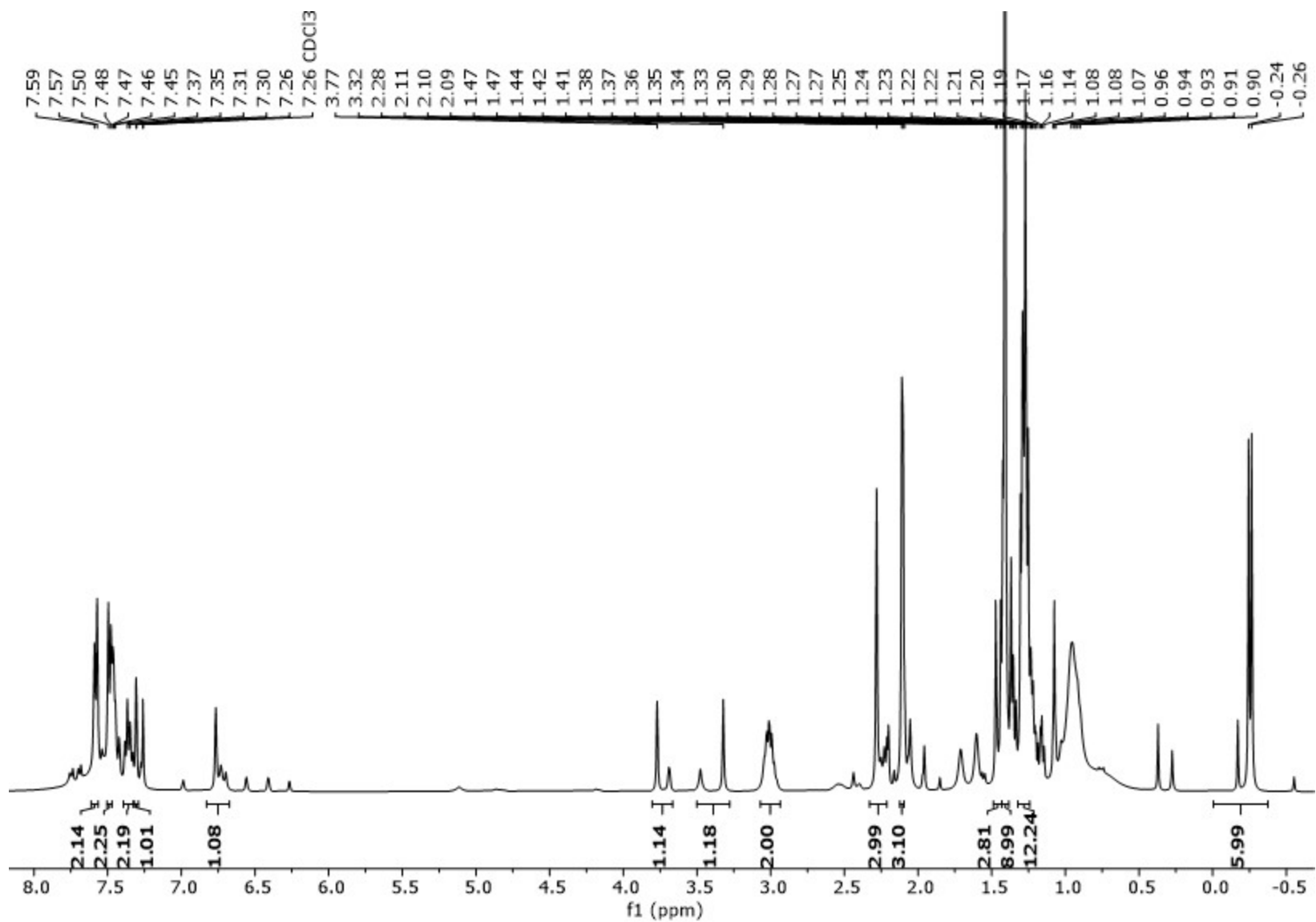


**Figure S22.** <sup>1</sup>H NMR spectrum (100 MHz, 25 °C, CDCl<sub>3</sub>) of **1j**.

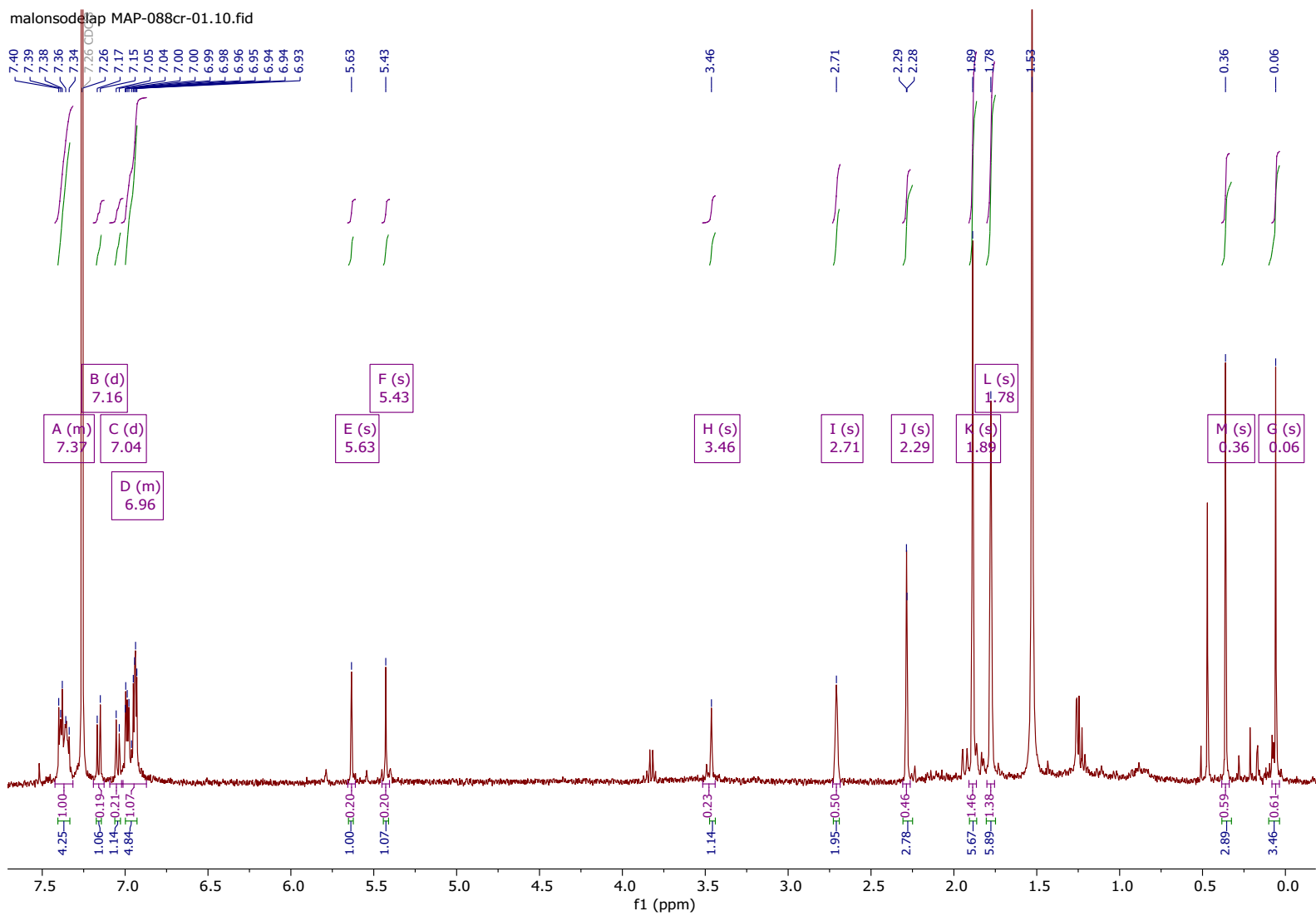
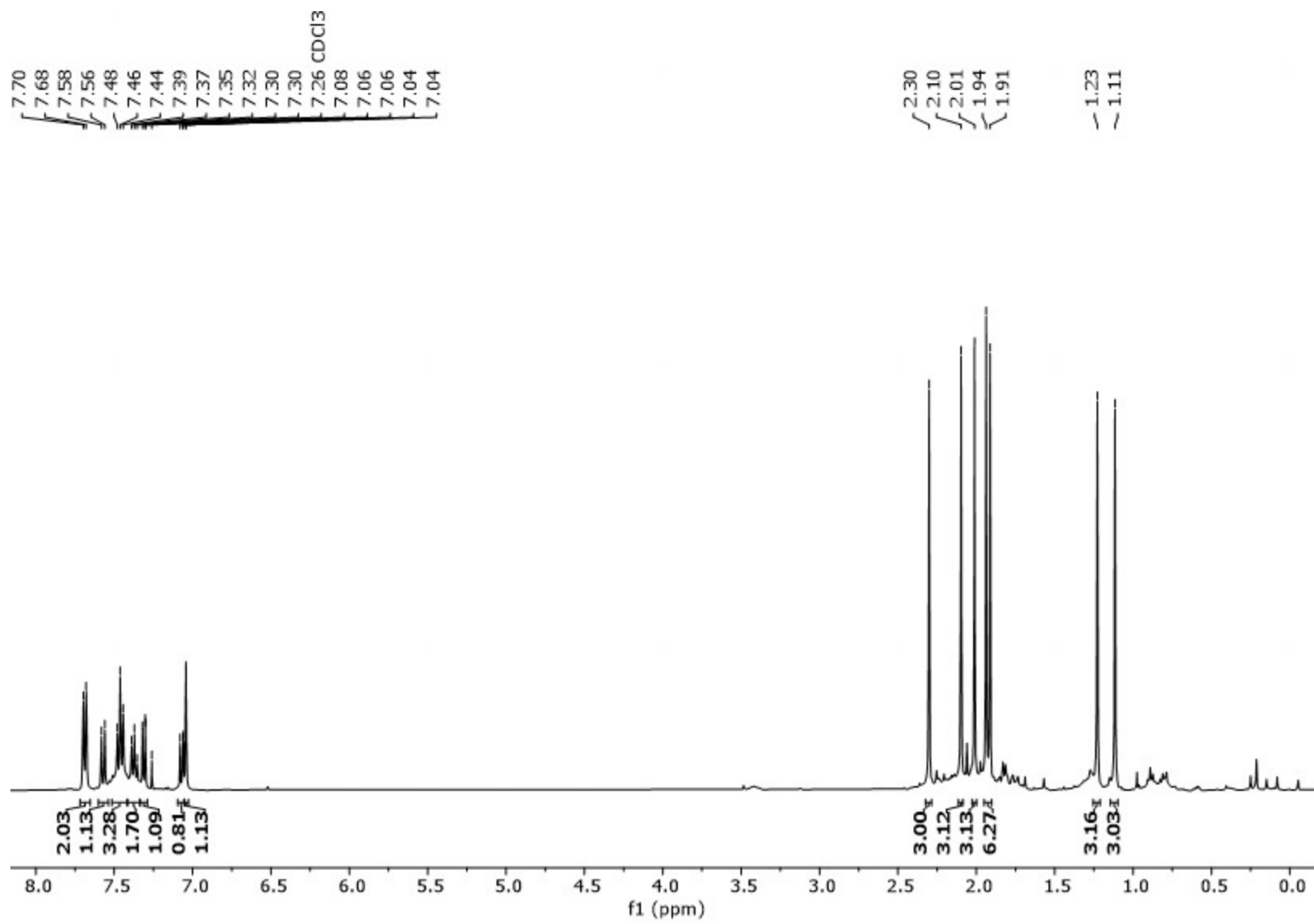
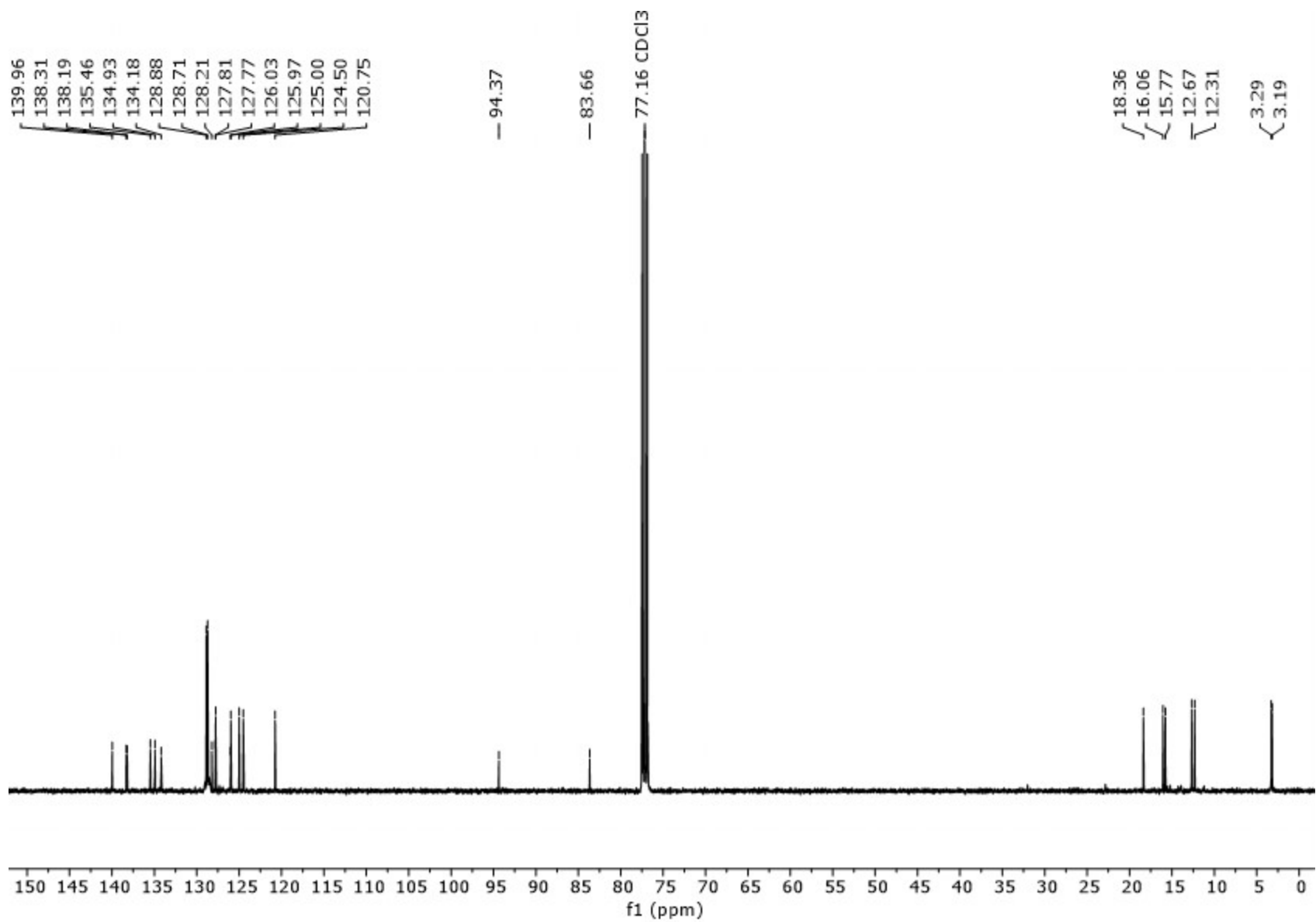


Figure S23. <sup>1</sup>H NMR spectrum (400 MHz, 25 °C, CDCl<sub>3</sub>) of **1k**.



**Figure S24.** <sup>1</sup>H NMR spectrum (400 MHz, 25 °C, CDCl<sub>3</sub>) of **2b-Zr**.



**Figure S25.**  $^{13}\text{C}\{^1\text{H}\}$  NMR spectrum (100 MHz, 25 °C,  $\text{CDCl}_3$ ) of **2b-Zr**.

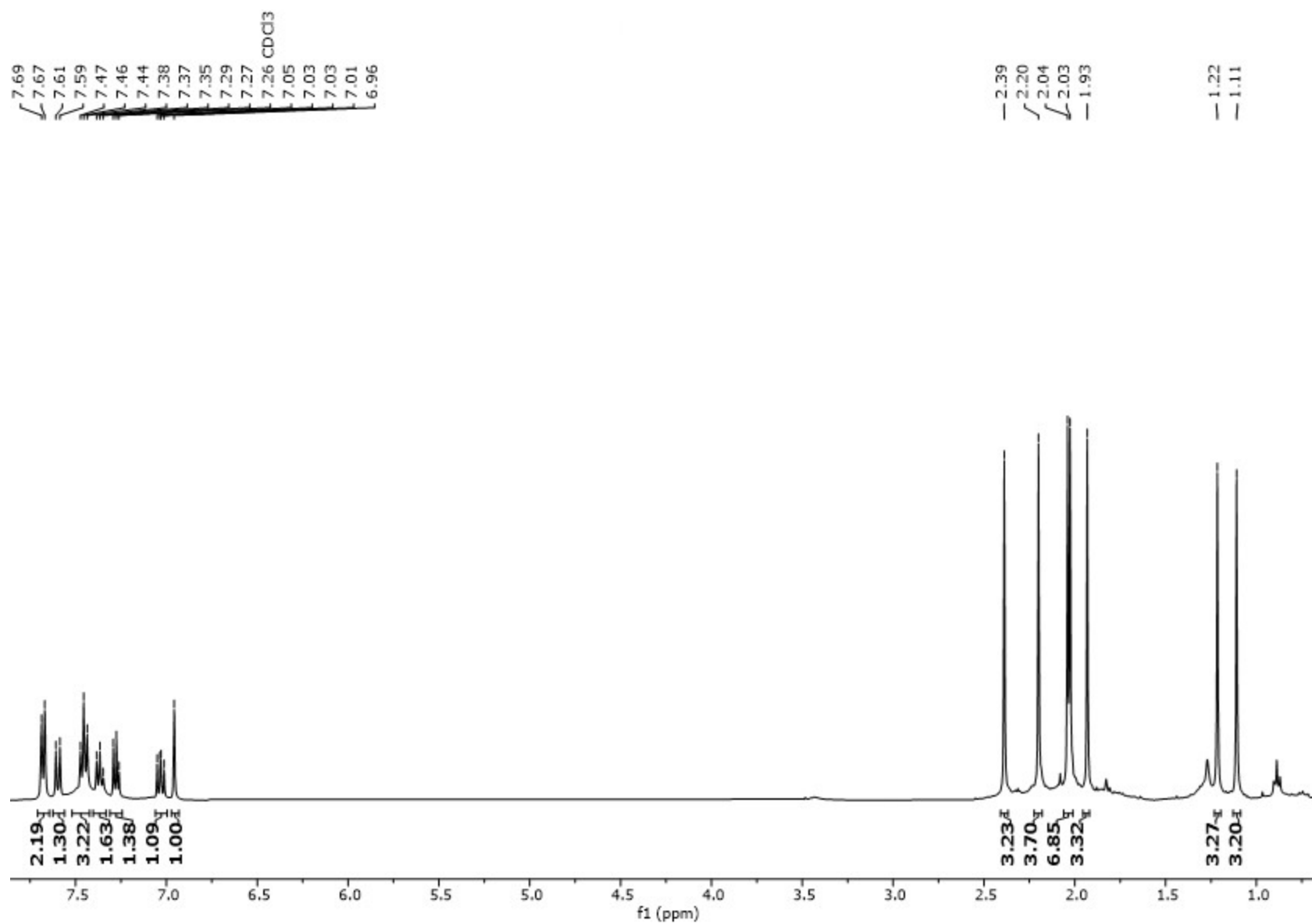


**Figure S26.** <sup>1</sup>H NMR spectrum (400 MHz, 25 °C, CDCl<sub>3</sub>) of **2b-Hf**.

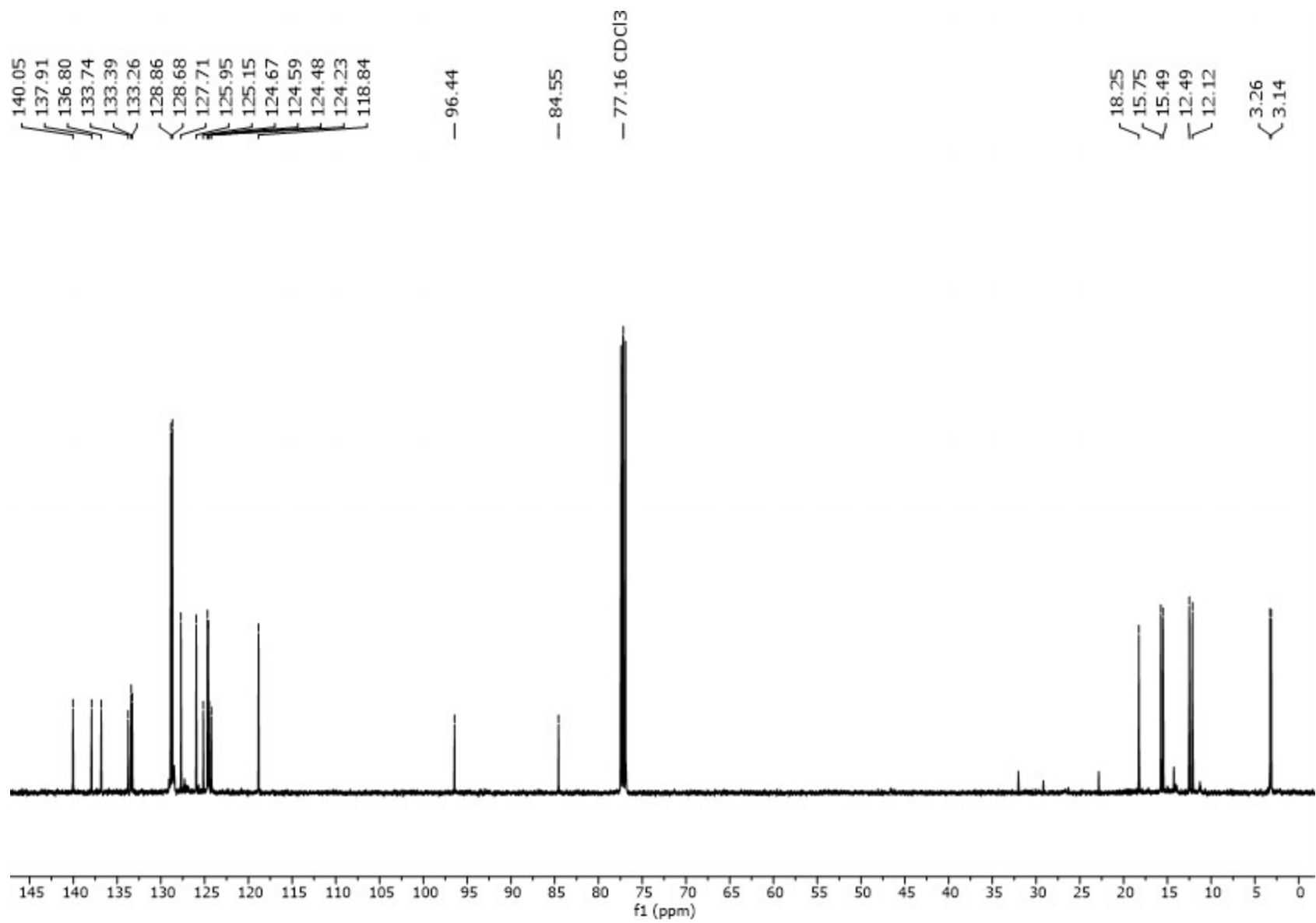


**Figure S27.**  $^{13}\text{C}\{^1\text{H}\}$  NMR spectrum (100 MHz, 25 °C,  $\text{CDCl}_3$ ) of **2b-Hf**.



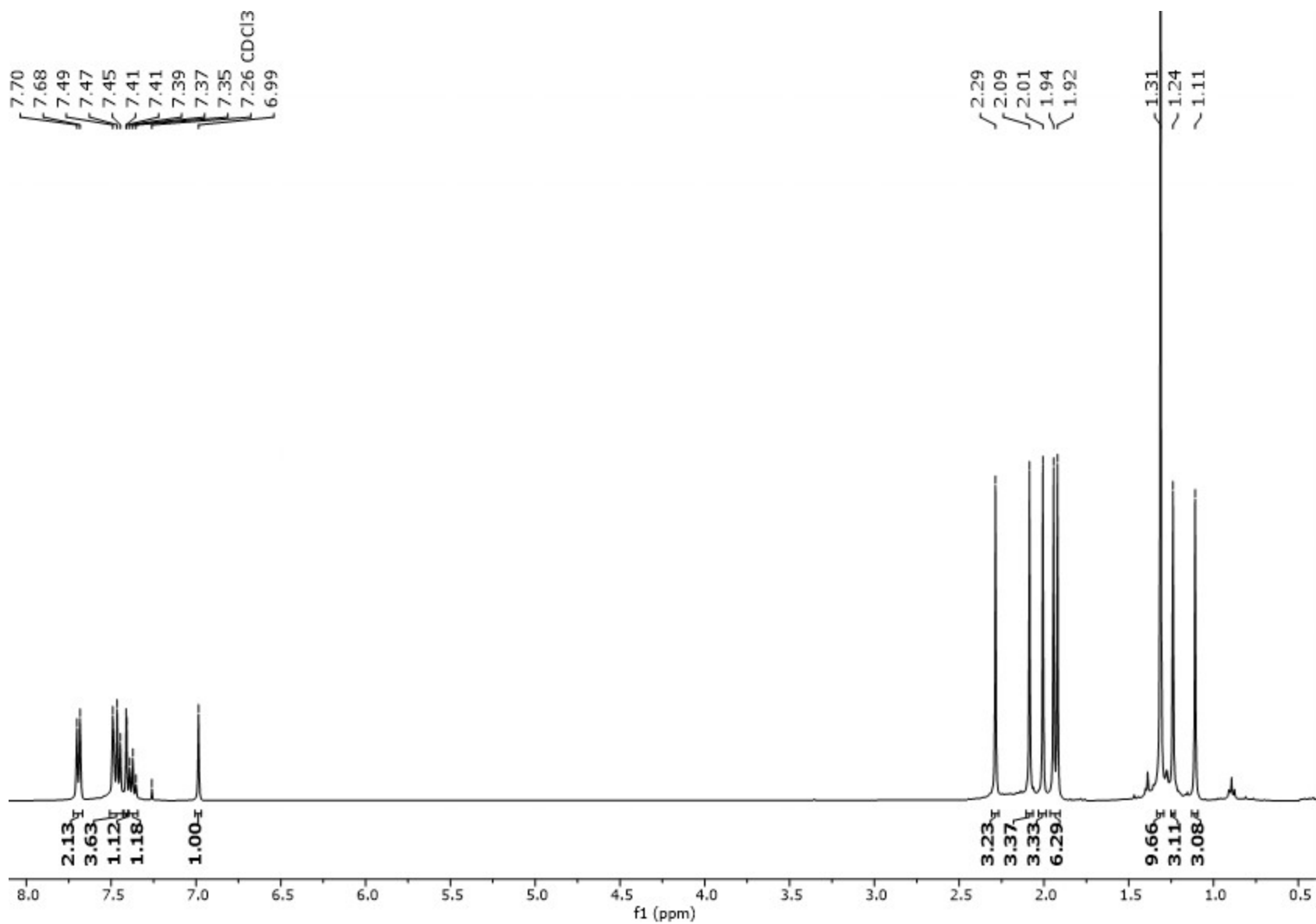
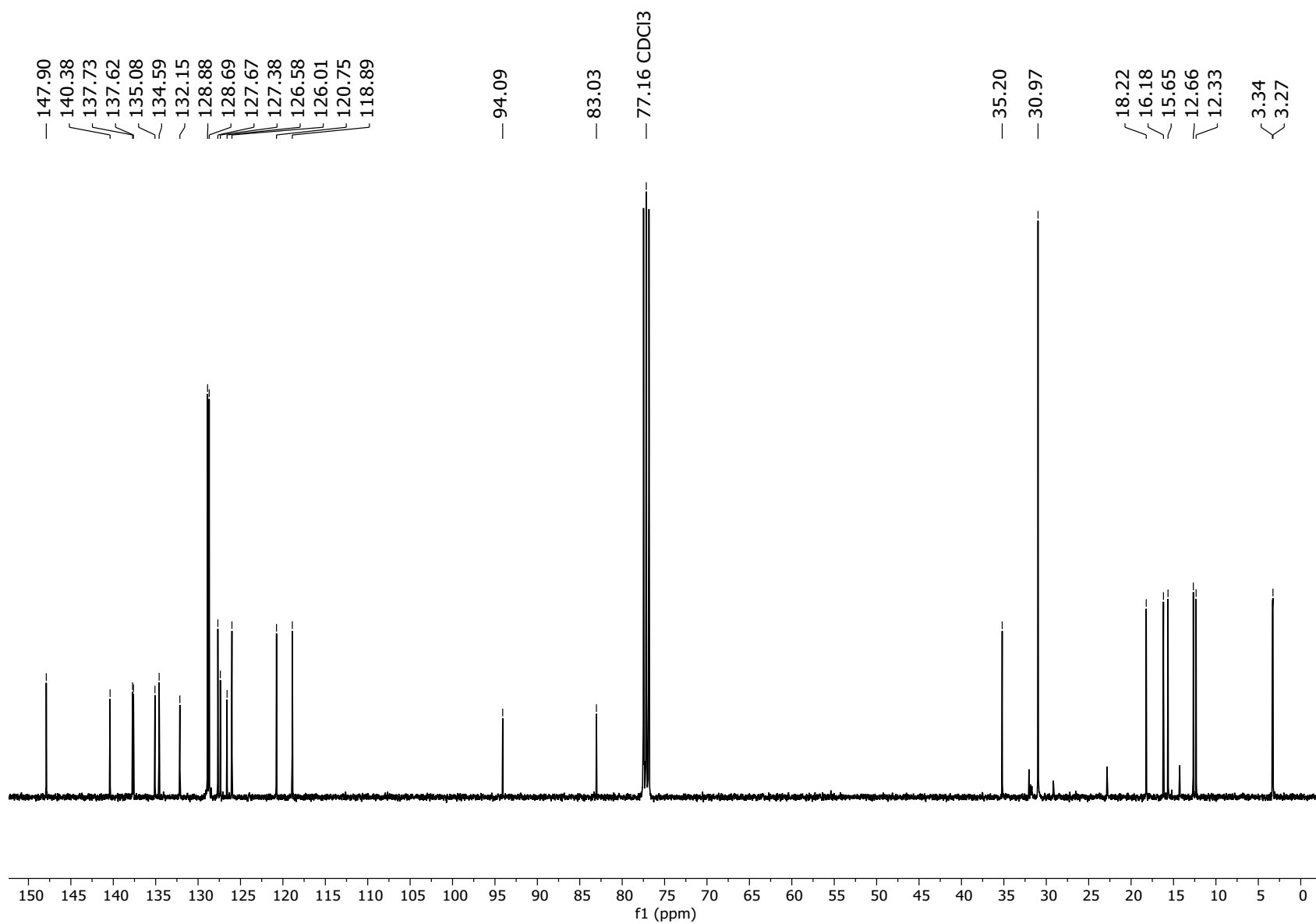
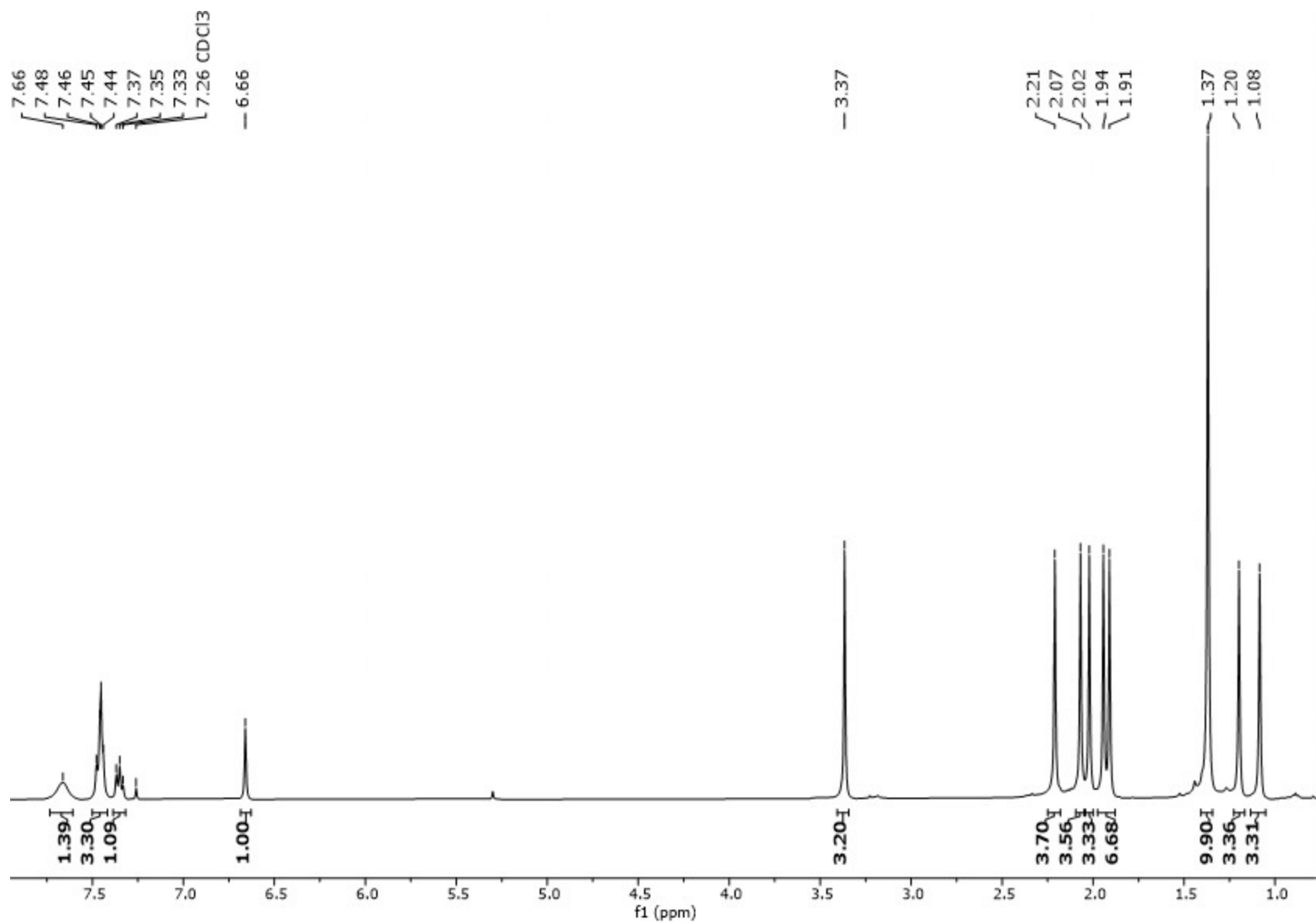


Figure S28. <sup>1</sup>H NMR spectrum (400 MHz, 25 °C, CDCl<sub>3</sub>) of 2c-Zr.



**Figure S29.**  $^{13}\text{C}\{^1\text{H}\}$  NMR spectrum (100 MHz, 25 °C,  $\text{CDCl}_3$ ) of **2c-Zr**.



**Figure S30.** <sup>1</sup>H NMR spectrum (400 MHz, 25 °C, CDCl<sub>3</sub>) of **2d-Zr**.

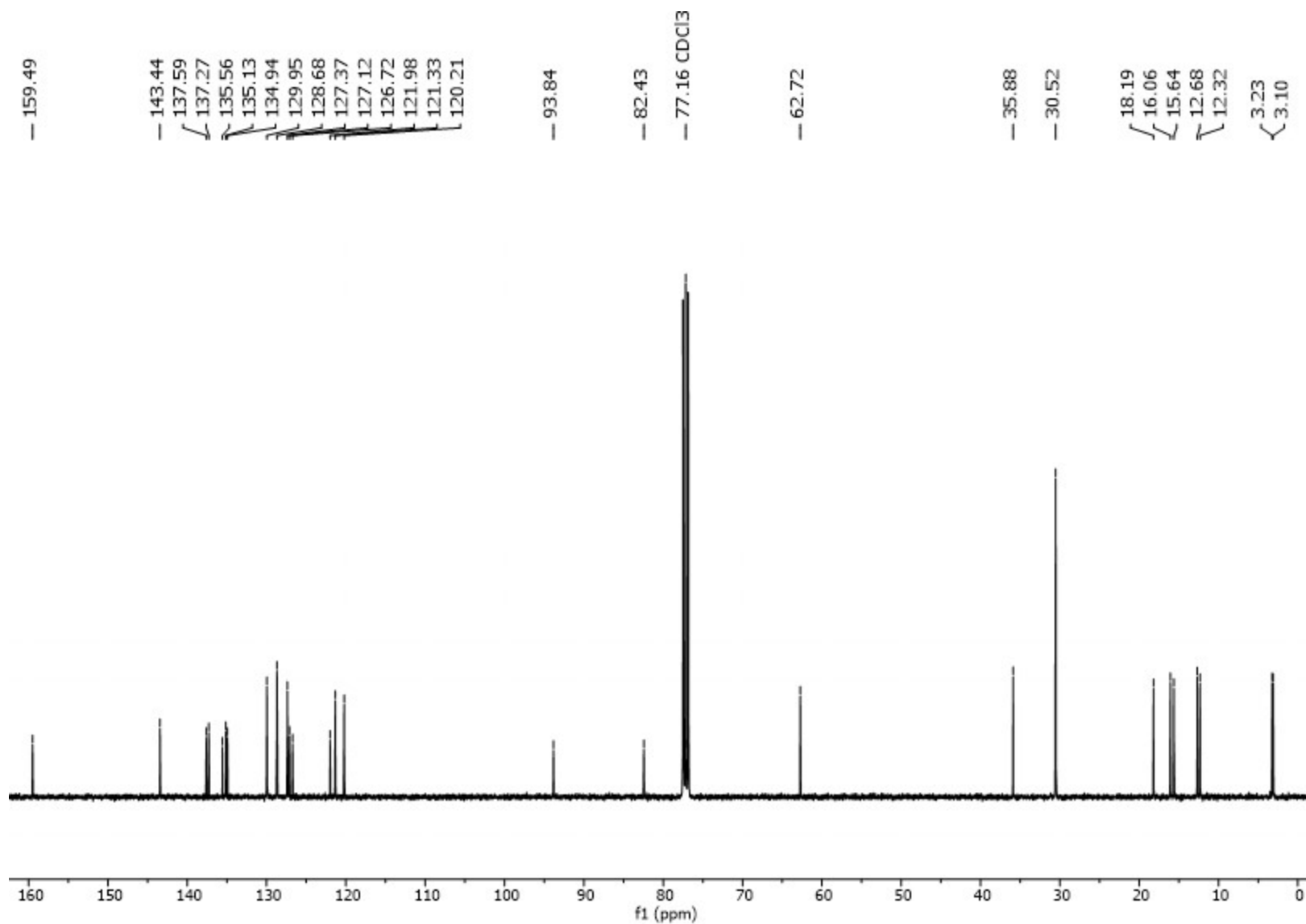


**Figure S31.**  $^{13}\text{C}\{^1\text{H}\}$  NMR spectrum (100 MHz, 25 °C,  $\text{CDCl}_3$ ) of **2d-Zr**.

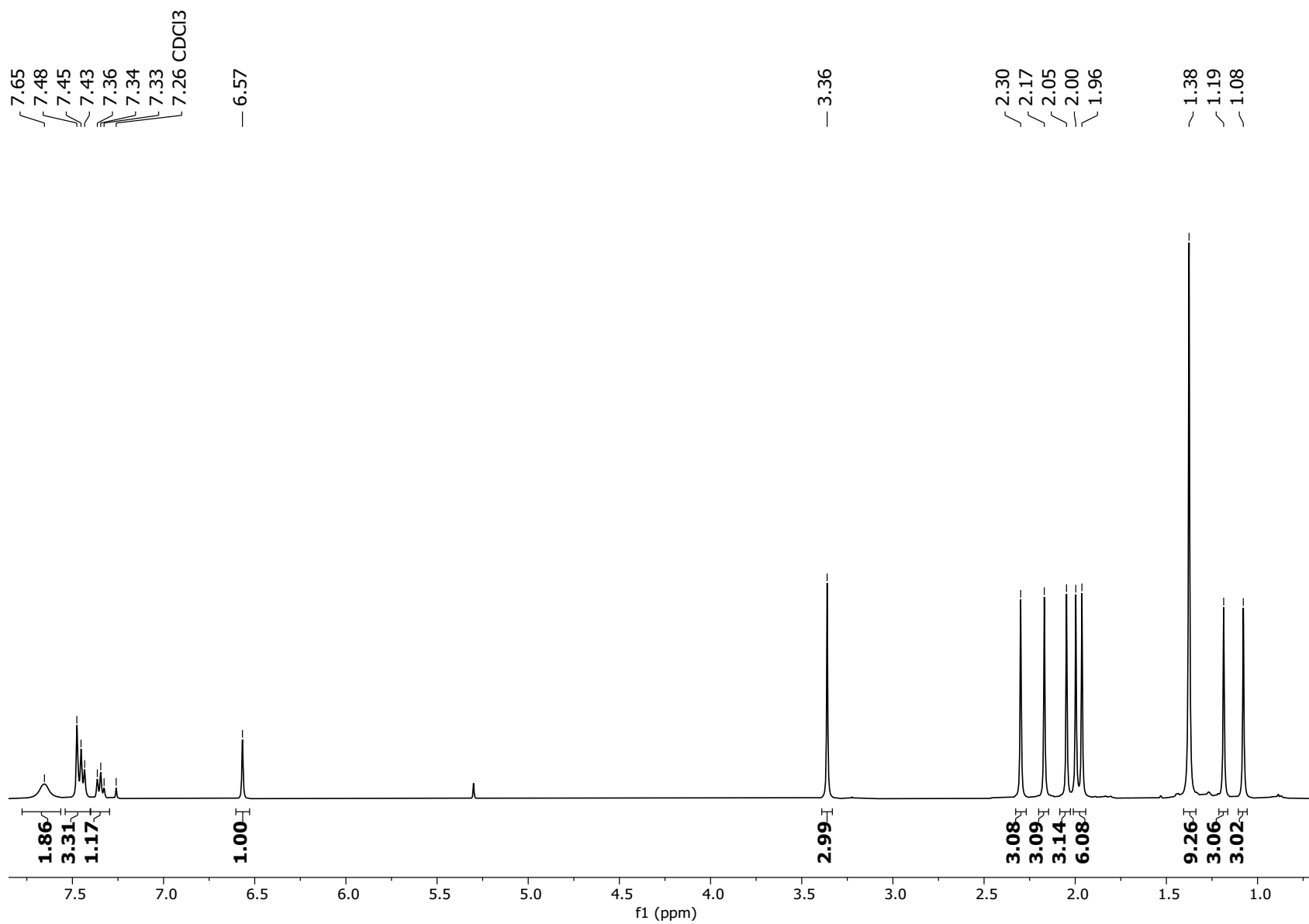


**Figure S32.** <sup>1</sup>H NMR spectrum (400 MHz, 25 °C, CDCl<sub>3</sub>) of **2d-Hf**.

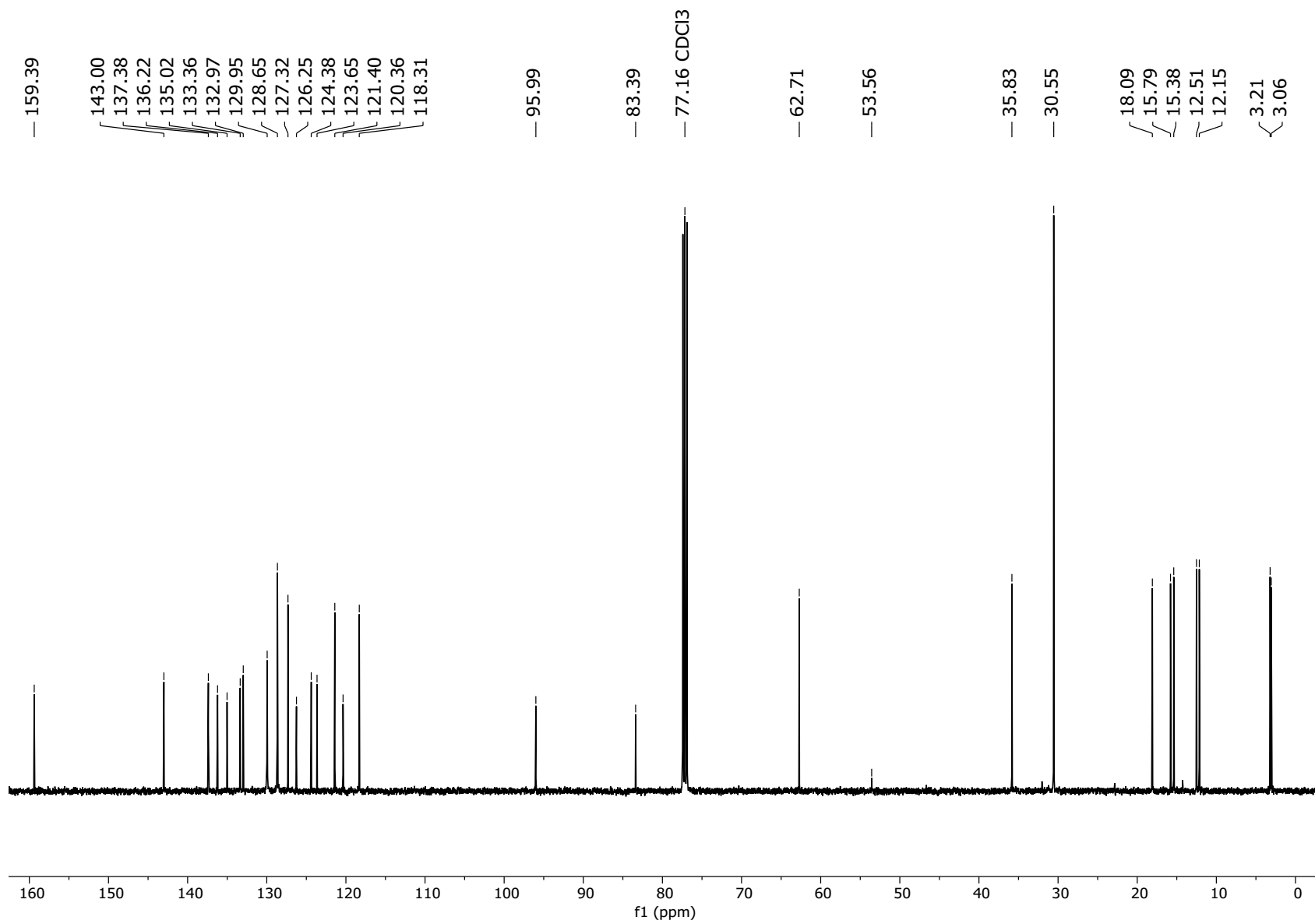


**Figure S33.**  $^{13}\text{C}\{^1\text{H}\}$  NMR spectrum (100 MHz, 25 °C,  $\text{CDCl}_3$ ) of **2d-Hf**.

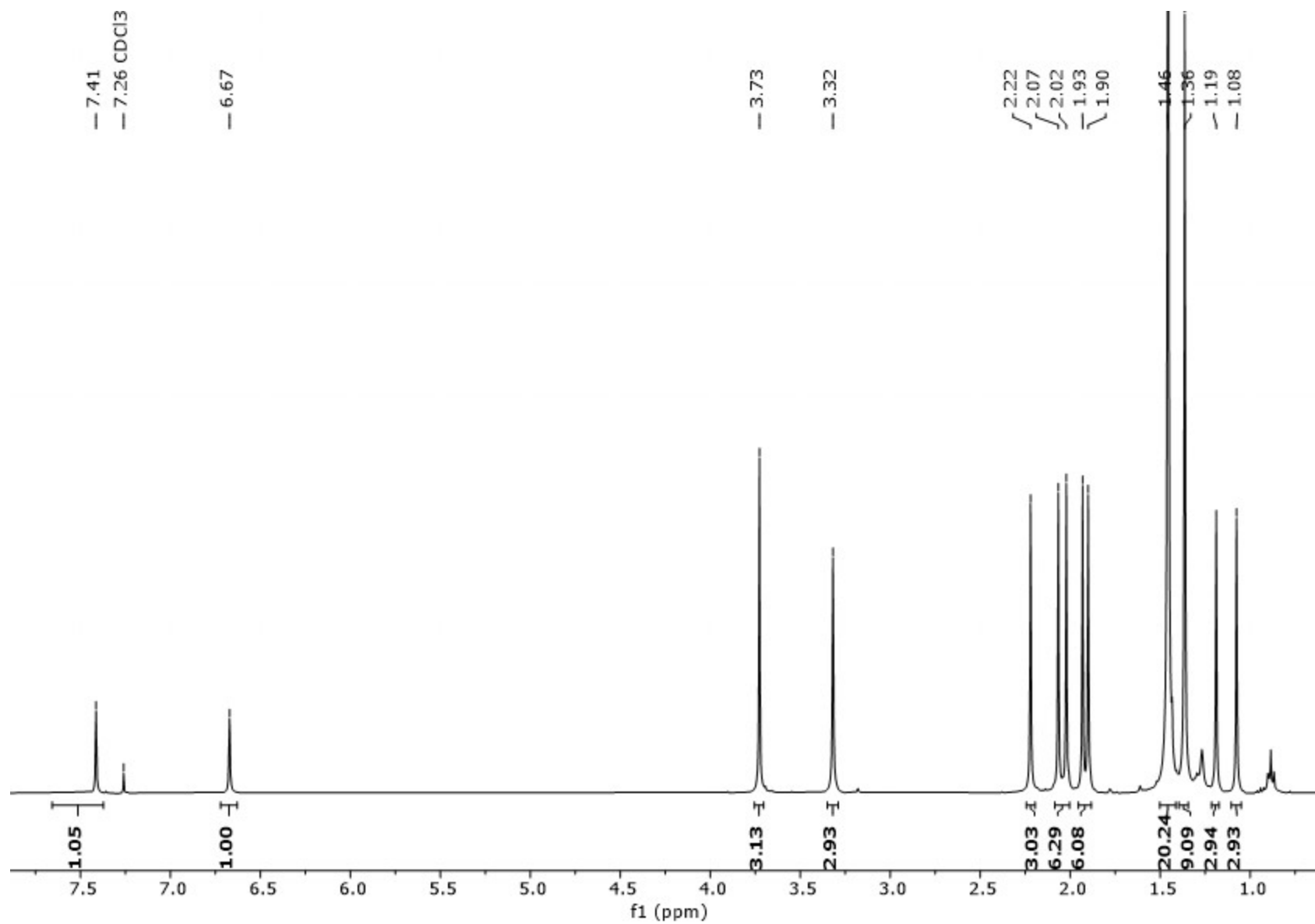


**Figure S34.** <sup>1</sup>H NMR spectrum (400 MHz, 25 °C, CDCl<sub>3</sub>) of **2e-Zr**.

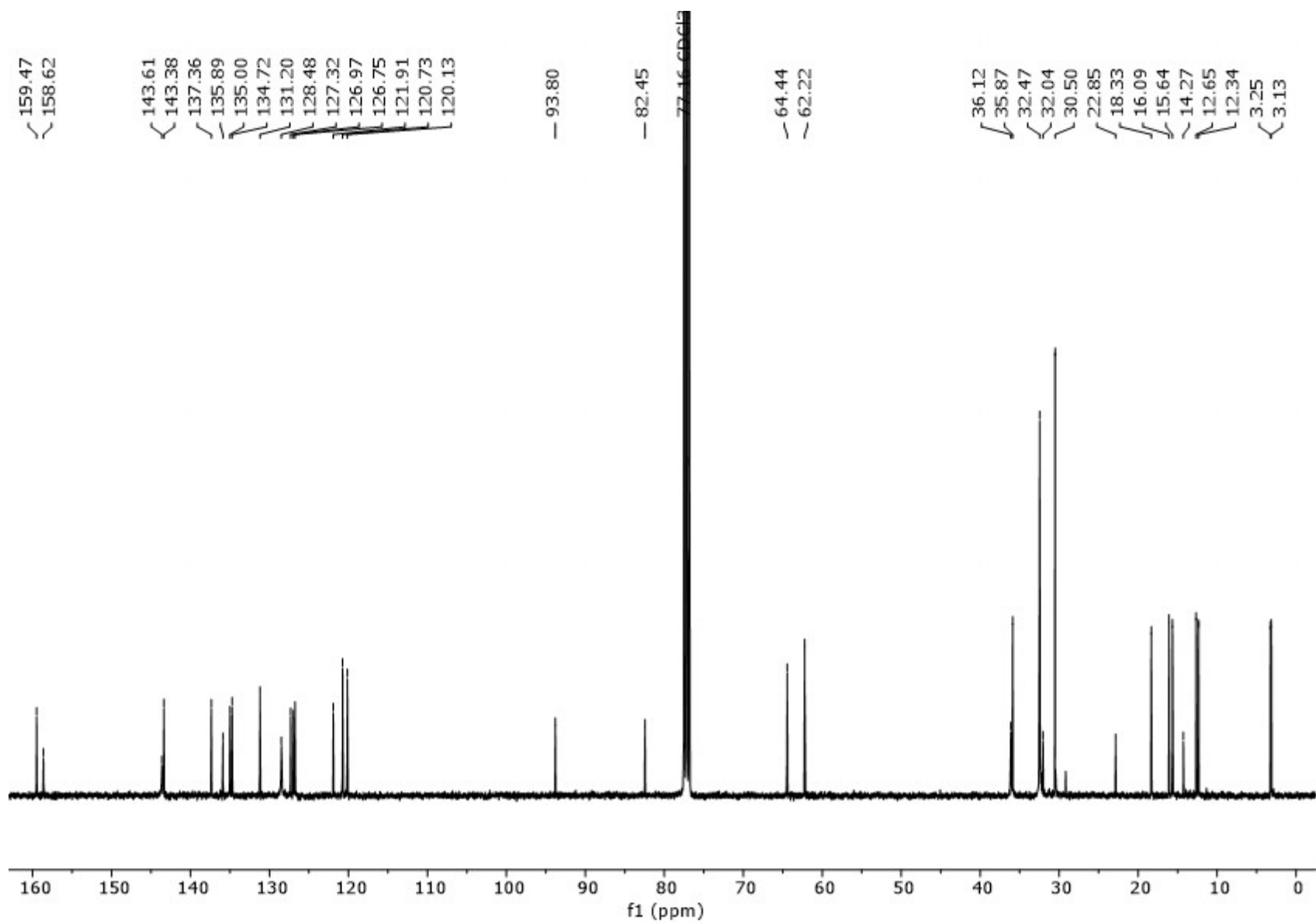


Figure S35.  $^{13}\text{C}\{^1\text{H}\}$  NMR spectrum (100 MHz, 25 °C,  $\text{CDCl}_3$ ) of **2e-Zr**.



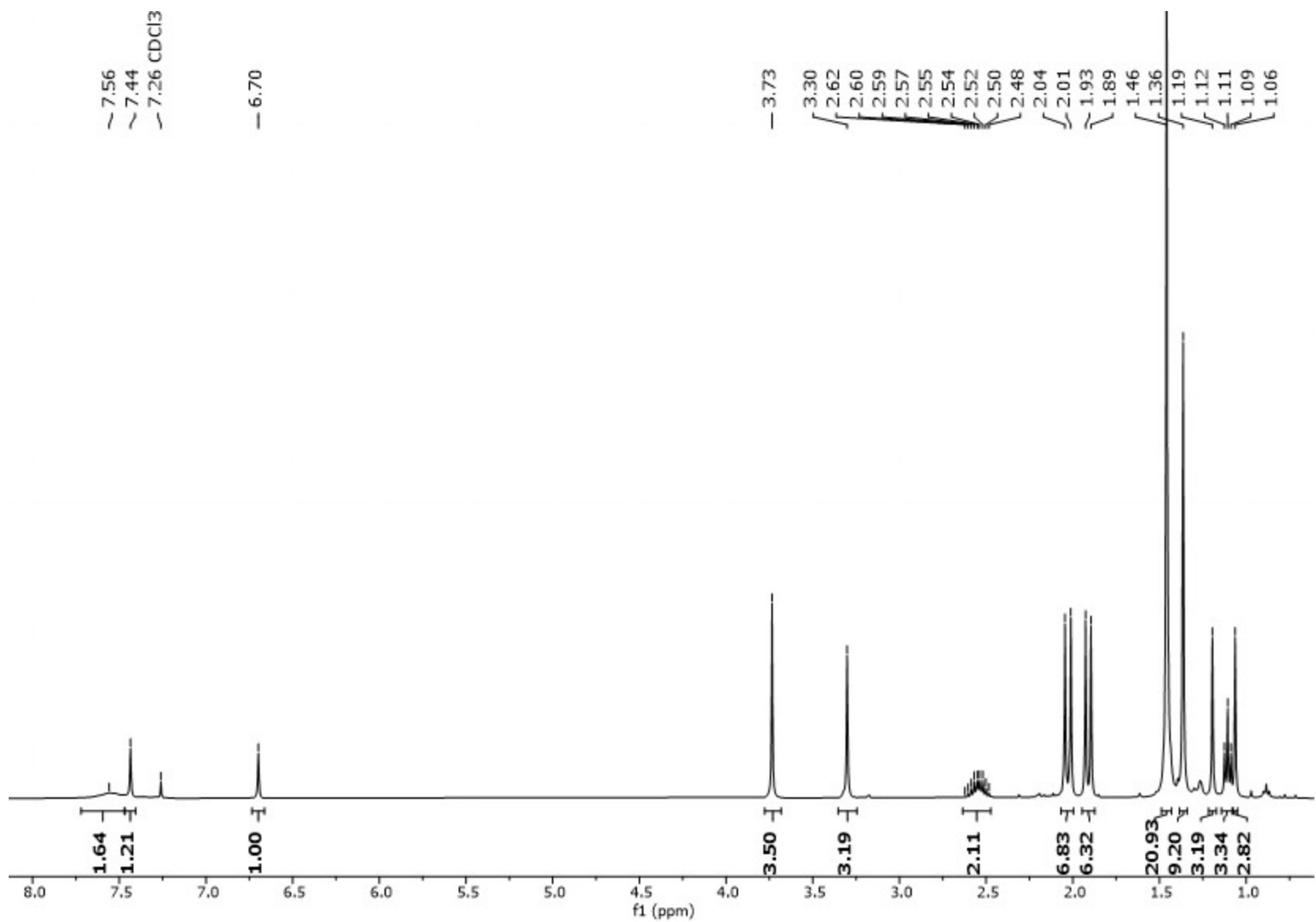


Figure S36. <sup>1</sup>H NMR spectrum (400 MHz, 25 °C, CDCl<sub>3</sub>) of **2f-Zr**.

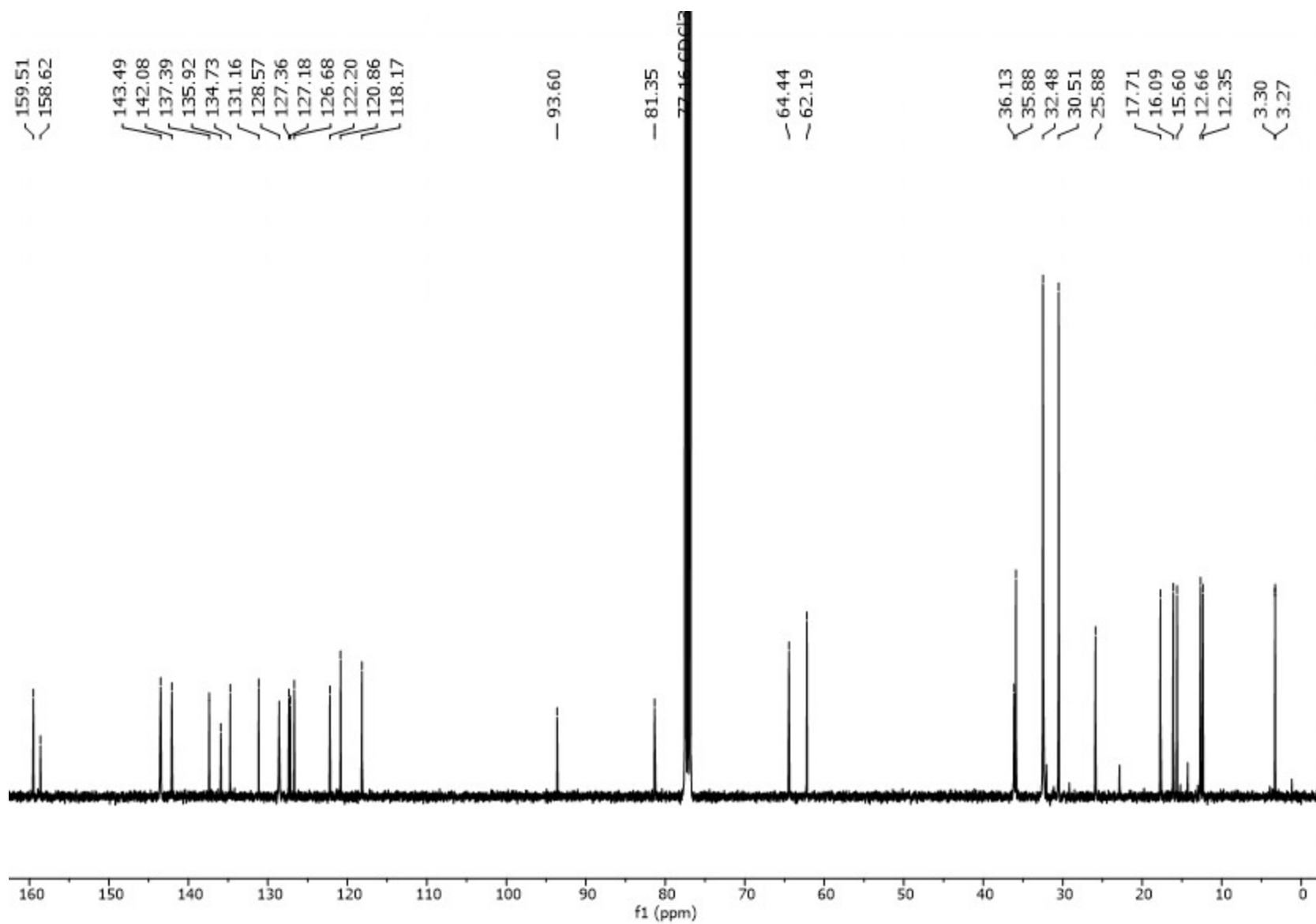


Figure S37.  $^{13}\text{C}\{^1\text{H}\}$  NMR spectrum (100 MHz, 25 °C,  $\text{CDCl}_3$ ) of **2f-Zr**.

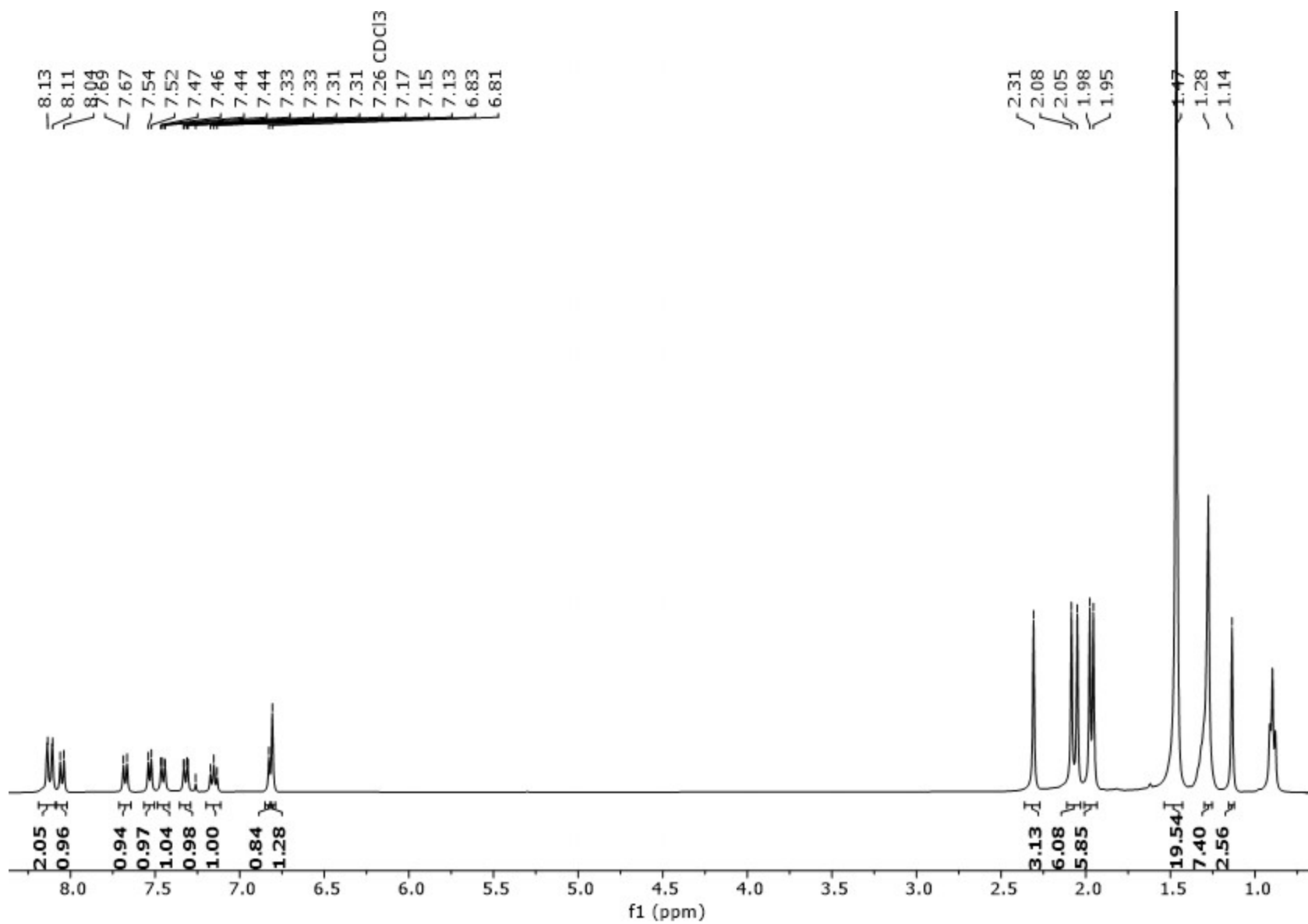
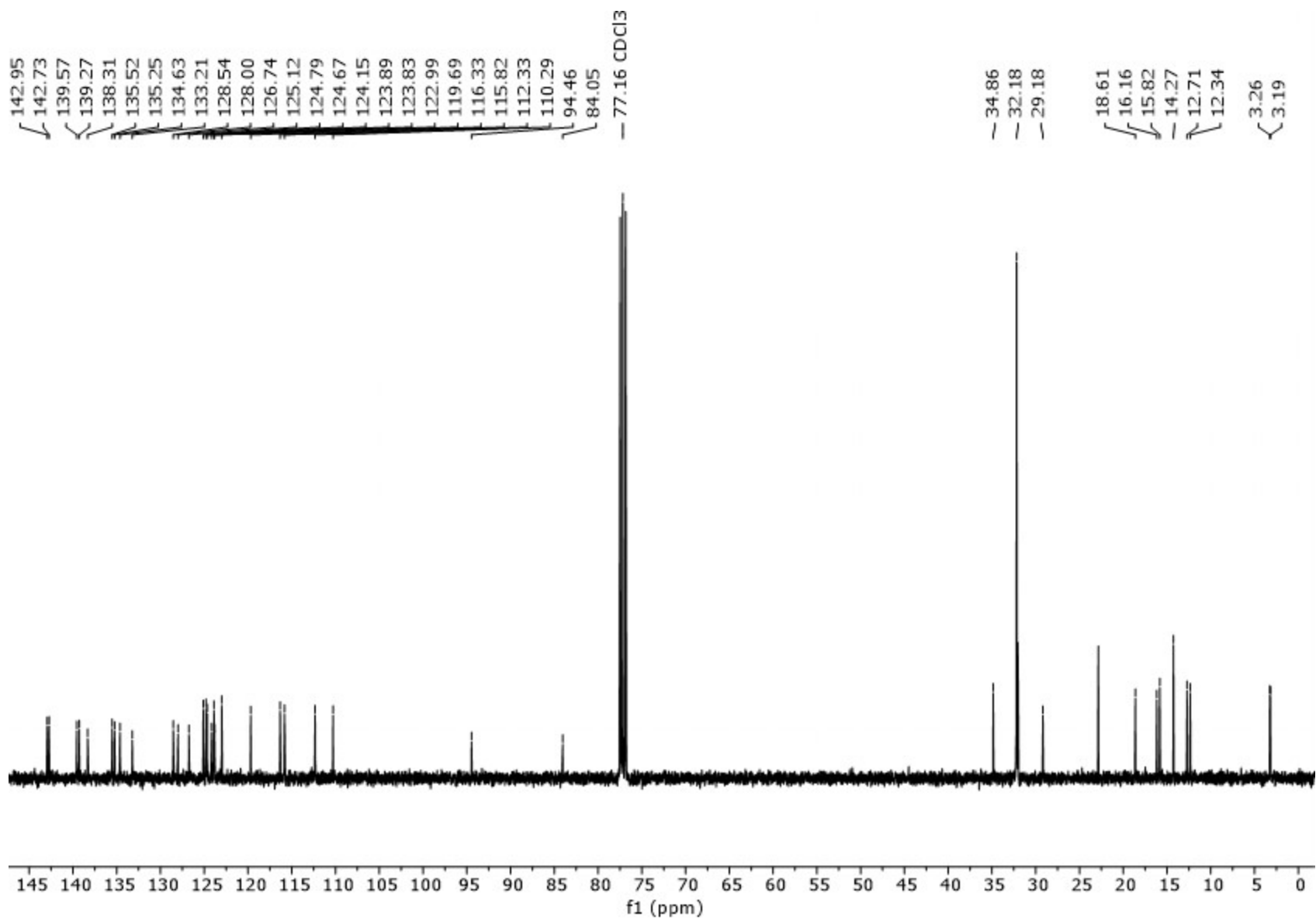


Figure S38. <sup>1</sup>H NMR spectrum (400 MHz, 25 °C, CDCl<sub>3</sub>) of **2g-Zr**.



**Figure S39.**  $^{13}\text{C}\{^1\text{H}\}$  NMR spectrum (100 MHz, 25 °C,  $\text{CDCl}_3$ ) of **2g-Zr**.

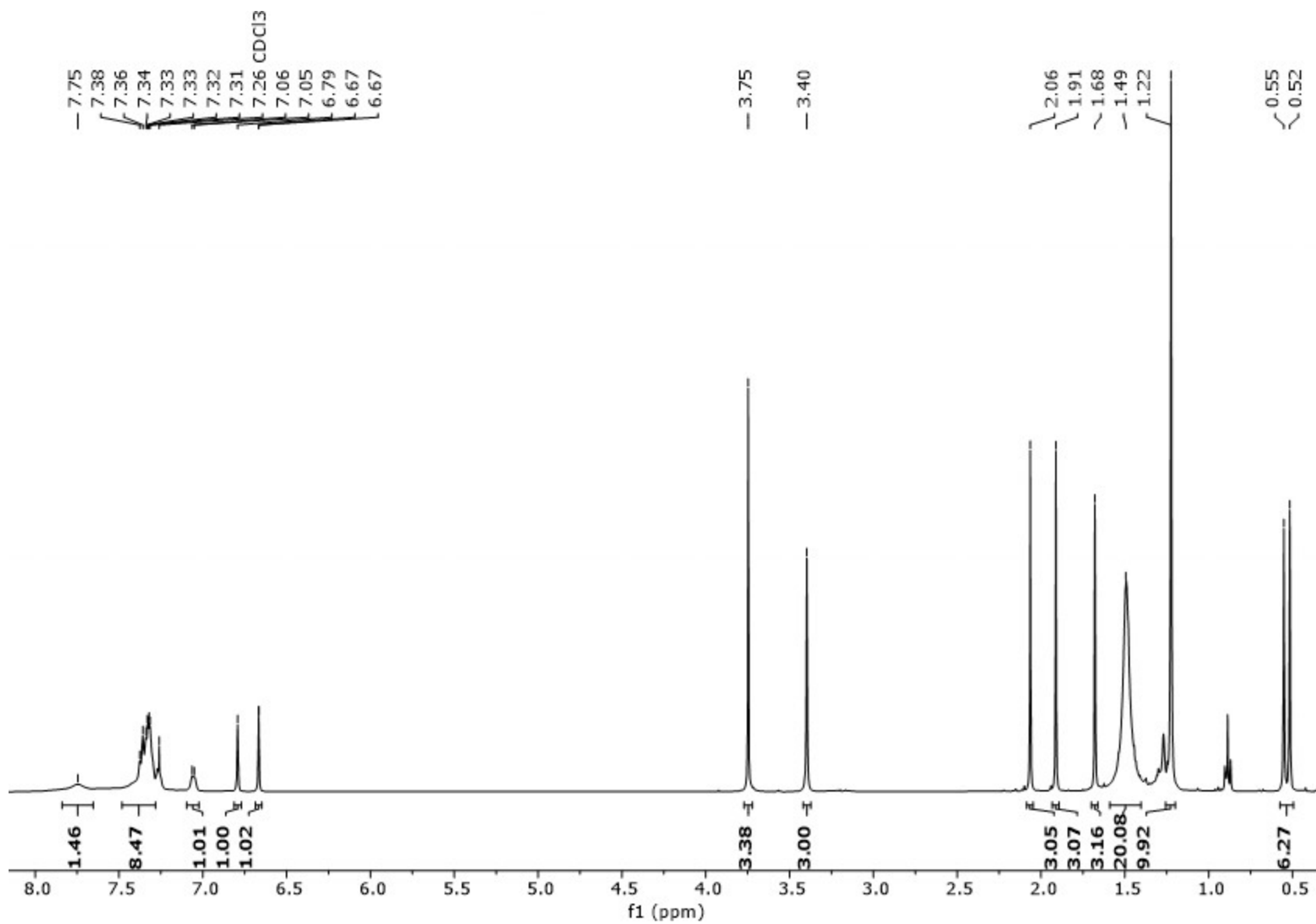
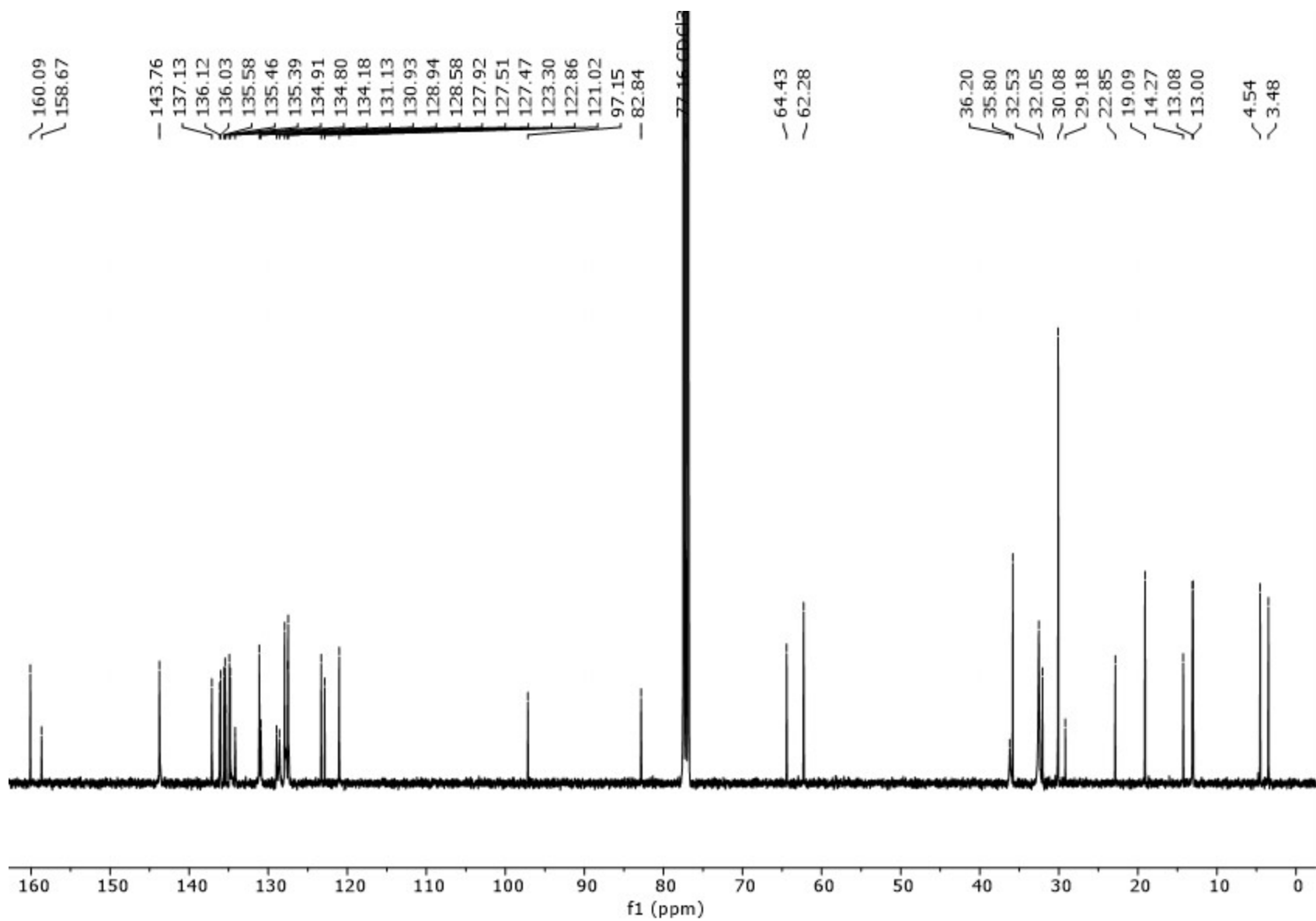
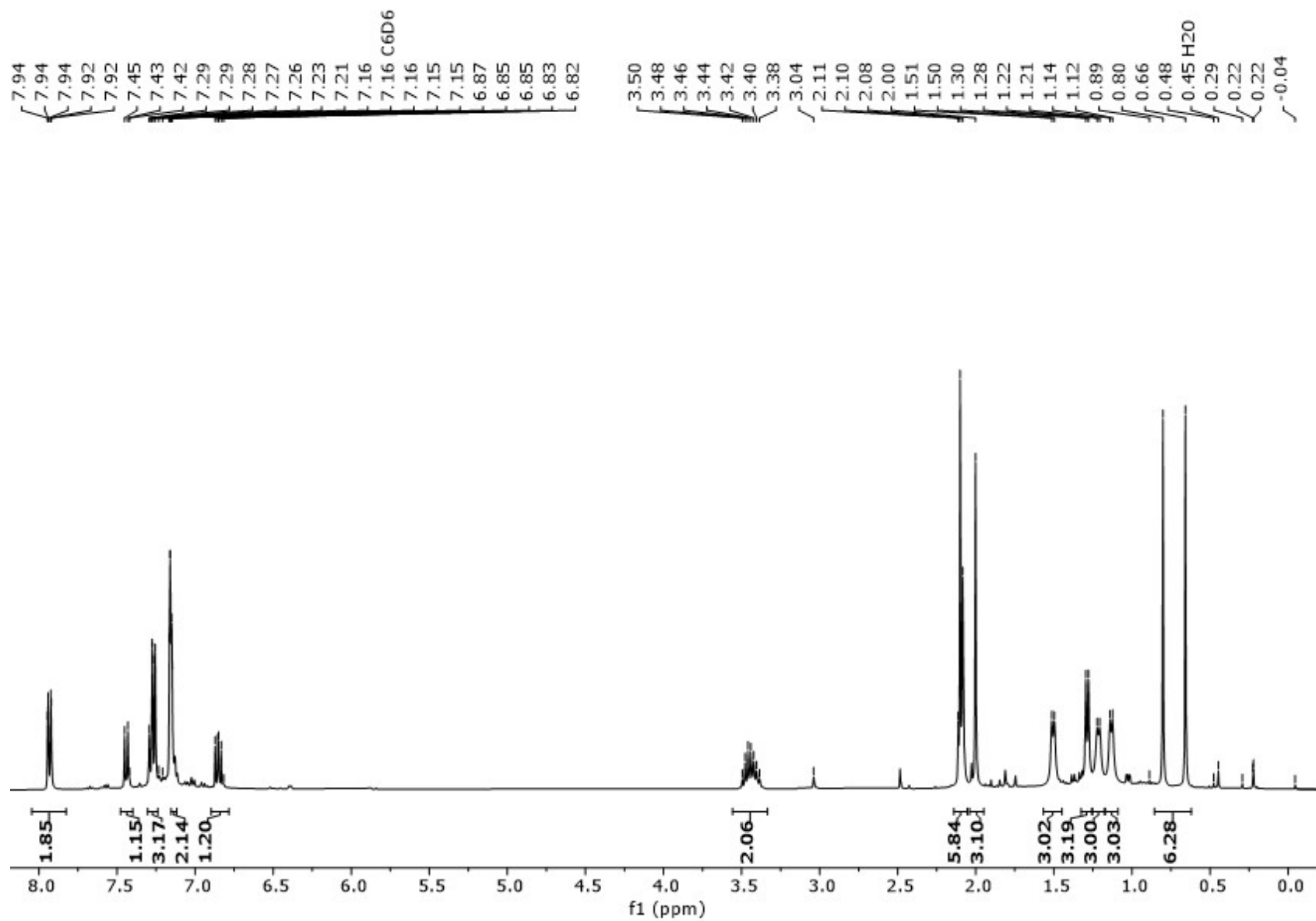


Figure S40. <sup>1</sup>H NMR spectrum (400 MHz, 25 °C, CDCl<sub>3</sub>) of **2h-Zr**.



**Figure S41.**  $^{13}\text{C}\{^1\text{H}\}$  NMR spectrum (100 MHz, 25 °C,  $\text{CDCl}_3$ ) of **2h-Zr**.



**Figure S42.**  $^1\text{H}$  NMR spectrum (400 MHz, 25 °C,  $\text{C}_6\text{D}_6$ ) of **2i-Zr**.

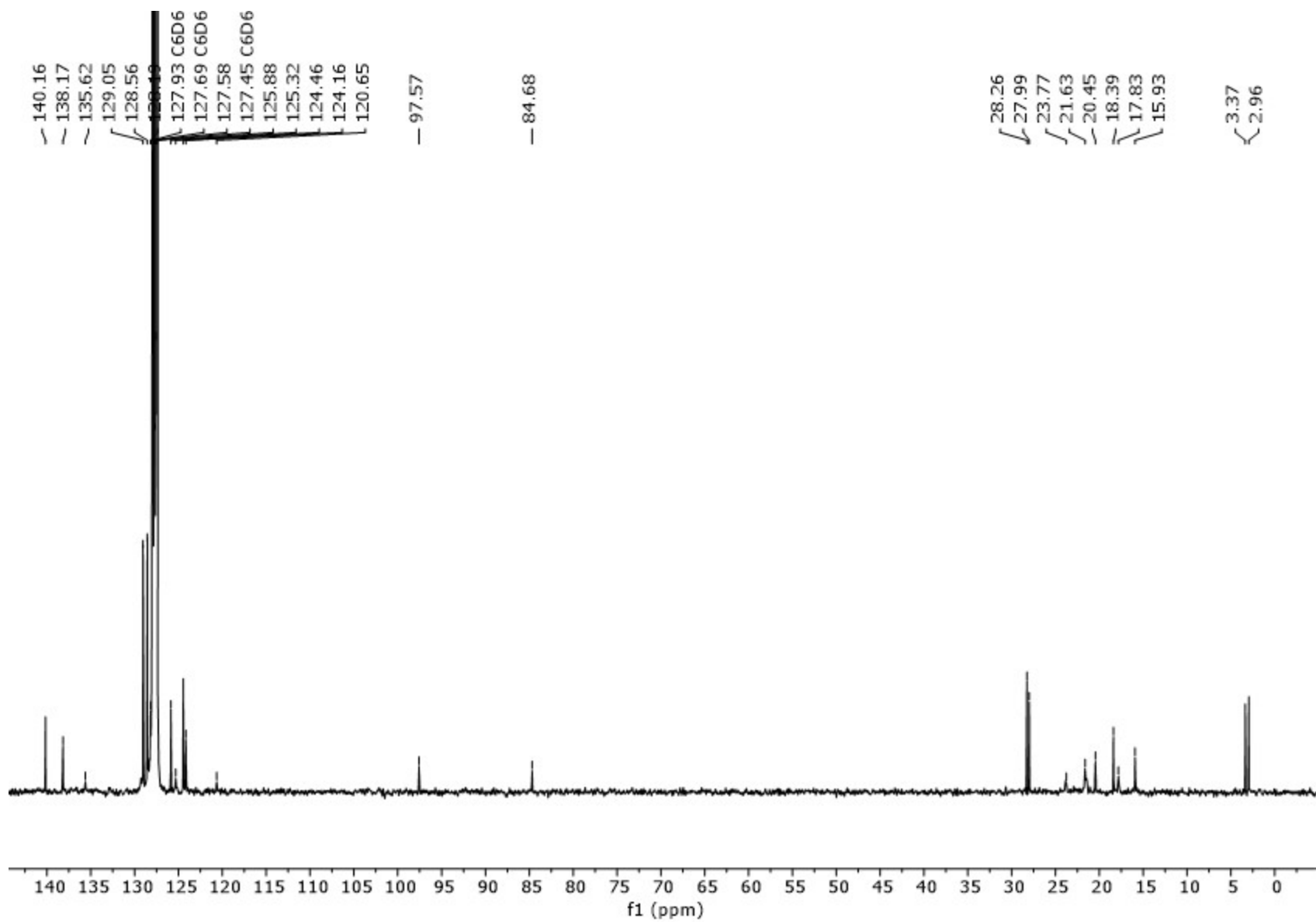


**Figure S43.**  $^{13}\text{C}\{^1\text{H}\}$  NMR spectrum (100 MHz, 25 °C,  $\text{C}_6\text{D}_6$ ) of **2i-Zr**.



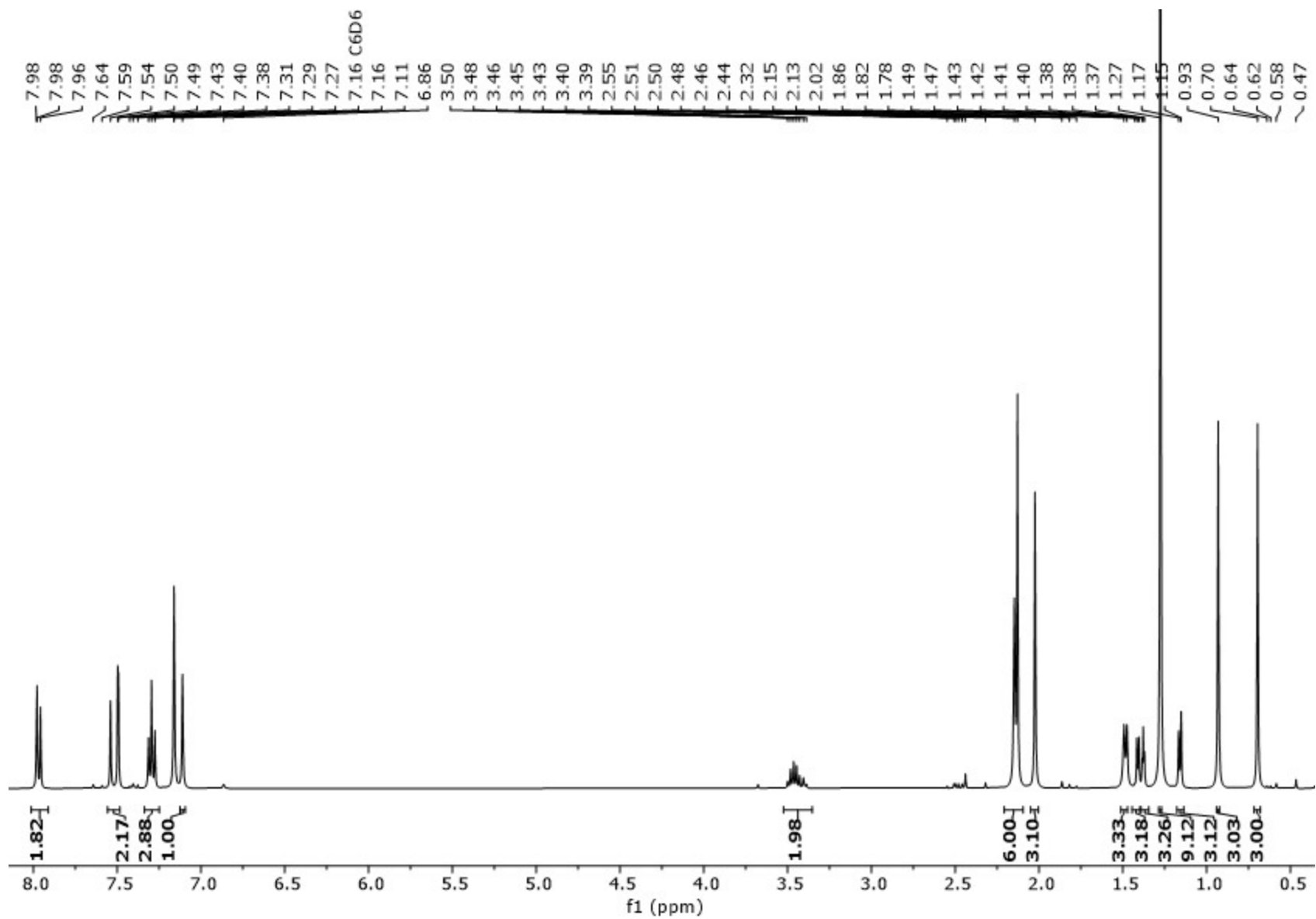
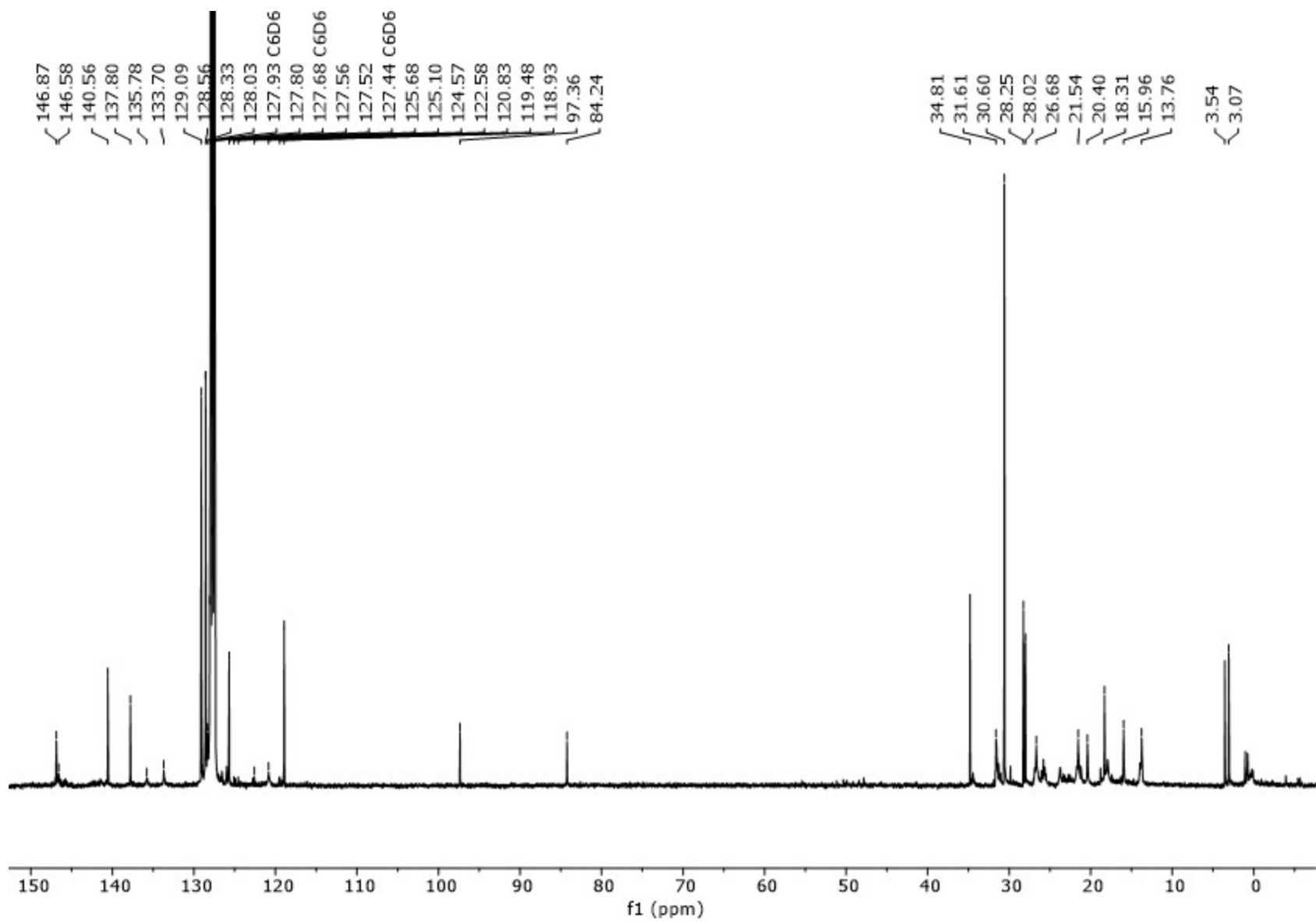
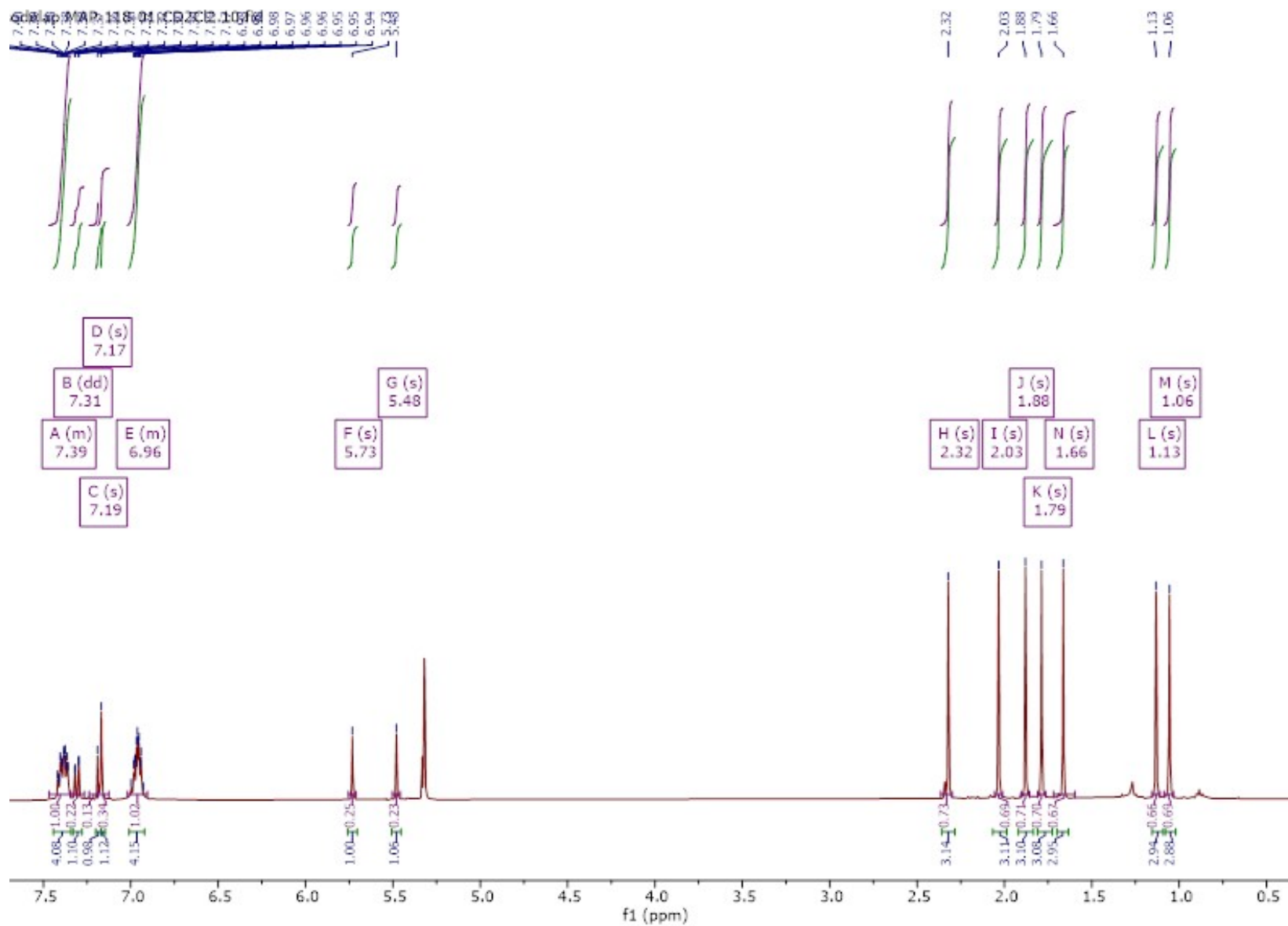


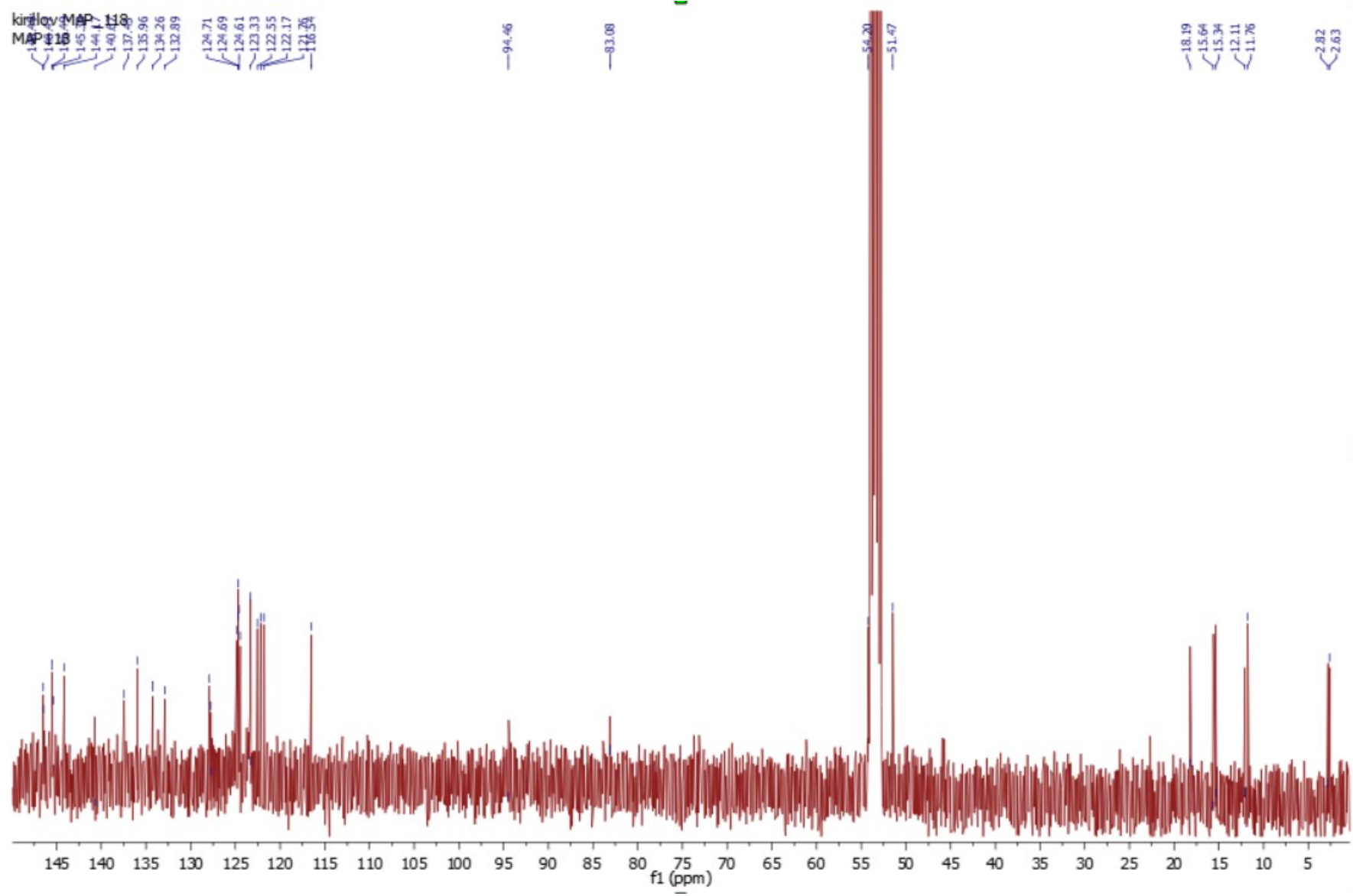
Figure S44.  $^1\text{H}$  NMR spectrum (400 MHz, 25 °C,  $\text{C}_6\text{D}_6$ ) of **2j-Zr**.



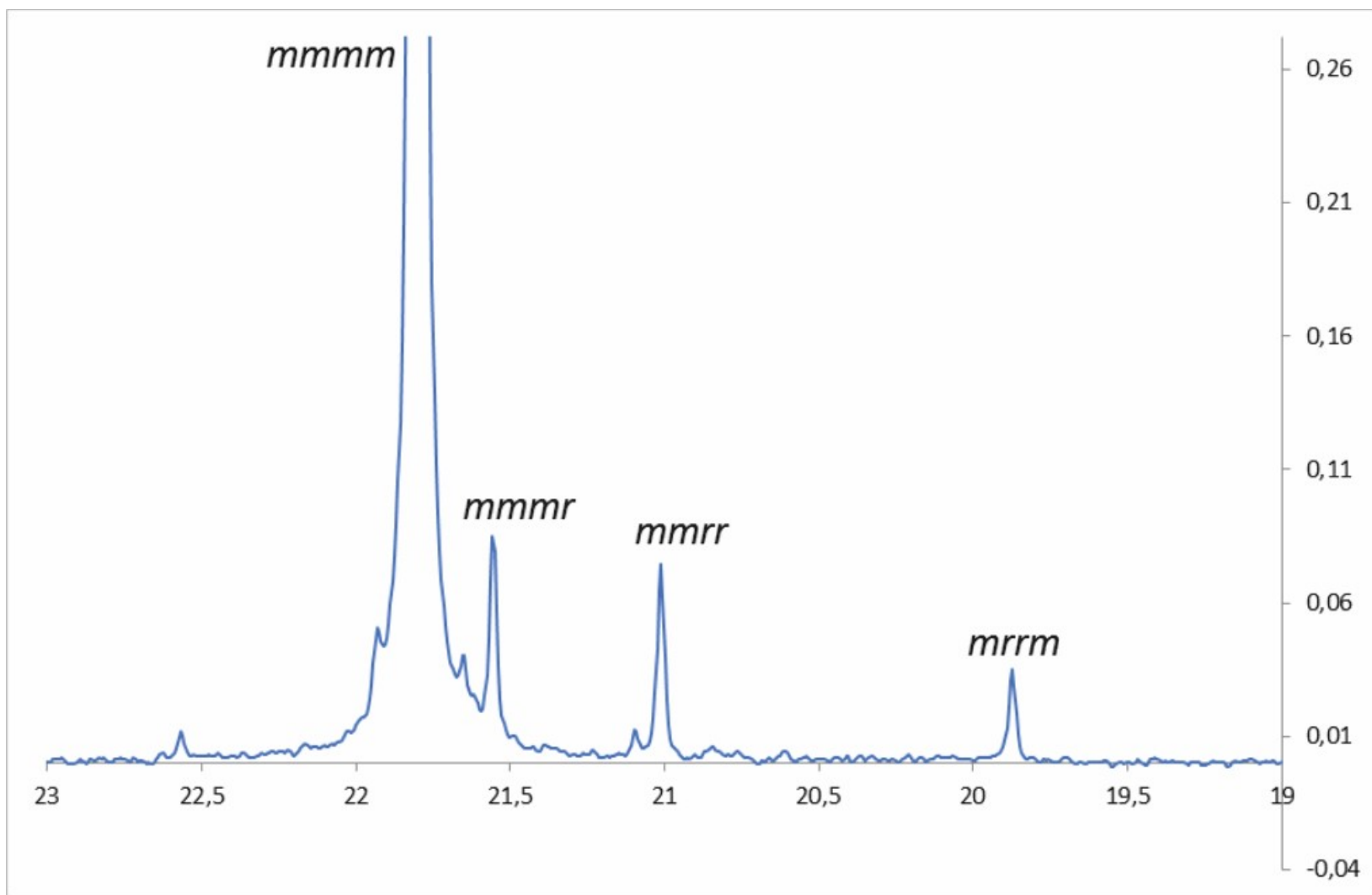
**Figure S45.**  $^{13}\text{C}\{^1\text{H}\}$  NMR spectrum (100 MHz, 25 °C,  $\text{C}_6\text{D}_6$ ) of **2j-Zr**.



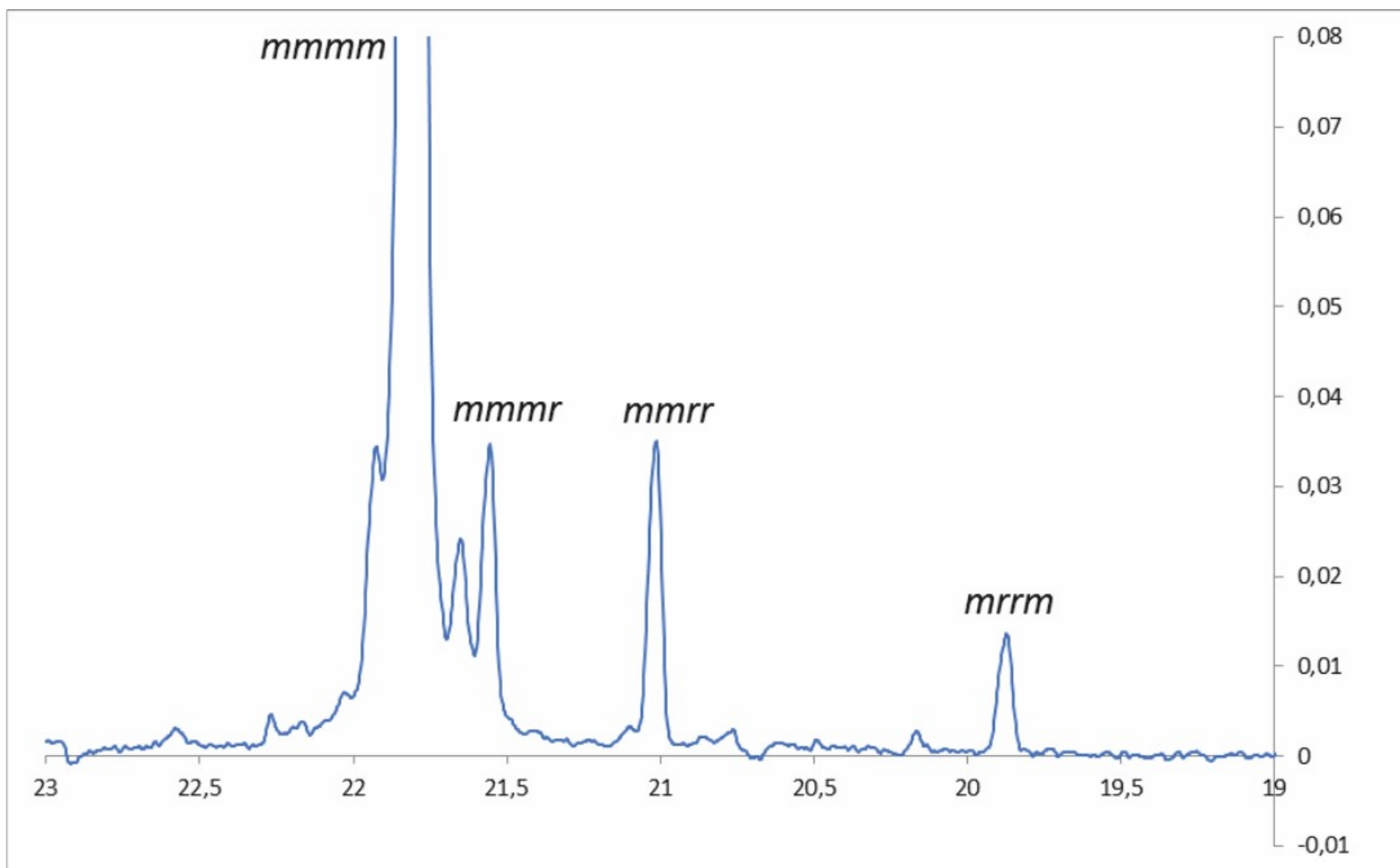
**Figure S46.** <sup>1</sup>H NMR spectrum (400 MHz, 25 °C, CD<sub>2</sub>Cl<sub>2</sub>) of **2k-Zr**.



**Figure S47.**  $^{13}\text{C}\{^1\text{H}\}$  NMR spectrum (100 MHz, 25 °C,  $\text{CD}_2\text{Cl}_2$ ) of **2k-Zr**.

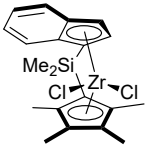
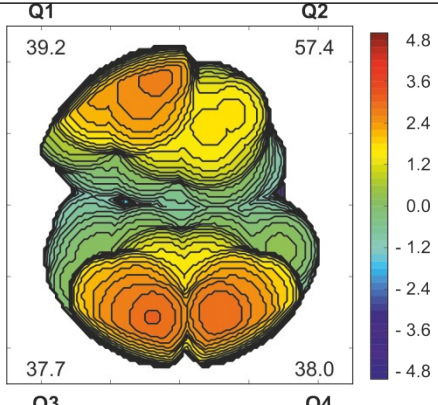
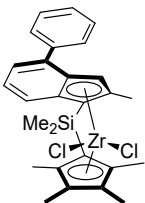
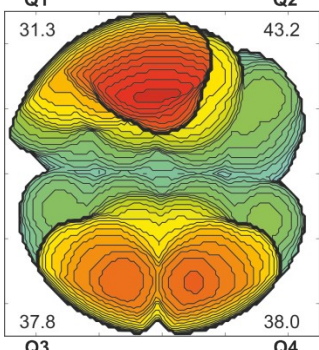
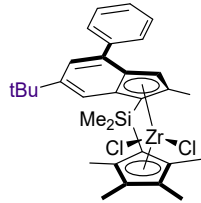
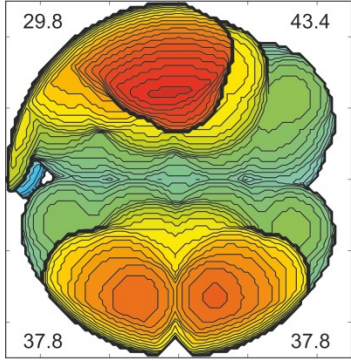
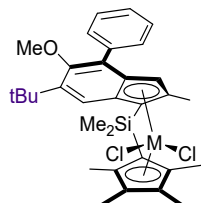
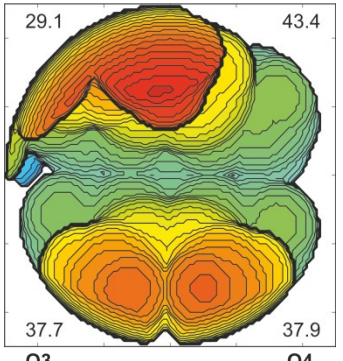


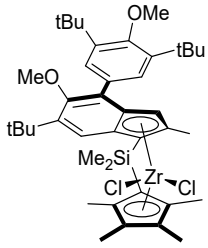
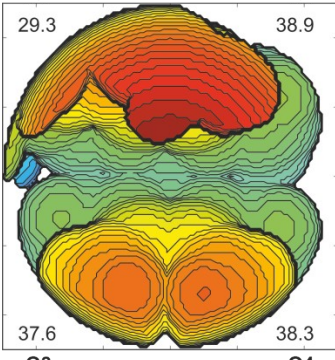
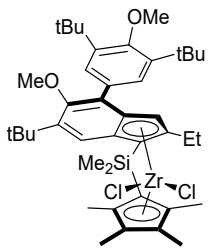
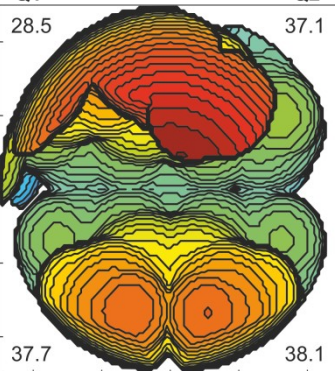
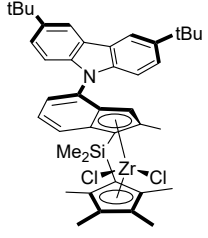
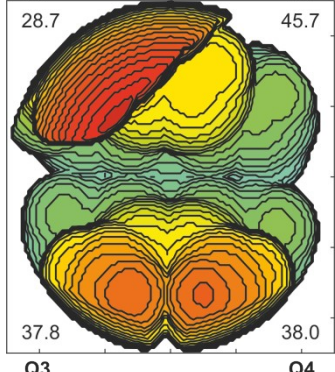
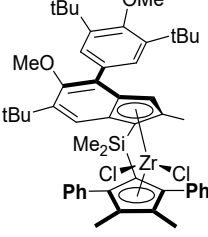
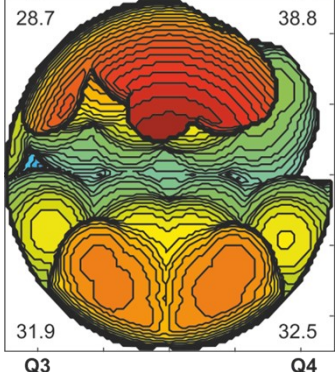
**Figure S48.**  $^{13}\text{C}\{^1\text{H}\}$  NMR spectrum (125 MHz, 135 °C,  $\text{C}_6\text{D}_6/\text{C}_6\text{H}_3\text{Cl}_3$ ) of an iPP sample obtained with precursor **2h-Zr** (Table 2, entry 14).



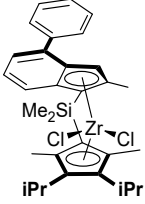
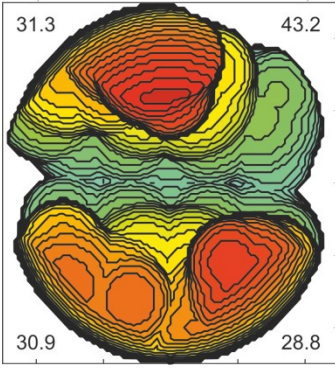
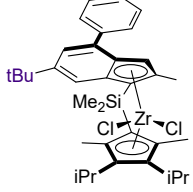
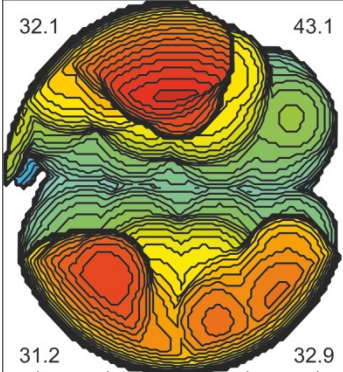
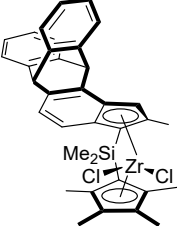
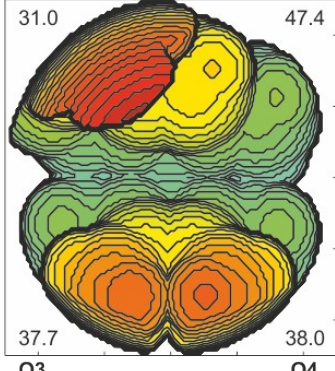
**Figure S49.**  $^{13}\text{C}\{^1\text{H}\}$  NMR spectrum (125 MHz, 135 °C,  $\text{C}_6\text{D}_6/\text{C}_6\text{H}_3\text{Cl}_3$ ) of an iPP sample obtained with precursor **2e-Zr** (Table 2, entry 8).

**Table S1.** Steric maps generated for the DFT-optimized (B3PW91/LANL2DZ) geometries of the synthesized {Cp/Ind} *ansa*-zirconocenes with sphere radius = 5 Å.<sup>18</sup>

Complex	Structure	Steric map, $\Delta\%V_{\text{free,Q1-Q4}}$	$\Delta\%V_{\text{free, total}}$
<b>2a-Zr</b>			43.1
<b>2b-Zr</b>			37.6
<b>2c-Zr</b>			37.2
<b>2d-Zr</b>			37.0

<p><b>2e-Zr</b></p>			<p>36.0</p>
<p><b>2f-Zr</b></p>			<p>35.4</p>
<p><b>2g-Zr</b></p>			<p>37.6</p>
<p><b>2h-Zr</b></p>			<p>33.0</p>



<p><b>2i-Zr</b></p>			<p>33.5</p>
<p><b>2j-Zr</b></p>			<p>34.8</p>
<p><b>2k-Zr</b></p>			<p>38.5</p>

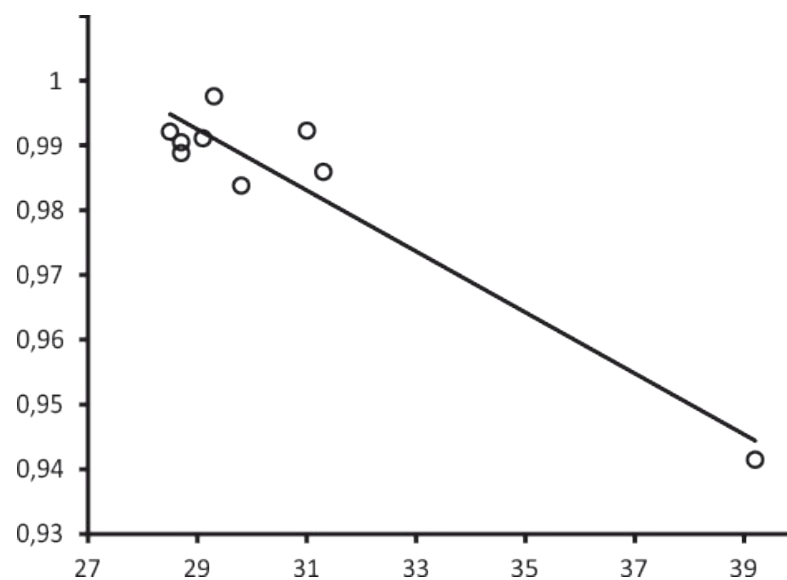


**Figure S50.** Plot of probabilistic descriptor  $b$  vs the  $\Delta\%V_{\text{free},Q1}$  of quadrants Q1 in metallocene complexes **2a-h,k-Zr** ( $R^2 = 0.900$ ).

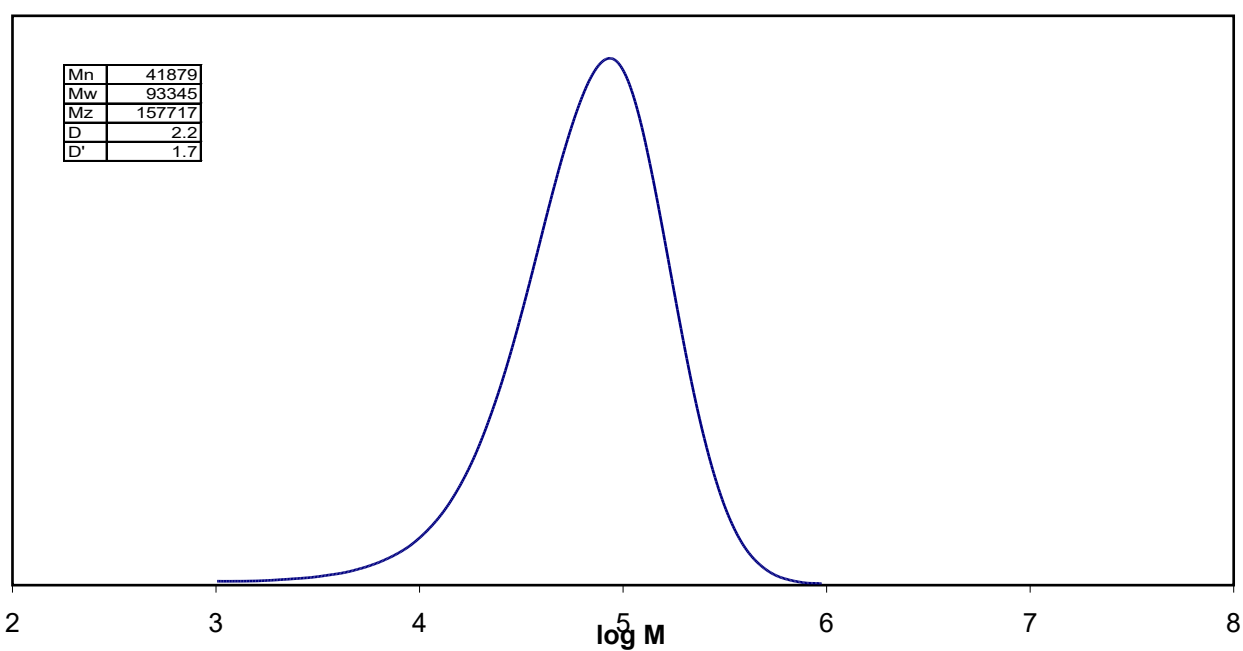


**Figure S51.** GPC trace for the iPP obtained with **2e-Zr** (Table 2, entry 9).

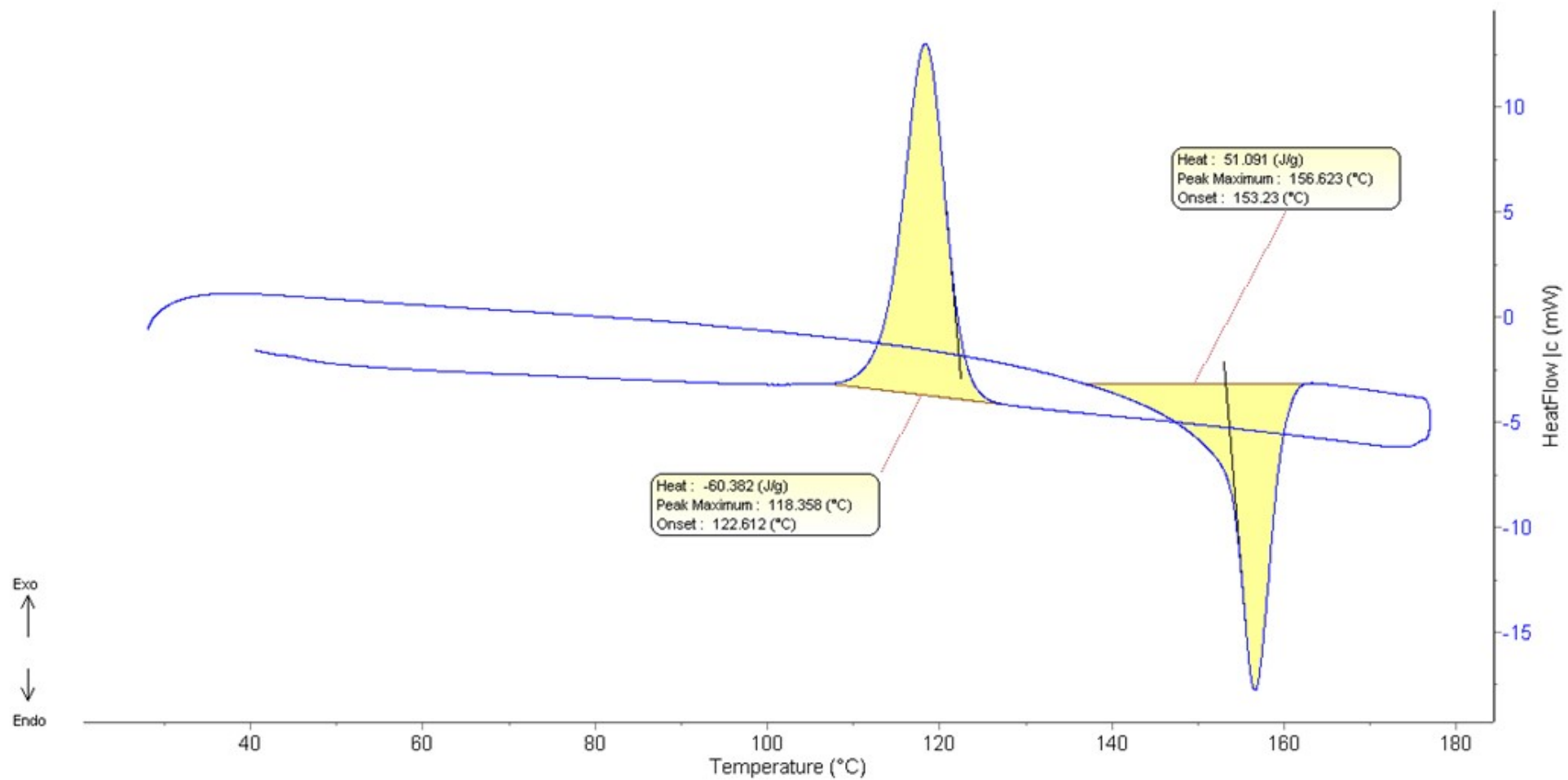


**Figure S52.** DSC curve for the iPP obtained with **2e-Zr** (Table 2, entry 9).

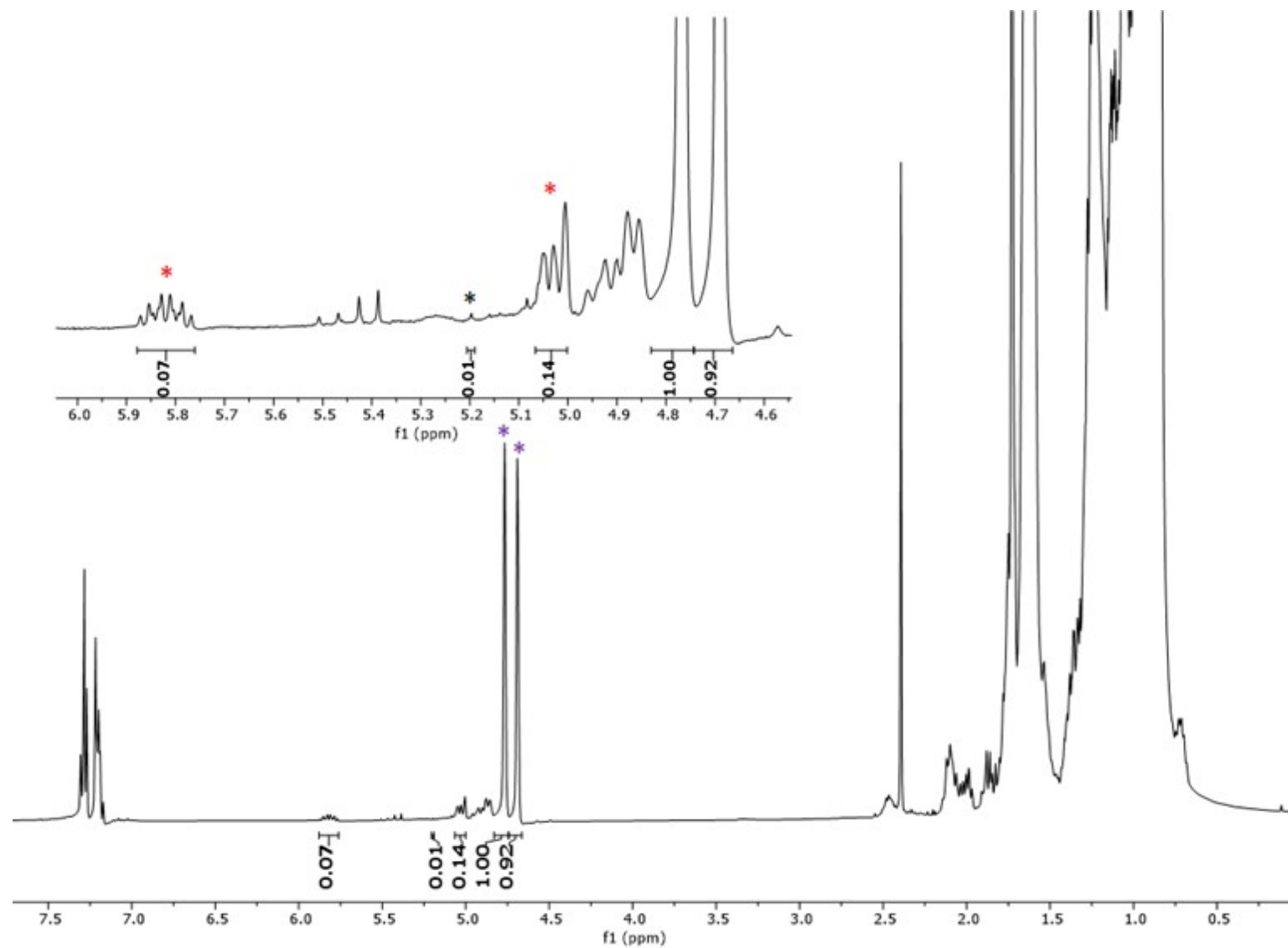


**Figure S53.** <sup>1</sup>H NMR spectrum (400 MHz, CDCl<sub>3</sub>, 25 °C) of oligomers produced with **2i-Zr** complex (Table 2, entry 16). \*Vinylidenic, \*Vinyllic, \*Isobutenyl end-groups. Ratio (93/6/<1).

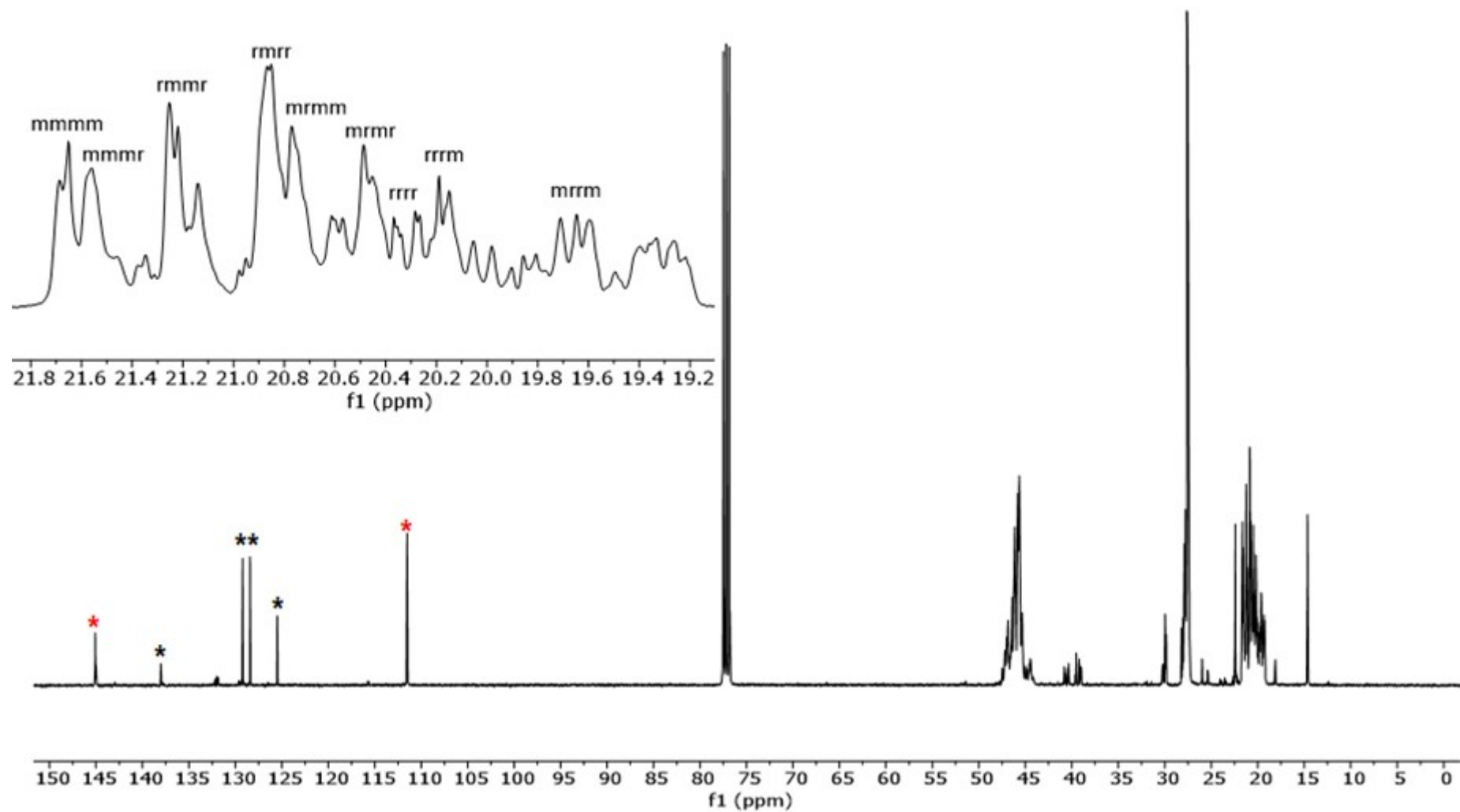


**Figure S54.**  $^{13}\text{C}\{^1\text{H}\}$  NMR spectrum (100 MHz, 25 °C,  $\text{CDCl}_3$ ) of oligomers produced with **2i-Zr**/MAO (Table 2, entry 16). \* stand for vinylidene chain ends, \*\* stand for residual toluene.

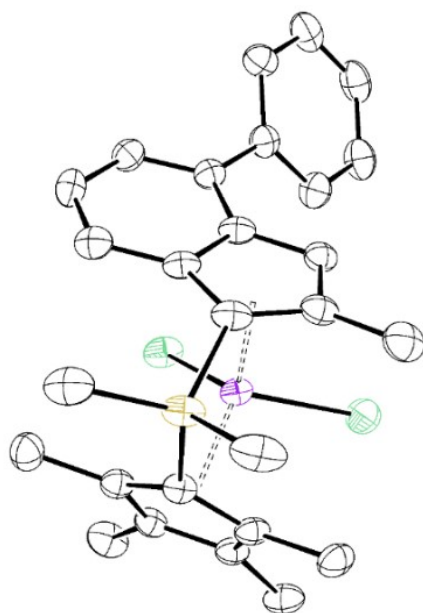


**Figure S55.** Molecular structures of **2b-Hf** (H atoms are omitted for clarity; ellipsoids are drawn at the 50% probability level).

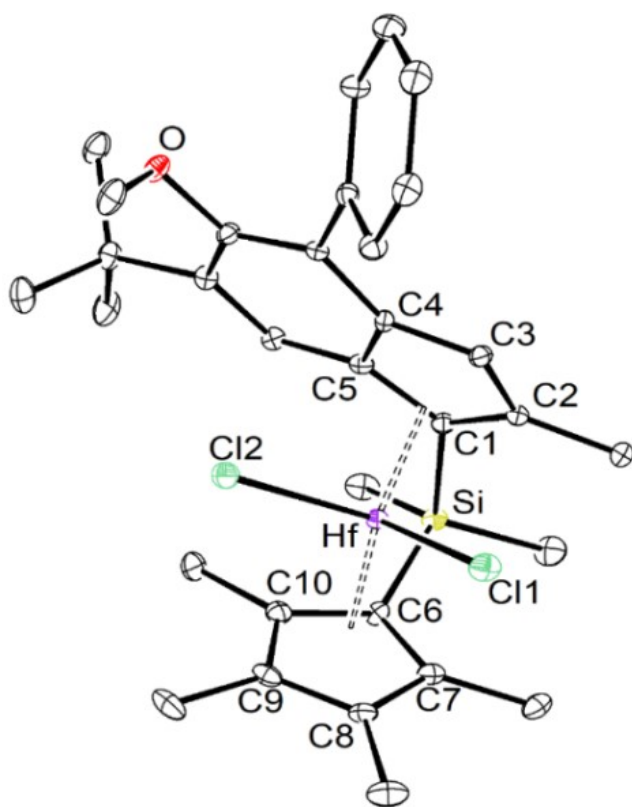


**Figure S56.** Molecular structures of **2d-Hf** (H atoms are omitted for clarity; ellipsoids are drawn at the 50% probability level).

**Table S2.** Summary of Crystal and Refinement Data for Complexes **2a,b-Zr**, **2b-Hf**, **2d-Zr,Hf**, **2e,f -Zr**.

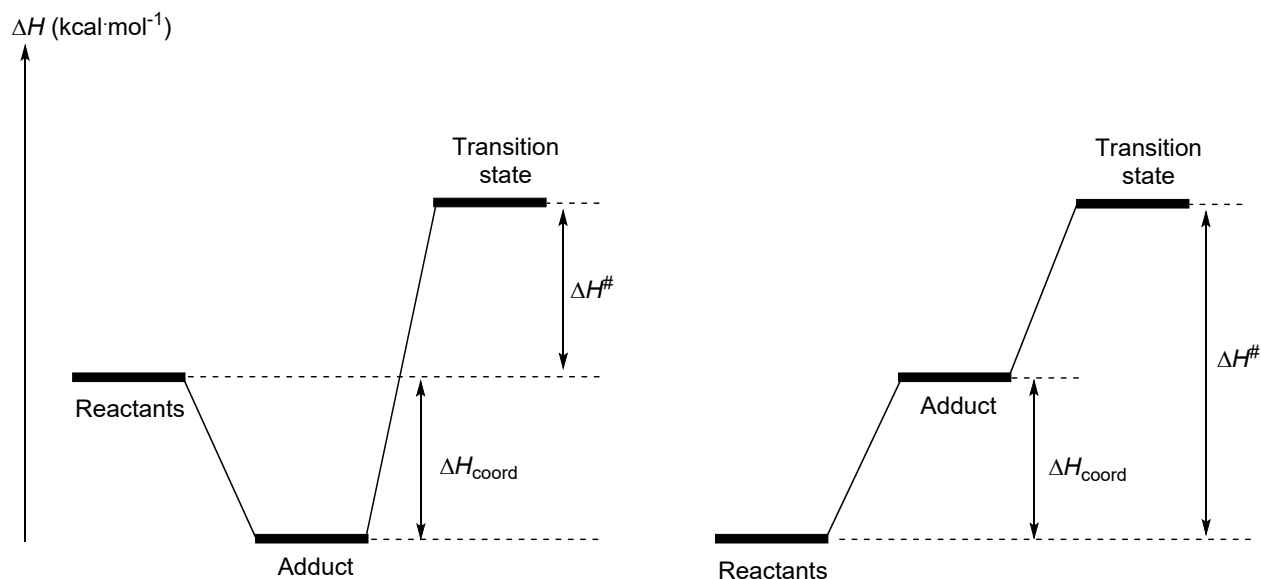
Complexes	<b>2a-Zr</b>	<b>2b-Zr</b>	<b>2b-Hf</b>	<b>2d-Zr</b>	<b>2d-Hf</b>	<b>2e-Zr</b>
Empirical formula	C20H24Cl2SiZr	C27H30Cl2SiZr	C27H30Cl2HfSi	C32H40Cl2OSiZr	C32H40Cl2HfOSi	C41H58Cl2O2SiZr
Formula weight	454.60	544.72	631.99	630.85	718.12	773.08
Temperature, K	150	150	150	150	150	150
Wavelength, Å	0.71073	0.71073	0.71073	0.71073	0.71073	0.71073
Crystal system	triclinic	triclinic	triclinic	monoclinic	monoclinic	triclinic
Space group	P -1	P -1	P -1	P 2 <sub>1</sub> /C	P 2 <sub>1</sub> /C	P 1
a, Å	9.640(2)	10.2268(13)	10.2320(15)	13.5939(16)	13.5837(12)	10.5046 (9)
b, Å	10.518(3)	11.5064	11.6128(15)	13.3843(13)	13.3364(11)	13.1681 (11)
c, Å	10.543(2)	12.7604(15)	12.8244(17)	17.1306(19)	17.0243(17)	17.5901 (15)
β, deg	71.581(9)	67.191(4)	67.625(5)	107.912(4)	107.861(3)	98.242 (3)
Volume, Å <sup>3</sup>	959.5(4)	1370.6(3)	1394.7(3)	2965.8(6)	2935.4(5)	2110.1 (3)
Z	2	2	2	4	4	2
Density (calc.), Mg/m <sup>3</sup>	1.573	1.320	1.505	1.413	1.625	1.217
Absorption coefficient, mm <sup>-1</sup>	0.913	0.652	3.986	0.615	3.801	0.446
Crystal size, mm <sup>3</sup>	0.110 x 0.080 x 0.070	0.340 x 0.270 x 0.240	0.180 x 0.120 x 0.090	0.310 x 0.180 x 0.120	0.300 x 0.130 x 0.130	0.220 x 0.090 x 0.040
Reflections collected	4222	25557	25697	21525	30160	37788
Independent reflections	2880	6280	6319	6750	6725	9542
Max. and min. transmission	0.938 , 0.714	0.855, 0.744	0.699, 0.506	0.929, 0.811	0.610, 0.465	0.982, 0.859
Data / restraints / parameters	4222 / 0 / 224	6280 / 0 / 287	6319 / 0 / 257	6750 / 0 / 345	6725 / 0 / 334	9542 / 0 / 442
Final R indices [I>2σ(I)]	0.0562 (0.1157)	0.0546 (0.1402)	0.0406 (0.1056)	0.0544 (0.1413)	0.0304 (0.0791)	0.0343 (0.0836)
R indices (all data)	0.0996 (0.1398)	0.0588 (0.1434)	0.0502 (0.1115)	0.0703 (0.1567)	0.0389 (0.0854)	0.0424 (0.0879)
Goodness-of-fit on F <sup>2</sup>	0.941	1.146	1.195	1.063	1.177	1.024
Largest diff. peak, e.Å <sup>-3</sup>	0.691 and -0.673	1.497 and -1.180	1.426 and -2.144	0.854 and -0.797	2.413 and -1.631	0.502 and -0.659

**Table S2 (continued).** Summary of Crystal and Refinement Data for Complexes **2f,j,k-Zr**.

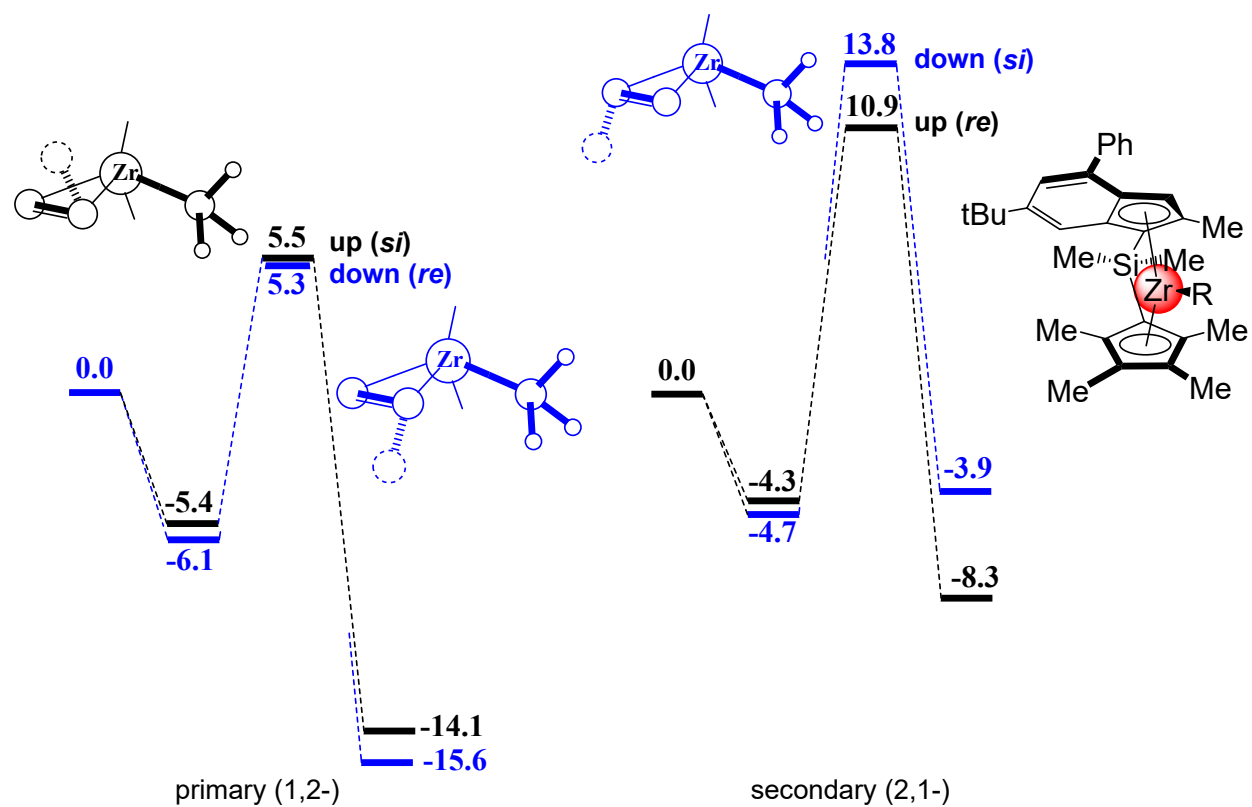
Complexes	<b>2f-Zr</b>	<b>2j-Zr</b> ·(toluene)	<b>2k-Zr</b>
Empirical formula	C42H60Cl2O2SiZr	(C35 H46 Cl2 Si Zr) <sub>3</sub> ·C7 H16	C35H34Cl2SiZr
Formula weight	787.11	2070.97	644.83 g/mol
Temperature, K	296	150	150
Wavelength, Å	0.71073	0.71073	0.71073
Crystal system	triclinic	triclinic	monoclinic
Space group	P 1	P -1	P 21/n
a, Å	9.2245 (8)	12.6320(8)	10.8073(10)
b, Å	9.6841 (8)	18.1924(14)	17.0431(16)
c, Å	24.836 (8)	23.8569(17)	15.6166(16)
β, deg	2094.7 (3)	85.210(2)	93.240(4)
Volume, Å <sup>3</sup>	97.894 (3)	5433.44	2871.8(5)
Z	2	2	4
Density (calc.), Mg/m <sup>3</sup>	1.248	1.266	1.491
Absorption coefficient, mm <sup>-1</sup>	0.451	0.508	0.635
Crystal size, mm <sup>3</sup>	0.410 x 0.270 x 0.090	0.490 x 0.350 x 0.300	0.090 x 0.050 x 0.040
Reflections collected	35578	25011	33115 / 6571
Independent reflections	9449	18204	5690
Max. and min. transmission	0.960, 0.877	0.996, 0.981	0.975, 0.913
Data / restraints / parameters	9449 / 0 / 449	24534 / 36 / 1153	6571 / 0 / 359
Final R indices [I>2σ(I)]	0.0692 (0.1942)	0.0568 (0.0988)	0.0278 (0.0635)
R indices (all data)	0.0809 (0.2107)	0.0375 (0.0891)	0.0358 (0.0674)
Goodness-of-fit on F <sup>2</sup>	1.030	1.026	1.027
Largest diff. peak, e.Å <sup>-3</sup>	1.263 and -0.641	1.097 and -0.616	0.415 and -0.339



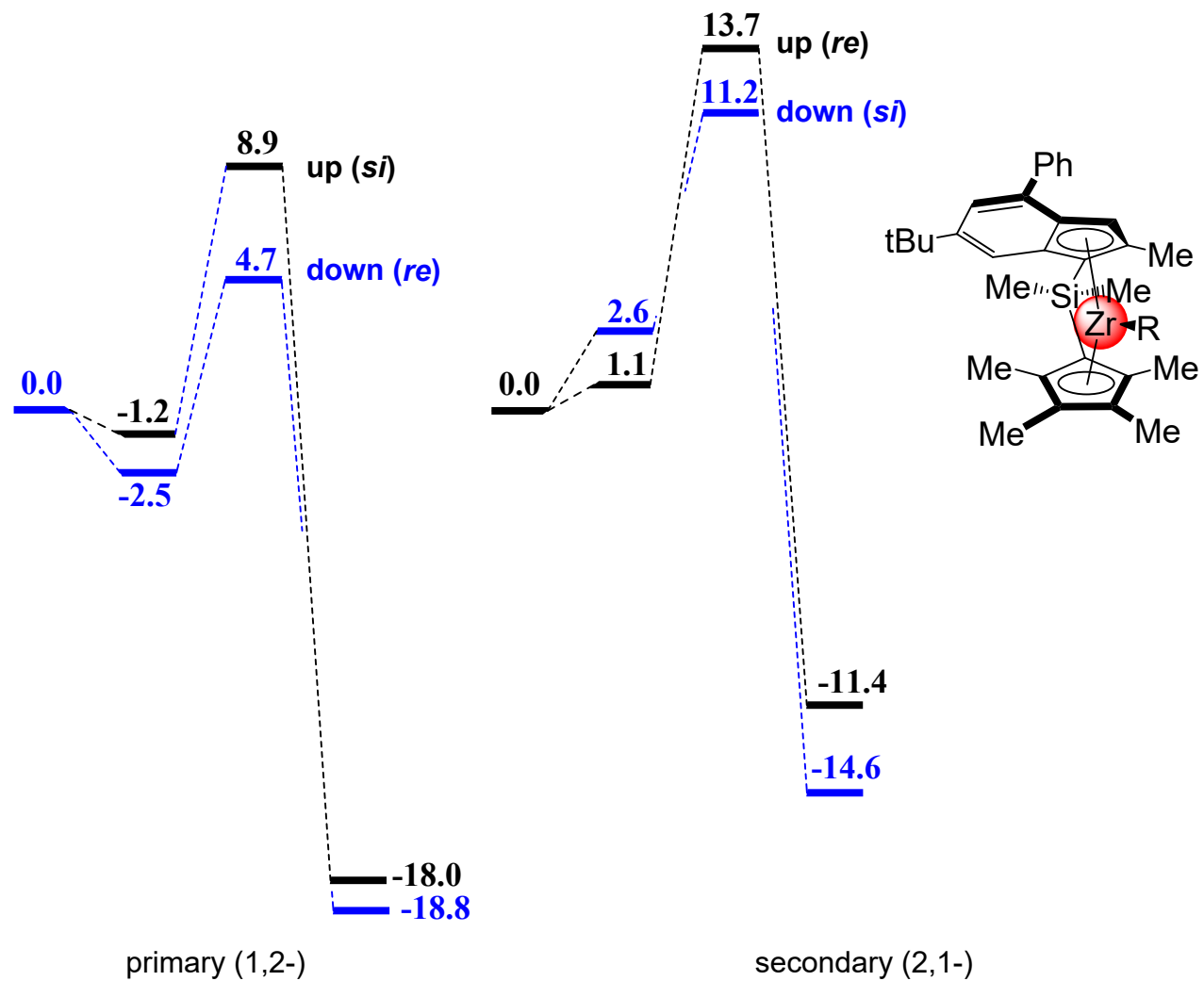
**Computational details.** All calculations were carried out with the Gaussian 09 suite of programs.<sup>19</sup> Zirconium atoms were treated with the very small core Stuttgart–Dresden effective core potential associated with its adapted basis sets and additional *f* and *g* polarization functions.<sup>20</sup> Carbon and hydrogen atoms were described with a 6-31G(d,p) double- $\zeta$  basis set.<sup>21</sup> Silicon atoms have been treated with the small core Stuttgart-Dresden effective core potential associated with its adapted basis set and additional *d* polarization functions.<sup>22</sup> Calculations were carried out at the DFT level of theory with the hybrid functional B3PW91.<sup>23</sup> Solvation energies were evaluated by a self-consistent reaction field (SCRF) approach based on accurate numerical solutions of the Poisson-Boltzmann equation by using the SMD solvation model.<sup>24</sup> Toluene was used as solvent. All geometries were optimized without any symmetry restriction and the nature of the extrema was verified by analytical frequency calculations. The calculation of electronic energies and enthalpies of the extrema of the potential energy surface (minima and transition states) were performed at the same level of theory as the geometry optimizations. Enthalpies were obtained at  $T = 298$  K within the harmonic approximation. The way how  $\Delta H^\ddagger$  was calculated is presented in Scheme S1. IRC calculations were performed to confirm the connections of the optimized transition states.



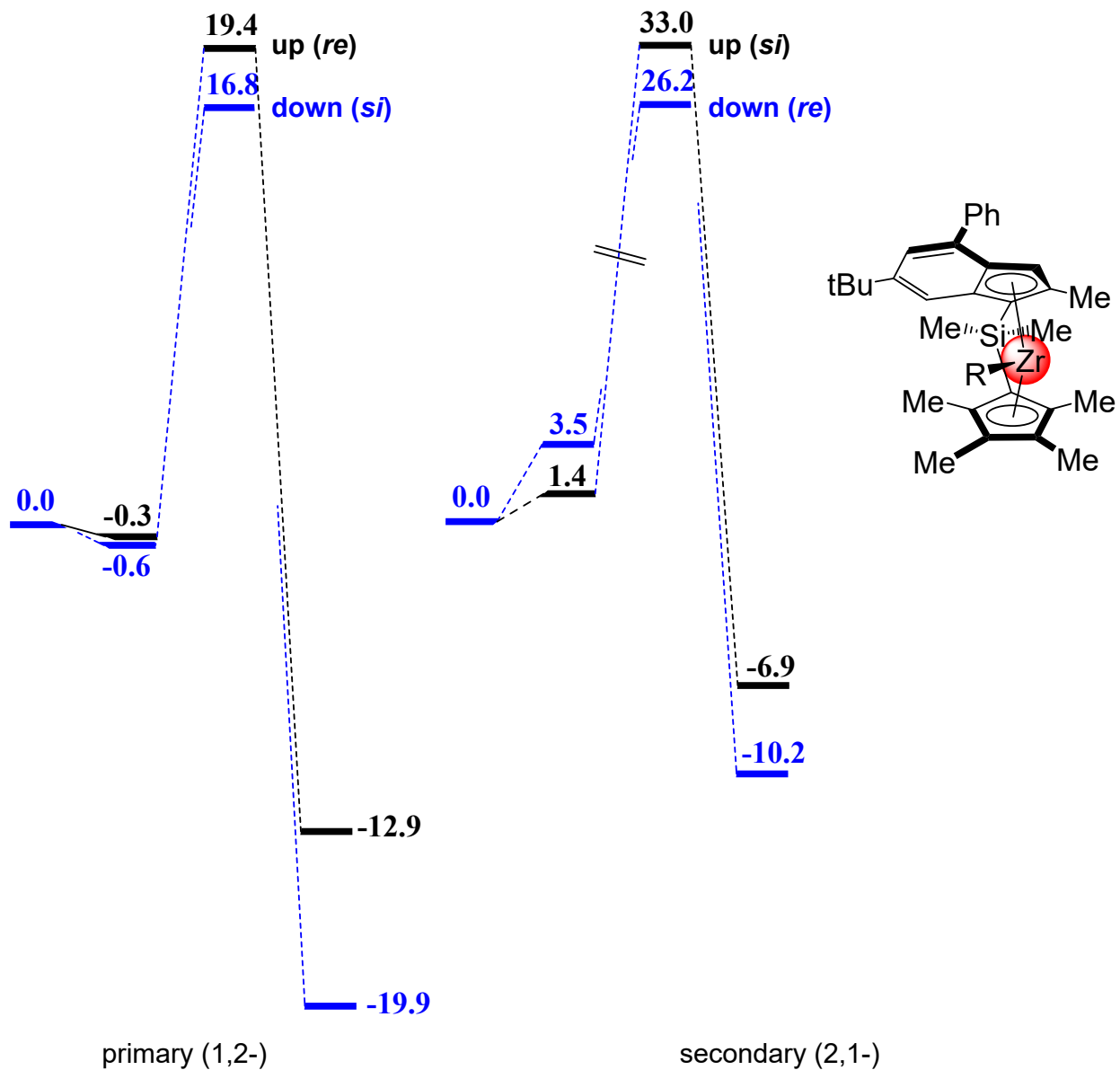
**Scheme S1.** Definition of  $\Delta H^\ddagger$  depending on the sign of  $\Delta H_{\text{coord}}$ .



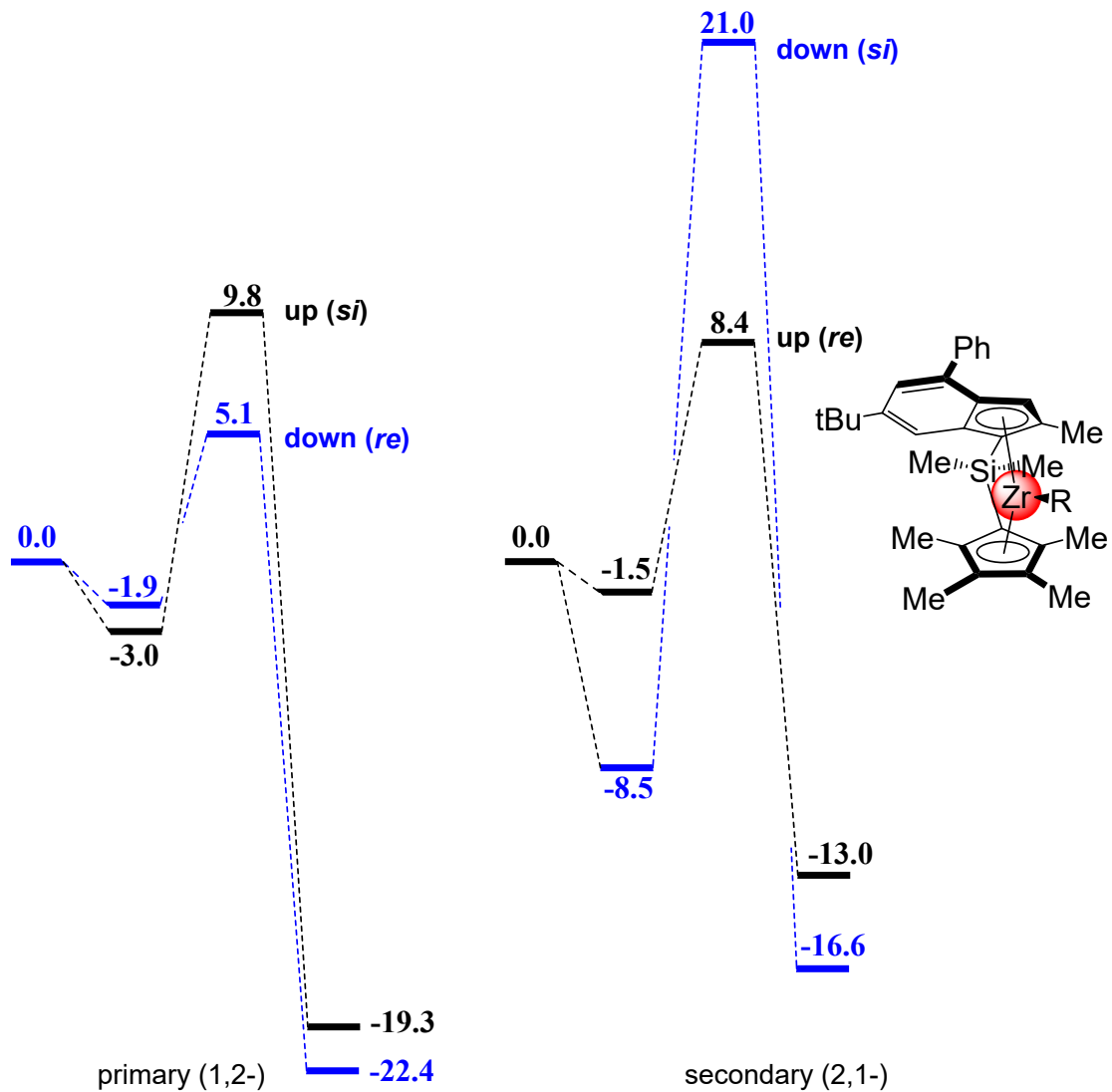
**Scheme S2.** DFT-calculated pathway for the first insertion of propylene in *Anti*-2c-Zr.



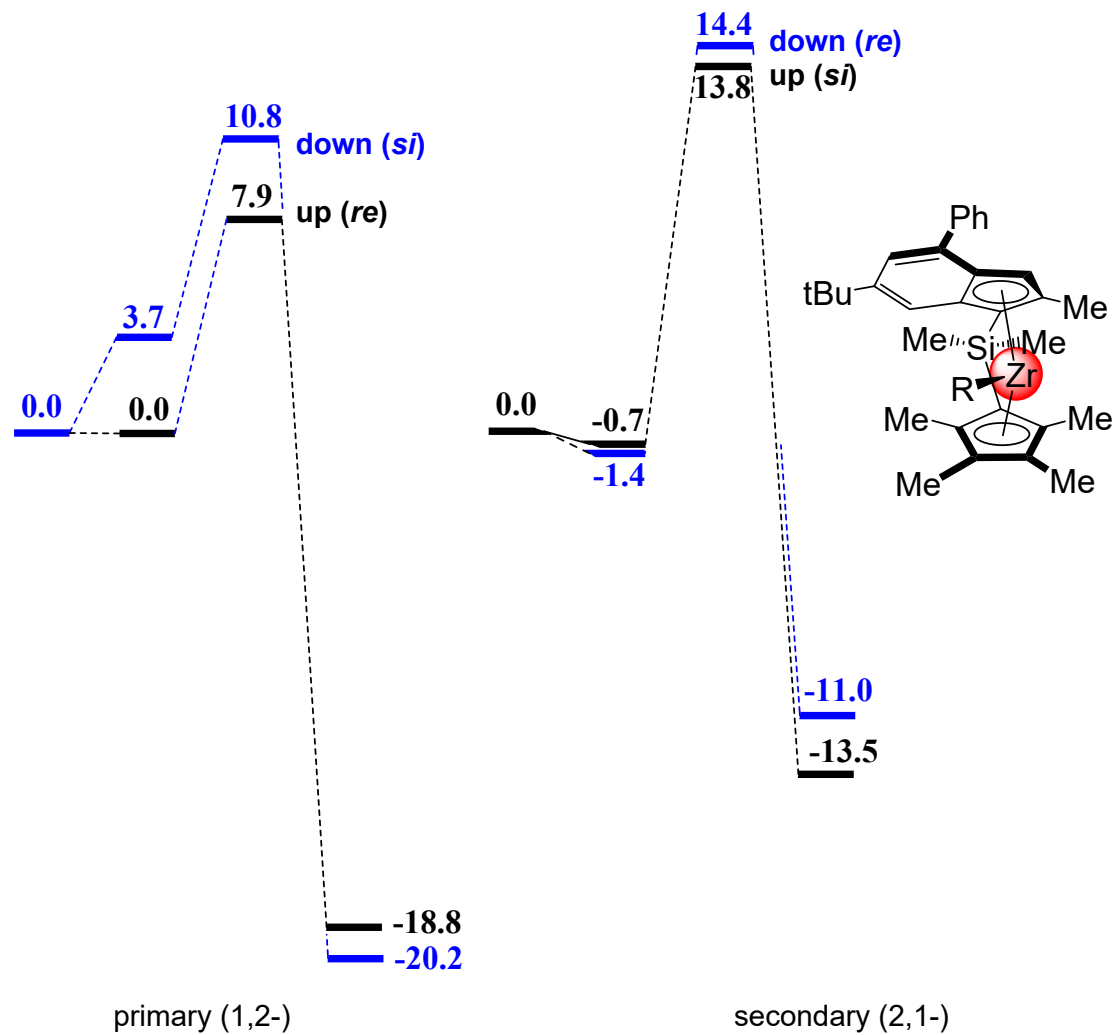
**Scheme S3.** DFT-calculated pathway for the second insertion of propylene in *Anti*-2c-Zr.



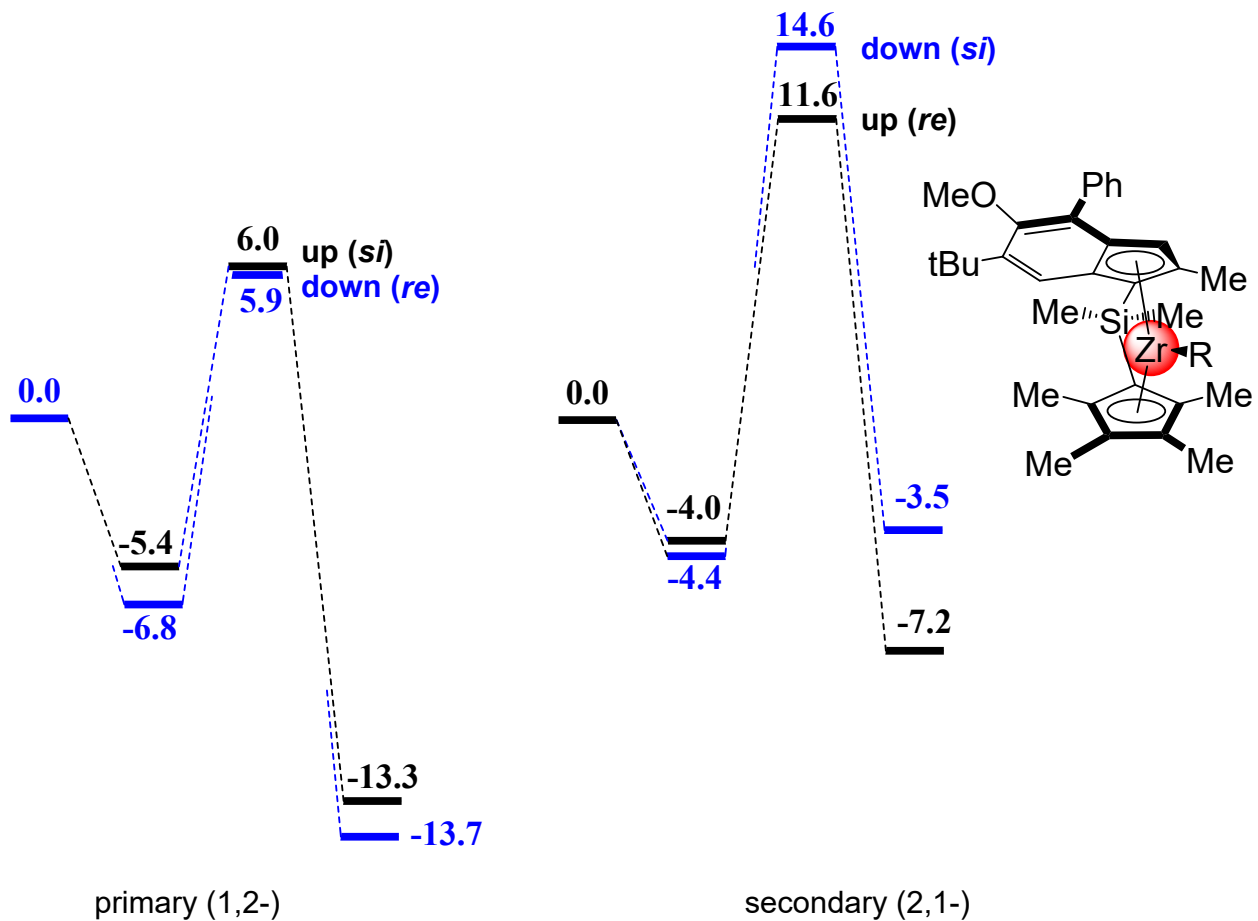
**Scheme S4.** DFT-calculated pathway for the second insertion of propylene in *Syn-2c-Zr*.



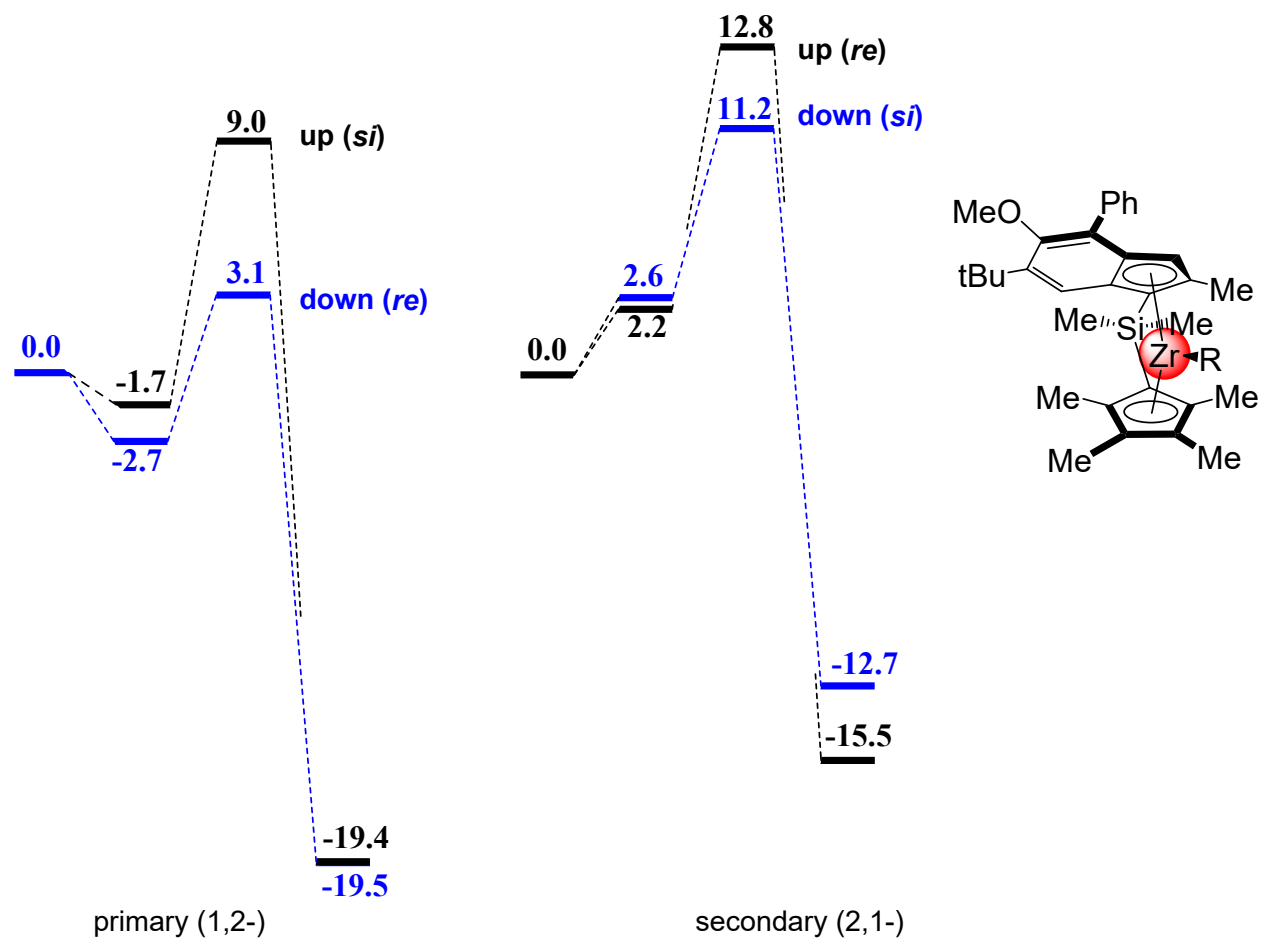
**Scheme S5.** DFT-calculated pathway for the third insertion of propylene in *Anti-2c-Zr*.



**Scheme S6.** DFT-calculated pathway for the third insertion of propylene in *Syn-2c-Zr*.

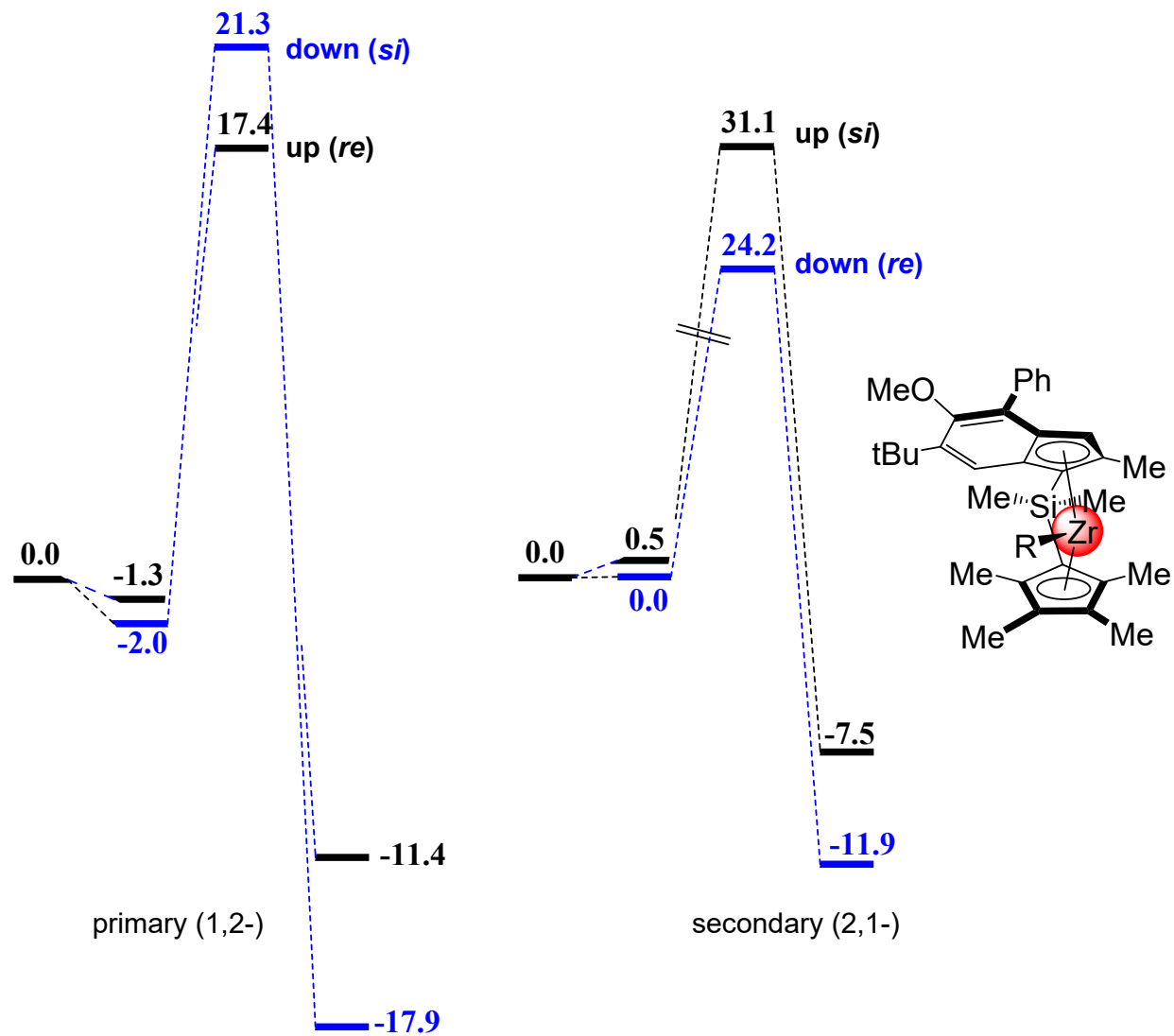


**Scheme S7.** DFT-calculated pathway for the first insertion of propylene in *Anti*-2d-Zr.

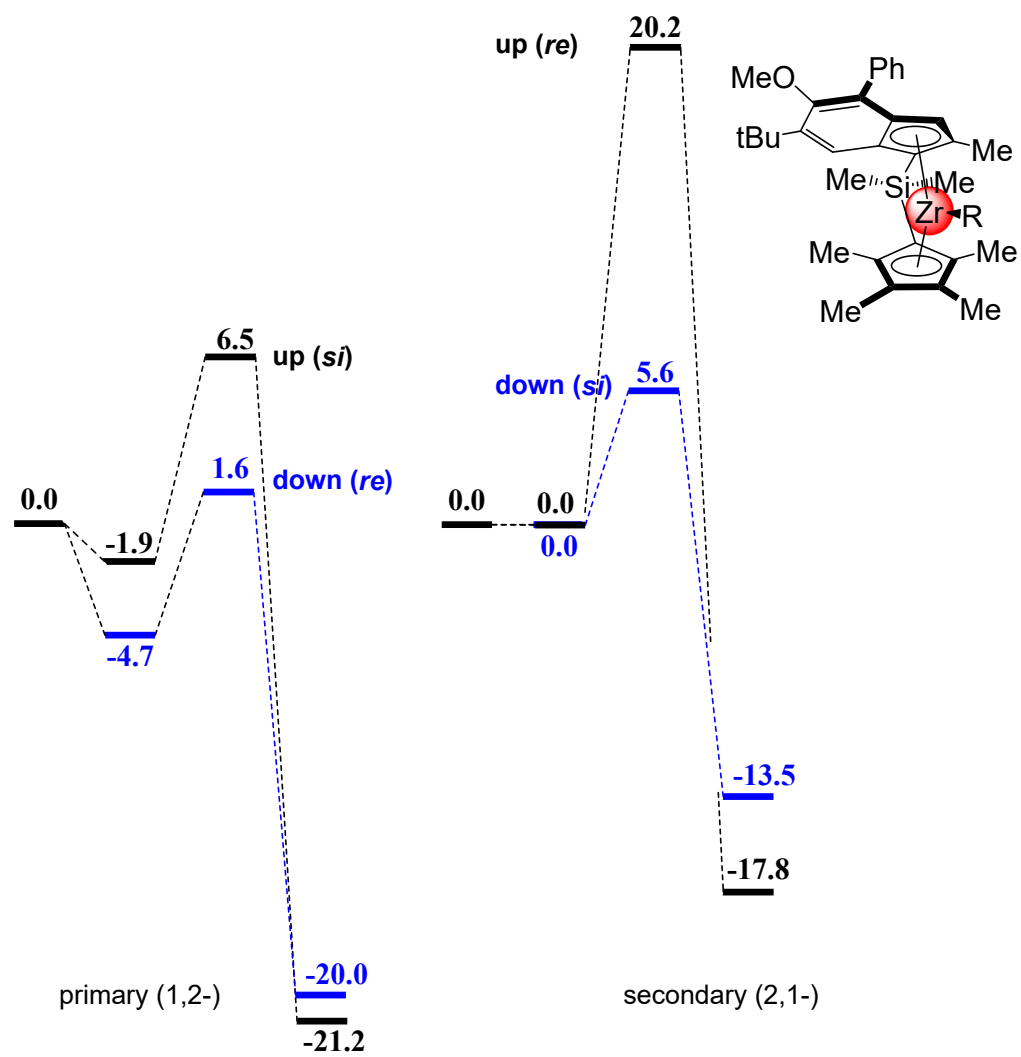


**Scheme S8.** DFT-calculated pathway for the second insertion of propylene in *Anti*-2d-Zr.

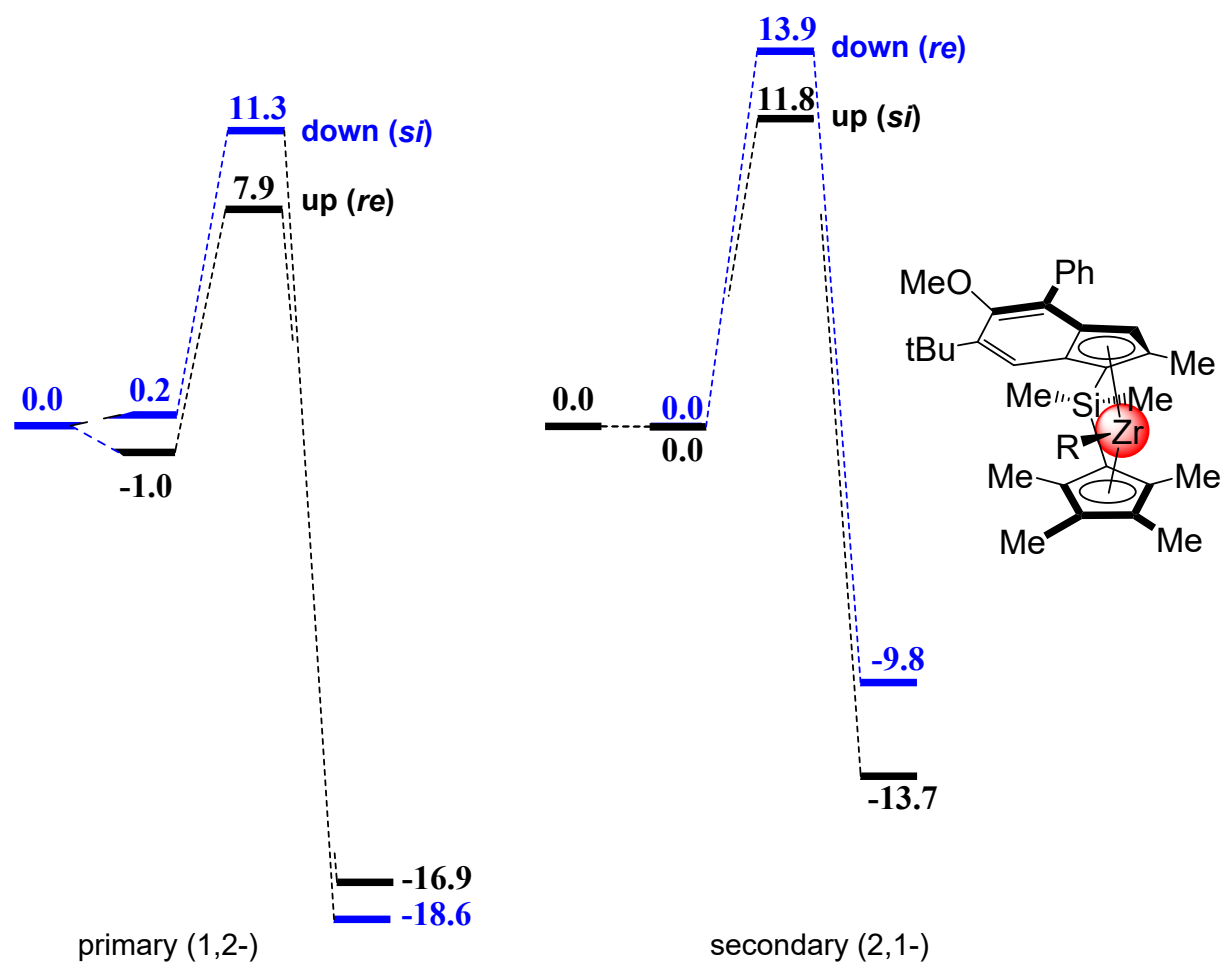




**Scheme S9.** DFT-calculated pathway for the second insertion of propylene in *Syn-2d-Zr*.



**Scheme S10.** DFT-calculated pathway for the third insertion of propylene in *Anti-2d-Zr*.



**Scheme S11.** DFT-calculated pathway for the third insertion of propylene in *Syn-2d-Zr*.

**Table S3.** Energetic data (kcal·mol<sup>-1</sup>) calculated for the three first propylene insertion steps with systems [3c-Zr-Me]<sup>+</sup> and [3d-Zr-Me]<sup>+</sup>.<sup>a</sup>

Reaction		[3c-Zr-Me] <sup>+</sup>			[3d-Zr-Me] <sup>+</sup>		
		$\Delta H$ (1 <sup>st</sup> insertion)	$\Delta H$ (2 <sup>nd</sup> insertion)	$\Delta H$ (3 <sup>d</sup> insertion)	$\Delta H$ (1 <sup>st</sup> insertion)	$\Delta H$ (2 <sup>nd</sup> insertion)	$\Delta H$ (3 <sup>d</sup> insertion)
<i>A-pr-si</i> (up)	Adduct	-5.4	-1.2	-3.0	-5.5	-1.7	-1.9
	TS	5.5 (10.9)	8.9 (10.1)	9.8 (12.8)	6.0 (11.5)	9.0 (10.7)	6.5 (8.4)
	Product	-14.1	-18.0	-19.3	-13.3	-19.5	-21.2
<i>A-pr-re</i> (down)	Adduct	-6.1	-2.5	-1.9	-6.8	-2.7	-4.7
	TS	5.3 (11.4)	4.7 (7.2)	5.1 (7.0)	5.9 (12.7)	3.1 (5.8)	1.6 (6.3)
	Product	-15.6	-18.8	-22.4	-13.7	-19.5	-20.0
<i>A-sec-si</i> (down)	Adduct	-4.7	2.6	-8.5	-4.4	2.6	-7.3
	TS	13.8 (18.5)	11.2	21.0 (29.5)	14.6 (19.0)	11.2	5.6 (12.9)
	Product	-3.9	-14.6	-16.6	-3.5	-12.7	-13.5
<i>A-sec-re</i> (up)	Adduct	-4.3	1.1	-1.5	-4.0	2.2	-0.8
	TS	10.9 (15.2)	13.7	8.4 (9.9)	11.6 (15.6)	12.8	20.2 (21.0)
	Product	-8.3	-11.4	-13.0	-7.2	-15.5	-17.8
<i>S-pr-si</i> (down)	Adduct		-0.6	3.7		-2.0	0.2
	TS	-	16.8 (17.4)	10.8		21.3 (23.3)	11.3
	Product		-19.9	-20.2		-17.9	-18.6
<i>S-pr-re</i> (up)	Adduct		-0.3	0.0		-1.3	-1.0
	TS	-	19.4 (19.7)	7.9	-	17.4 (18.7)	7.9 (8.9)

	Product		-12.9	-18.8		-11.4	-16.9
<i>S</i> -sec- <i>si</i> (up)	Adduct		1.4	-0.7		0.5	-0.2
	TS	-	33.0	13.8 (14.5)	-	31.1	11.8 (12.0)
	Product		-6.9	-13.5		-7.5	-13.7
<i>S</i> -sec- <i>re</i> (down)	Adduct		3.5	-1.4		0.0	-1.4
	TS	-	26.2	14.4 (15.8)	-	24.2	13.9 (15.3)
	Product		-10.2	-11.0		-11.9	-9.8

<sup>a</sup> The values for the insertion barriers were calculated as  $\Delta H_{\text{ins}}^{\ddagger} = H_{\text{TS}} - H_{\text{Reactants}}$ . The values in brackets for the insertion barriers were calculated as  $\Delta H^{\ddagger} = H_{\text{TS}} - H_{\text{Adduct}}$ .

## References

- 1 Feitler, D.; Whitesides, G. M. Convenient Preparations of 1,2,3,4,5-Pentamethylcyclopentadiene and 1-Ethyl-2,3,4,5-tetramethylcyclopentadiene. *Inorganic Chemistry* **1976**, *15*, 466–469.
- 2 McKittrick, M. W.; Lones, C. W. Toward Single-Site Functional Materials-Preparation of Amine-Functionalized Surfaces Exhibiting Site-Isolated Behavior. *Chem. Mater.* **2003**, *15*, 1132–1139.
- 3 Barton, J. W.; Shepherd, M. K.; Benzocyclo-octenes. Part 5. Thermal rearrangements of benzocyclo-octenes to benzo[a]cyclopropa[c,d]pentalenes. *J. Chem. Soc., Perkin Trans. 1* **1986**, 961–966.
- 4 Nifant'ev, I. E.; Ivchenko, P. V.; Bagrov, V. V.; Churakov, A. V.; Mercandelli, P. 5-Methoxy Substituted Zirconium Bis-indenyl ansa-Complexes: Synthesis, Structure, and Catalytic Activity in the Polymerization and Copolymerization of Alkenes. *Organometallics* **2012**, *31*, 4962–4970.
- 5 Borealis AG European Appl. 09153718.3 2010.
- 6 Diemer, V.; Chaumeil, H.; Defoin, A.; Fort, A.; Boeglin, A.; Carré, C., Syntheses of Sterically Hindered Zwitterionic Pyridinium Phenolates as Model Compounds in Nonlinear Optics. *Eur. J. Org. Chem.* **2008**, 1767–1776.
- 7 Following the procedure for the Suzuki-Coupling as described in Reference 8, 1d was prepared starting from 4-bromo-2-methyl-1H-indene and phenyl boronic acid.
- 8 Izmer, V. V.; Lebedev, A. Y.; Kononovich, D. S.; Borisov, I. S.; Kulyabin, P. S.; Goryunov, G. P.; Uborsky, D. V.; Canich, J. A. M.; Voskoboynikov, A. Z. ansa-Metallocenes Bearing 4-(N-Azoly)-2-methylindenyl and Related Ligands: Development of Highly Iselective Catalysts for Propene Polymerization at Higher Temperatures. *Organometallics* **2019**, *38*, 4645–4657.
- 9 Quindt, V.; Saurenz, D.; Schmitt, O.; Schär, M.; Dezember, T.; Wolmershäuser, G.; Sitzmann, H. Bulky Peralkylated Cyclopentadienes by Extension of Jutzi's Pentamethylcyclopentadiene Procedure. *J. Organomet. Chem.* **1999**, *579*, 376–384.
- 10 Kulyabin, P. S.; Goryunov, G. P.; Sharikov, M. I.; Izmer, V. V.; Vittoria, A.; Budzelaar, P. H. M.; Busico, V.; Voskoboynikov, A. Z.; Ehm, C.; Cipullo, R.; Uborsky, D. V. Ansa-Zirconocene Catalysts for Isotactic-Selective Propene Polymerization at High Temperature: A Long Story Finds a Happy Ending. *J. Am. Chem. Soc.* **2021**, *143*, 7641–7647.
- 11 Villaseñor, E.; Gutierrez-Gonzalez, R.; Carrillo-Hermosilla, F.; Fernández-Galán, R.; López-Solera, I.; Fernández-Pacheco, A. R.; Antiñolo, A. Neutral Dimethylzirconocene Complexes as Initiators for the Ring-Opening Polymerization of epsilon-Caprolactone. *Eur. J. Inorg. Chem.* **2013**, *13*, 1184–1196.
- 12 Lee, M. H.; Han, Y.; Kim, D.-H.; Hwang, J.-W.; Do, Y. Isospecific Propylene Polymerization by C1-Symmetric Me<sub>2</sub>Si(C<sub>5</sub>Me<sub>4</sub>)(2-R-Ind)MCl<sub>2</sub> (M = Ti, Zr) Complexes. *Organometallics* **2003**, *22*, 2790–2796.
- 13 Friederichs, N. H.; Vittoria, A.; Cipullo, R.; Busico, V.; Borisov, I.; Guzeev, B. A.; Mladentsev, D. Y.; Sharikov, M. I.; Uborsky, D.; Voskoboynikov, A.; Coen, H. (Sabice Global Technologies B.V.) PCT Int. Appl. WO 18/058630, 2018.
- 14 Sheldrick, G. M. SHELXT – Integrated Space-Group and Crystal-Structure Determination. *Acta Crystallogr. Sect. Found. Adv.* **2015**, *71*, 3–8.

- 
- 15 Sheldrick, G. M. Crystal Structure Refinement with SHELXL. *Acta Crystallogr. Sect. C Struct. Chem.* **2015**, *71*, 3–8.
- 16 Van der Sluis, P.; Spek, A. L. BYPASS: An Effective Method for the Refinement of Crystal Structures Containing Disordered Solvent Regions. *Acta Crystallogr. A.* **1990**, *46*, 194–201.
- 17 Spek, A. L. Single-Crystal Structure Validation with the Program PLATON. *J. Appl. Crystallogr.* **2003**, *36*, 7–13
- 18 Cavallo, L.; Scarano, V.; Oliva, R.; Poater, A.; Serra, L.; Petta, A.; Cao, Z.; Falivene, L. Towards the online computer-aided design of catalytic pockets. *Nat. Chem.* **2019**, *11*, 872–879.
- 19 Gaussian 09, Revision **D.01**, Frisch, M. J.; Trucks, G. W.; Schlegel, H. B.; Scuseria, G. E.; Robb, M. A.; Cheeseman, J. R.; Scalmani, G.; Barone, V.; Mennucci, B.; Petersson, G. A.; Nakatsuji, H.; Caricato, M.; Li, X.; Hratchian, H. P.; Izmaylov, A. F.; Bloino, J.; Zheng, G.; Sonnenberg, J. L.; Hada, M.; Ehara, M.; Toyota, K.; Fukuda, R.; Hasegawa, J.; Ishida, M.; Nakajima, T.; Honda, Y.; Kitao, O.; Nakai, H.; Vreven, T.; Montgomery, J. A., Jr.; Peralta, J. E.; Ogliaro, F.; Bearpark, M.; Heyd, J. J.; Brothers, E.; Kudin, K. N.; Staroverov, V. N.; Kobayashi, R.; Normand, J.; Raghavachari, K.; Rendell, A.; Burant, J. C.; Iyengar, S. S.; Tomasi, J.; Cossi, M.; Rega, N.; Millam, M. J.; Klene, M.; Knox, J. E.; Cross, J. B.; Bakken, V.; Adamo, C.; Jaramillo, J.; Gomperts, R.; Stratmann, R. E.; Yazyev, O.; Austin, A. J.; Cammi, R.; Pomelli, C.; Ochterski, J. W.; Martin, R. L.; Morokuma, K.; Zakrzewski, V. G.; Voth, G. A.; Salvador, P.; Dannenberg, J. J.; Dapprich, S.; Daniels, A. D.; Farkas, Ö.; Foresman, J. B.; Ortiz, J. V.; Cioslowski, J.; Fox, D. J. Gaussian, Inc., Wallingford CT, **2009**.
- 20 (a) Andrae, D.; Haeussermann, U.; Dolg, M.; Stoll, H.; Preuss, H. *Theor. Chim. Acta* **1990**, *77*, 123-141. (b) Martin, J. M. L.; Sundermann, A. *J. Chem. Phys.* **2001**, *114*, 3408-3420.
- 21 Hehre, W. J.; Ditchfield, R.; Pople, J. A. *J. Chem. Phys.* **1972**, *56*, 2257-2261.
- 22 Bergner, A.; Dolg, M.; Kuechle, W.; Stoll, H.; Preuss, H. *Mol. Phys.* **1993**, *80*, 1431.
- 23 (a) Becke, A. D. *J. Chem. Phys.* **1993**, *98*, 5648-5652. (b) Burke, K.; Perdew, J. P.; Yang, W. in *Electronic Density Functional Theory: Recent Progress and New Directions*, Eds: Dobson, J. F.; Vignale, G.; Das, M. P., Plenum, New York, **1998**.
- 24 Marenich, A. V.; Cramer, C. J.; Truhlar, D. G. *J. Phys. Chem. B* **2009**, *113*, 6378-6396.